Engineering Properties of Stabilized Marine Clay Using Basic Oxygen Furnace Steel Slag: Strength Development and Expansion Behaviour

（製鋼スラグを用いて改良した海成粘土の工学的性質：強度発現および膨張特性）

D165358

Cikmit, Arlyn Aristo

Doctoral Thesis

Supervisor: Prof. Takashi Tsuchida

Hiroshima University

September 2019

In the Name of Allāh, the Most Gracious, the Most Merciful

ABSTRACT

The recycling of slag is a strategic issue in countries with huge iron and steel manufacturing industries. Japan itself annually produced 30 million tons of slag, 8.3% of the total worldwide production 360 million tons (globalslag.com). Most steel slag generated in Japan is used as a raw material in cement industries (~66%), road base material (~12%), concrete aggregate (~7%), and raw material for fertilizer and other miscellaneous applications (~15%). Over 39 million tons of steel slag was produced in 2010 and ~5% of it was dumped in disposal facilities (Horii et al., 2013). The significant number of unused steel slag that ends up in disposal site is not only uneconomical but also not environmentally friendly, thus an alternative and sustainable method to increase the recycling rate is necessary (JSCE, 2017; Oss, 2012).

This study was achieved as a fundamental study of engineering properties of stabilized dredged marine clay (DMC) with basic oxygen furnace (BOF) slag to enhance and broaden the use of BOF slag in civil works. Four main studies were performed: (i)Strength development and microstructural characteristic of DMC with BOF slag, (ii)Particle size effect of BOF slag in the stabilization of DMC, (iii)Expansion characteristic of BOF slag mixed with DMC, (iv)Time-delay effect on the strength development of stabilized DMC with BOF slag.

In investigating the compressive strength and expansion rate of the stabilized DMC with BOF slag, a laboratory vane shear, and unconfined compression. An accelerated expansion test was performed to measure the expansion of specimens in this study. Scanning electron microscope and energy dispersive spectroscopy were adapted to observe the microstructure of stabilized DMC with BOF slag.

Overall, the study results indicate that BOF slag is satisfactory to stabilize DMCs. Strength of the stabilized DMC with BOF slag (SMSS) develops significantly with time; classified into three stages, (i) inactive zone (0.5 to 5 hours), (ii) active zone (5 hours to 3 days), and (iii) moderate zone (3 to 90 days). Empirical equations for each zone were proposed based on the volumetric solid content, initial water content, strength at 1 h of curing, and strength increment coefficients. Moreover, the reticulation structure of the amorphous C-S-H gel and platy AFm phases on all

samples were observed, with intergrowths of rod-like ettringite within the flat clay structure and flocculated clay-cement cluster, and the cementitious compounds became more evident with an increase in the BOF slag content and curing time.

The study results showed that the strength was significantly affected by different maximum particle sizes, despite the same free lime content. The larger the maximum grain size of BOF aggregate, the lower the final strength developed. An equation to predict the strength development of a larger maximum grain-size from a smaller maximum grain-size was proposed using a modified BOF slag rate of addition and its calculated specific surface area. Further analysis indicates that the equation is feasible for predicting the strength development of an actual construction from a laboratory test results.

The heavyweight characteristic of steel slag gives it the potential to be used in various civil engineering constructions. However, controlling its volume instability is challenging. The study of the expansion mechanism of steel slag mixed with soft marine clay and determine the maximum steel slag addition is essential in order to achieve a heavyweight geomaterial which still in compliance with the allowable expansion. A series of expansion tests on steel slag mixed with soft clay were performed and evaluated. Scanning electron microscopy (SEM) and energy-dispersive spectroscopy (EDS) were conducted to support the tests. Our results showed that the removal of fine content in steel slag is not effective for alleviating expansion. In the steel slag mixed with soft clay, the soft clay provided spaces that absorbed the volumetric change of the steel slag, and 60% was found to be the maximum volumetric addition to the soft clay, exhibiting 0.24%–0.35% of the volumetric expansion. The addition of 60% of steel slag produced 24.3 kN/m3 of unit weight, which is preferable for certain submerged fill purposes. SEM and EDS analysis results showed more microcracks and less existence of the C-S-H phase in 45%–60% of steel slag addition than in 70–100%, which explains the occurrence of less volumetric expansion. Further observation indicates that the amount of free CaO and free MgO most likely controls the final volume expansion, whereas the grain size distribution varies the increment of the volumetric change.

In the fourth study, Time-delay effect on the strength development of stabilized DMC with BOF slag, s series of strength test was performed on the specimens with various different time-delay intervals between the mixing and the pouring of the sample. It is found that at the early development, the strength was highly affected by the

disturbance. However, after 28 days, the strength of specimen with disturbance 2, 5 and 7 hours developed onto a similar strength exhibited in the specimen without disturbance. For 20% BOF slag addition, the specimens of 1, 2, and 3 days disturbance exhibited strength ratio of 0.92, 0.64, and 0.54, respectively. For 30% BOF slag addition, the specimens with 1, 2, and 3 days disturbance were able to develop with a strength ratio of 0.7, 0.5 and 0.52 to that without disturbance, respectively. The strength of the specimens with various RSS values and different time-disturbances can be referred by a single line with a high coefficient determination, 0.94. As a conclusion, the stabilized DMC with BOF slag has a self-recovery feature that allows it to mobilize its strength after a disturbance occurs.

TABLE OF CONTENTS

LIST OF FIGURES

LIST OF TABLE

Chapter 1

Introduction

TABLE OF CONTENTS

1.1 Background

The recycling of slag is a strategic issue in countries with huge iron and steel manufacturing industries. Japan itself annually produced 30 million tons of slag, 8.3% of the total worldwide production 360 million tons (globalslag.com). Most steel slag generated in Japan is used as a raw material in cement industries (~66%), road base material (~12%), concrete aggregate (~7%), and raw material for fertilizer and other miscellaneous applications (~15%). Over 39 million tons of steel slag was produced in 2010 and ~5% of it was dumped in disposal facilities (Horii et al., 2013). The significant number of unused steel slag that ends up in disposal site is not only uneconomical but also not environmentally friendly, thus an alternative and sustainable method to increase the recycling rate is necessary (JSCE, 2017; Oss, 2012).

For past decades, the BOF slag coming from a steel-making process is relatively lower in utilization than the slag from an iron-making process i.e GGBF slag. One of the reasons is due to the volume instability of the BOF slag. (Geiseler, 1996; Juckes, 2003; Shi, 2004; Yildirim and Prezzi, 2011). This study concentrates more in improving the recycling rate of the BOF slag by providing a comprehensive understanding of the property and characteristic of BOF slag to massively use it in broad applications.

The hydration of both lime and dolomites mainly causes the volume instability (expansion) of the steel slag. During the BOF steel-making process, 10-20% steel scraps and 80-90% molten iron are charged into basic oxygen furnaces. In order to remove the impurities from the steel, the furnace is also charged with fluxing agents, such as lime (CaO) and/or dolomite [$MgCa(CO_3)_2$] along with pure oxygen. Since the lime or dolomite do not burn thoroughly, it remains and precipitates in molten slag (Shi, 2004; Wachsmuth et al., 1981; Yildirim and Prezzi, 2015). It is widely known that when in contact with water, the free lime reacts and form hydroxides that can cause volume expansion. For its volume instability, most applications of BOF slag in civil works are implemented by diminishing the free-lime rather than benefitting from it.

The idea of soil stabilization using BOF slag coming from the necessity to meet the demand for fill materials. The stabilization of dredged soil is considered to

be a good method to simultaneously recycle the BOF slag and dredged soils. Poh H. Y. et al. (2006) initiated the possibility of steel slag as a stabilizer in soil stabilization by investigating the effect of fine-steel-slag addition and activator agent to two different English clays. They reported that it takes a minimum 15-20% of fine steel slag and an activator (quicklime or cement) to significantly increase the soil strength. In practical purposes, especially a low-strength material of fill construction, one can possibly replace the common stabilizer such as cement to achieve a decent geomaterial in off-shore fill construction. Therefore, recent studies were carried out to provide a comprehensive understanding of the physical and chemical characteristic of stabilized soils with BOF slag so that the BOF slag can be massively recycled and used in broad applications.

1.2 Objectives

The goal of this research was to provide a comprehensive understanding of the physical and chemical characteristic of stabilized soils with basic oxygen furnace slag so that it can be massively used in broad applications. The specific objectives of this research were:

1) To investigate the strength development of dredged clay stabilized with basic oxygen furnace slag at various curing times in order for it to be used as a geo-material in geotechnical applications.
2) To further understand the soil stabilization using BOF slag by observing its microstructural and mineralogical properties.
3) To investigate the effects of a different maximum grain-size of BOF slag on the strength development of stabilized dredged marine clay.
4) To investigate the expansion mechanism of steel slag mixed with dredged soil and steel slag without fine particle.
5) To determine the maximum steel slag addition possible to dredged marine clay such that it remains in compliance with the allowable volume expansion.

1.3 Thesis outline

An outline of the research topics studied in this thesis is presented as follows:

- **Chapter 1** provides the background information, the purpose of research and the outline of the thesis.
- **Chapter 2** focuses on a literature review of related topics in the introduction section, especially on the physical and chemical characteristic, and the strength-mobilization mechanism of the stabilized soils with BOF slag. The thesis is divided into five chapters that provide the overall results of the study investigated in this thesis.
- **Chapter 3** addresses the time-strength relationship of the stabilized soils with BOF slag. Early-curing and later-curing specimens were tested using a laboratory vane shear (LVS) test and an unconfined compressive (UC) test, respectively. The macrostructural and mineralogy of the specimens were investigated using a scanning electron microscope and an energy dispersive spectroscopy (EDS). A strength estimation equation was proposed to estimate the strength development of the stabilized soils.
- **Chapter** 4 covers a study on the effects of different grain size distributions (GSD) of BOF slag to the stabilized soils. Various GSDs were used to stabilize the soft soil. An equation to estimate the strength development of the stabilized soil with various GSD of BOF slag was proposed.
- In **Chapter 5**, the expansion characteristic of the BOF slag mixed with soft soil, and the BOF slag with and without fine particles were investigated. The volumetric change was tested using an expansion apparatus specialized for materials subject to hydration.
- **Chapter 6** covers the effects of disturbance (time-delay between mixing and the fill) to the strength development of the stabilized soils. The various time-delay disturbances were applied to the specimens and the strength development of the specimens from the early curing time was observed.
- **Chapter 7** presents the main findings and overall conclusions of this study. Some recommendations for future research were also listed in this chapter.

1.4 References

Geiseler, J. (1996). Use of steelworks slag in Europe. Waste Management *16*, 59–63.

Horii, K., Kitano, Y., Tsutsumi, N., and Kato, T. (2013). Processing and Reusing Technologies for Steelmaking Slag. 123–129.

JSCE (2017). Technical manual steelmaking slag treated soil for harbor, airport, and coastal construction projects (Japan society of civil engineering).

Juckes, L.M. (2003). The volume stability of modern steelmaking slags. Mineral Processing and Extractive Metallurgy *112*, 177–197.

Oss, H.G. van (2012). Slag-iron and steel, annual review 2006. 2012 Mineral Industry Surveys, U.S Geological Survey, Reston, VA.

Poh H. Y., Ghataora Gurmel S., and Ghazireh Nizar (2006). Soil Stabilization Using Basic Oxygen Steel Slag Fines. Journal of Materials in Civil Engineering *18*, 229–240.

Shi, C. (2004). Steel Slag—Its Production, Processing, Characteristics, and Cementitious Properties. Journal of Materials in Civil Engineering *16*, 230–236.

Wachsmuth, F., Geiseler, J., Fix, W., Koch, K., and Schwerdtfeger, K. (1981). Contribution to the Structure of BOF-Slags and its Influence on Their Volume Stability. Canadian Metallurgical Quarterly *20*, 279–284.

Yildirim, I.Z., and Prezzi, M. (2011). Chemical, Mineralogical, and Morphological Properties of Steel Slag.

Yildirim, I.Z., and Prezzi, M. (2015). Geotechnical Properties of Fresh and Aged Basic Oxygen Furnace Steel Slag. Journal of Materials in Civil Engineering *27*, 04015046.

Chapter 2

Literature Review

TABLE OF CONTENTS

2.1 Dredged marine soil

Dredged-marine (DM) soil is soft clay or soft silty clay that coming from a dredging process of a sea bottom. Port construction and maintenance field annually produced the DM soil as a consequent to create navigable channels (de Wit, 2005). DM clay is highly compressible and has a low unit weight depending on the initial moisture and coarse material content (Bartos, 1977a). The initial moisture content of marine clay is approximately 0.9-1.0 of its liquid limit at sea bottom. It increases drastically due to the act of dredging (Van Leussen and Nieuwenhuis, 1984), for instance, using a grab type dredger, the moisture content of DM soils raise to ~1.2-1.3 times (Terashi and Katagiri, 2005). Typically, a small amount of sand particle can be found as the dredged soil constituent; its content varies depending on how far the dredging takes place from the nearest estuary.

In order to progressively recycle DM soils, various studies (Chiu et al., 2009; Federico et al., 2015; Kang et al., 2015; Tang et al., 2001; Wang et al., 2017) on the stabilization and improvement of its physical properties have been performed. Van Leussen and Nieuwenhuis (1984) studied the soil mechanics aspect of dredging to ease the dredging practice by collecting comprehensive data from various actual constructions. DM clay commonly ends up at disposal facility. However, to reduce the cost, it is alternatively stabilized prior to its utilization as a geomaterial in civil works. The improvement of DM soils can be both mechanically (sand compaction or vertical drain), and or chemically (cement stabilization or other stabilization agents) executed. Other potential uses of dredged soils such as the cover of construction, liners, gas vent, leachate drains were proposed and investigated by (Bartos, 1977b).

2.2 Soft soil stabilization

Soil stabilization is any method of changing the natural condition of soil to meet an engineering purpose (Ingles and Metcalf, 1972). The bearing capability, tensile and compressive strength, and overall performance of soil can be improved by applying a certain type of techniques such as mechanical, biological, or chemical stabilization or combined method of stabilization (Kirsch and Bell, 2012).

As previously described, there are various methods to improve the nature of the soil, but in this study, I will only discuss the chemical stabilization of soil.

For years, the soil stabilization using chemically-active binders has become a prominent method to improve the poor ground condition. Portland cement, lime or other chemically-active binder are preferred since it assures the durability and the instant strength modification (Chiu et al., 2009; Federico et al., 2015; Kang et al., 2015; Rogers and Roff, 1997; Tang et al., 2001; Wang et al., 2017). Comprehensive studies on the effect of inorganic content (Kang et al., 2017; Paria and Yuet, 2006), clay structure and mineralogy (Sasanian and Newson, 2014; Vakili et al., 2013), low and high plasticity (Amu et al., 2005), stress-strain, strength development, have indicated the reliability of Portland cement in stabilizing various type of soils. The advance information and meticulous research on the cement stabilization invite more practitioners to widespread use it in civil works.

2.3 Basic oxygen furnace steel slag

Figure 2- 1 Classifications of slag and its process (NSA, 2010).

Basic oxygen furnace (BOF) steel slag is a by-product produced during the steel manufacturing process. Generally, slag can be classified into two types, a granulated

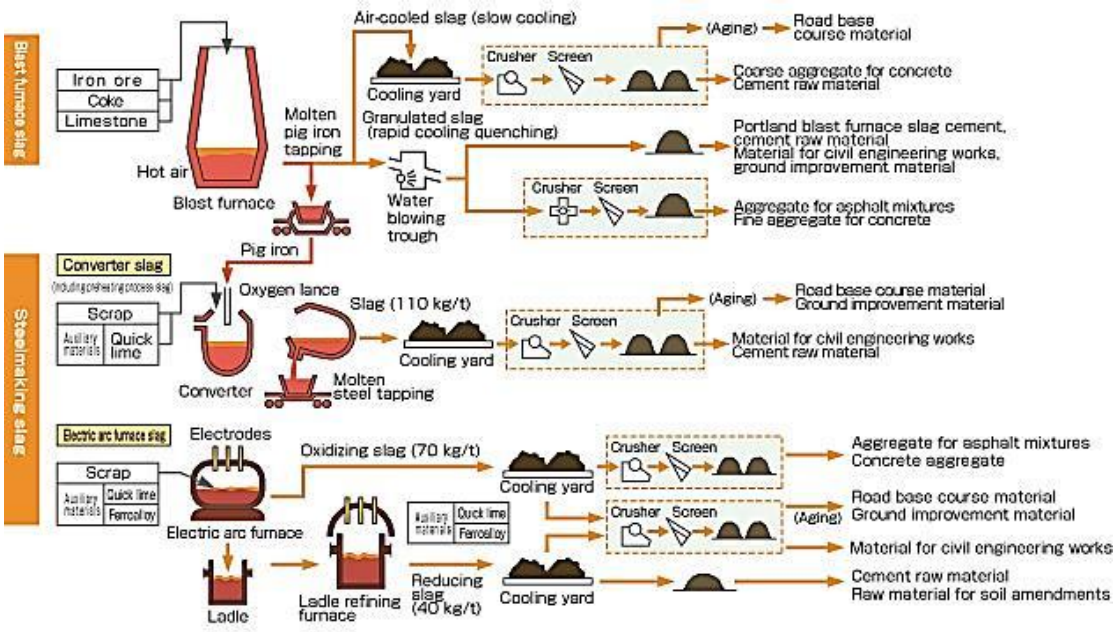

blast furnace (GBF) slag coming from an iron-manufacturing process, and a steelmaking/converter slag coming from an iron-to-steel-conversion process. Steelmaking slag itself is classified into two types, BOF slag and electric arc furnace slag (EAF), based on its method of the process involved during the conversion (Shi, 2004; Yildirim and Prezzi, 2011). During the iron-to-steel conversion process, basic oxygen furnace is charged with approximately 10-20% steel scraps and 80-90% molten iron. An oxygen lance lowered into the furnace blows 99% pure oxygen to remove the impurities of the charge (Brandt and Warner, 1999). Along with the oxygen blowing, lime (CaO) and/or dolomite ($MgCa(CO_3)_2$) are charged to remove unwanted chemical elements in steel. Since the lime and dolomite do not react thoroughly, a little amount of lime (CaO) and magnesia (MgO) remain and exist in steel slag.

2.3.1 Free lime content

Free lime is the undissolved lime in a steel refining process that accompanies steelmaking slag. Generally, free lime can be distinguished into three forms: (i) undissolved particles; (ii) lime precipitated from the melt during cooling; (iii) free lime that comes from tricalcium silicate when it transformed to dicalcium silicate (Juckes, 2003). The hydration of free lime in steelmaking slag is the main factor of the volume instability of steelmaking slag, although the hydration of magnesia may also contribute in some cases (Sorlini et al., 2012). The free lime of unassimilated origin occurs in large nodules (lime pocket) which is regarded as the most likely to cause damaging expansion. The precipitated lime in the molten slag has also been implicated in volumetric instability, but according to Inoue and Suito (1995), a decent amount of combined FeO and MnO made the precipitated lime less-reactive to hydration. The lime from the dissociated tricalcium silicate is more prone to hydration, however, it is normally small and enclosed within the mass of dicalcium silicate that will block it from outside pore water. Thus, the contribution of free lime (the precipitated lime and the free lime from dissociated tricalcium silicate) to the expansion during hydration appears to be small if not negligible.

Figure 2-2 shows a relationship among precipitated lime, residual free lime, and total free lime content reported by Wachsmuth et al. (1981). The figure indicates that if the total free lime content in the steelmaking slag is less than 4%, the source of

free lime is mainly from the precipitation of lime in molten slag. Whereas, if the total free lime content is more than 4%, the total free lime mainly comes from the undissolved lime since the precipitated lime does not alter much with total free lime (Wachsmuth et al., 1981). The hydration of free lime in steel slag is mainly contributed by the hydration of residual/undissolved lime (Geiseler, 1996). Without access to water from fractures or pores, the pocket lime or the residual surrounded by steel slag (Figure 2-3), may not be able to hydrate. However, due to the grinding process, the residual lime can be exposed to water.

There are various tests to determine the free lime content in steelmaking slag, such as ethylene glycol extraction (Delimi et al., 1991; Javellana and Jawed, 1982; Kato et al., 2014; MacPherson and Forbrich, 1937), X-ray diffraction (Vaverka and Sakurai, 2014), and Cathodoluminescence method (Hiroki et al., 2019). The ethylene-glycol-extraction method is considered to be the easiest and the most common in industrial products because it takes relatively faster than other methods; Goto and Kakita (1955) reported that free lime in several kinds of slags was successfully determined in only 30 minutes. Kato et al., (2014) reported that occasionally the ethylene-glycol-extraction method cannot distinguish the different form of calcium, thus, they proposed an X-ray diffraction method for meticulous results.

2.3.2 Expansion behavior of steel slag

The act of adapting steel slag as aggregate, cementitious materials, or a heavyweight geomaterial can increase the rate of steel slag utilization; by delicately controlling its volume instability, it can be adapted in various civil engineering works.

The volume instability or expansion of steel slag is mainly caused by the hydration of both free lime and free magnesium in steel slag (Collins and Ciesielski, 1994). In contact with water, the free lime rapidly hydrates to cause large volume expansion over a short time (weeks), whereas free magnesia takes a relatively long period of time (years) to complete and therefore it causes a long-term expansion (Emery, 1974; Juckes, 2003). One study reported that the portion of expansion caused by free magnesia is very small compared to that of free lime (Sorlini et al., 2012), and yet it often causes cracks and volumetric since the hydration of free magnesia continuously takes place over several years. Some expansion of fragments can be accommodated by the porosity or cracks within the aggregate.

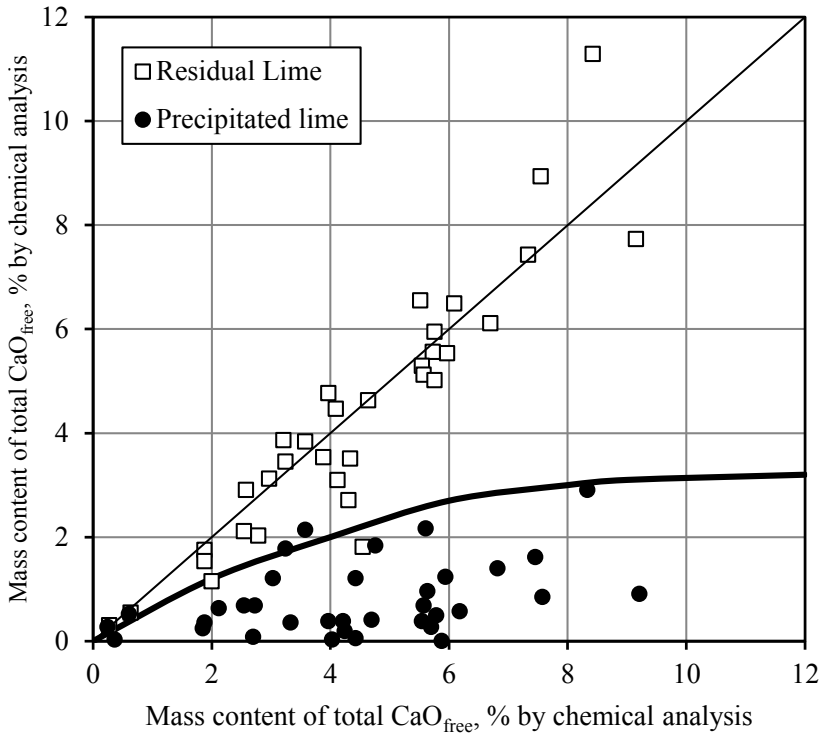

Figure 2- 2 Fractions of residual lime and precipitated lime as a function of total free lime (Wachsmuth et al., 1981)

Figure 2- 3 Free lime pocket inside a gravel-size steel slag aggregate (Yildirim and Prezzi, 2009).

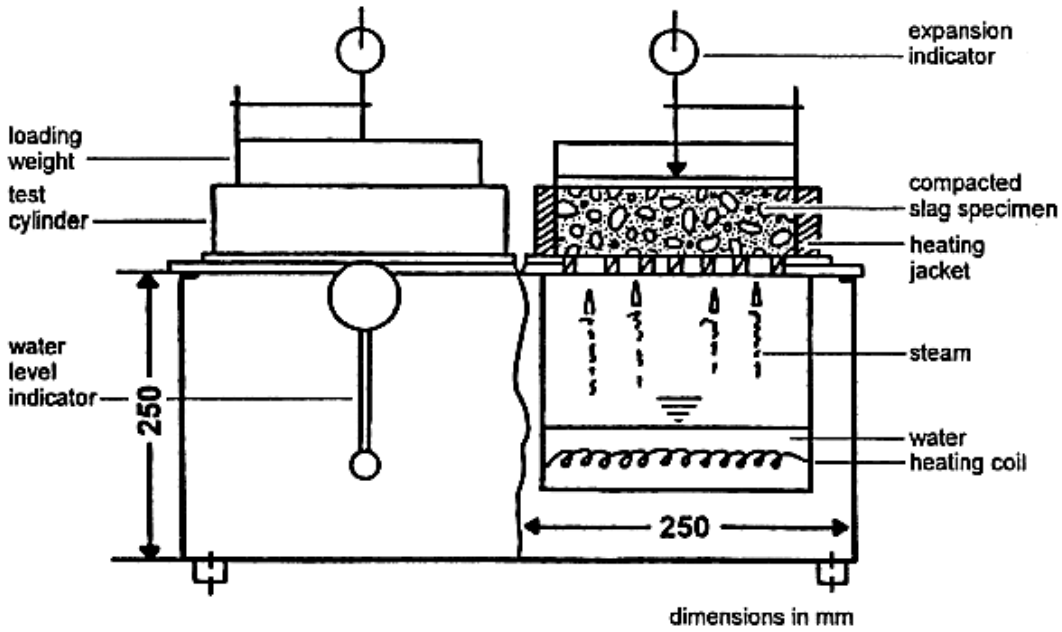

Figure 2- 4 Principle of the steam test of expansion (Motz and Geiseler, 2001).

As discussed by Juckes (2003), an assessment of the extent of any expansion that might occur over the years is a necessity if a steel slag is used as a bound or unbound aggregate. There are different ways to accelerate the hydration process so that the time-span of the expansion test will be much shorter: raising the temperature and the pressure (autoclave expansion test), cycle of temperature (JIS A 5015) immersion of sample in hot water (ASTM D4792; CR M Belgium), or exchange the water in liquid with water vapor (Motz and Geiseler, 2001; Ramachandran et al., 1964). To validate the chosen type of the expansion test, the results of the expansion test must be confirmed whether the test is revealing the same reaction and mechanism with the object of an application or not. He also added that the expansion value of aggregate, for instance, 5% in an expansion test does not mean a road containing this aggregate will eventually expand by a factor of 5%. It is possibly less, more or not expand at all, but the actual expansion will depend on such factors as grading, compaction, or any steps involved in road construction (Verhasselt and Choquet, 1989; Yildirim and Prezzi, 2009).

Wang et al. (2010) attempted to explain the expansion behavior of steel slag through the chemical and physical change of steel slag. Often the physical portion of volume change is underestimated or neglected. As previously described, the chemical part was mainly caused by the hydration of lime that caused a change of specific gravity; lime (CaO) which initially had a specific gravity of 3.34 transformed into

$Ca(OH)_2$ which had a 2.23 specific gravity. At the same amount of mass, the change of specific gravity caused the solid phase to expand; the volume change is 97.92% of the initial volume. Physically, when the lime hydrates, the increase in the solid phase simultaneously caused an increase of void volume. The portion of volume expansion by the increase by void volume is around 34.40% (assuming steel slag has a spherical form). Therefore the actual volume expansion is 97.92%+34.4%-4.54%= 127.78% of the initial volume. He further proposed an equation to predict the final volume of steel slag (E_s) expansion as follows:

$$E_S = 0.38.\gamma_s F \quad (1)$$

where γ_s is a constant for particular slag (g/cm^3) and F is free lime content of the slag.

2.4 Applications of steel slag

The recycling of slag is a strategic issue in countries with huge iron and steel manufacturing industries. Japan itself annually produced 30 million tons of slag, 8.3% of the total worldwide production 360 million tons (globalslag.com). Most steel slag generated in Japan is used as a raw material in cement industries (~66%), road base material (~12%), concrete aggregate (~7%), and raw material for fertilizer and other miscellaneous applications (~15%). Over 39 million tons of steel slag was produced in 2010 and 8% of it was dumped in disposal facilities (Horii et al., 2013). The significant number of unused steel slag that ends up in disposal site is not only uneconomical but also not environmentally friendly, thus an alternative and sustainable method to increase the recycling rate is necessary (JSCE, 2017; Oss, 2012).

2.4.1 Steel slag in road construction

A large body of research shows that the BOF slag can fulfill the demand of aggregate in road construction. Ahmedzade and Sengoz, (2009) studied the influence of steel slag on the mechanical properties and electrical conductivity of hot mix asphalt (HMA) mixtures. They reported that the steel slags as a road construction aggregate are able to produce a better resistance to permanent deformation and higher stiffness than limestone in hot mixed asphalt. Kandhal and Hoffman (1997) suggested that

steel slag can replace either fine or coarse aggregates and that encouraging a 100% replacement would cause over-asphalting and in-service traffic compaction, resulting in flushing. One study found that steel slag can be used in asphalt concrete mixes; 25% replacement of limestone with steel slag was found to be optimum that can improve the mechanical properties of asphalt concrete (Asi et al., 2007). Pasetto and Baldo (2010) reported that the use of slags allowed the very high performances of high modulus asphalt even with a low polymer concentration of bitumens. They further claimed that the used of two types of slags is feasible and can comply with the asphalt mix design criteria: good values of Marshall stability and Marshall quotient, and high workability. Xue et al. (2006) investigated the feasibility of steel slag usage in an express-highway construction. Figure 2-6 shows the comparison of different material and steel slag in compressive strength. It is found that with intense and various tests performed, a certain mix with a high-quality control of steel slag

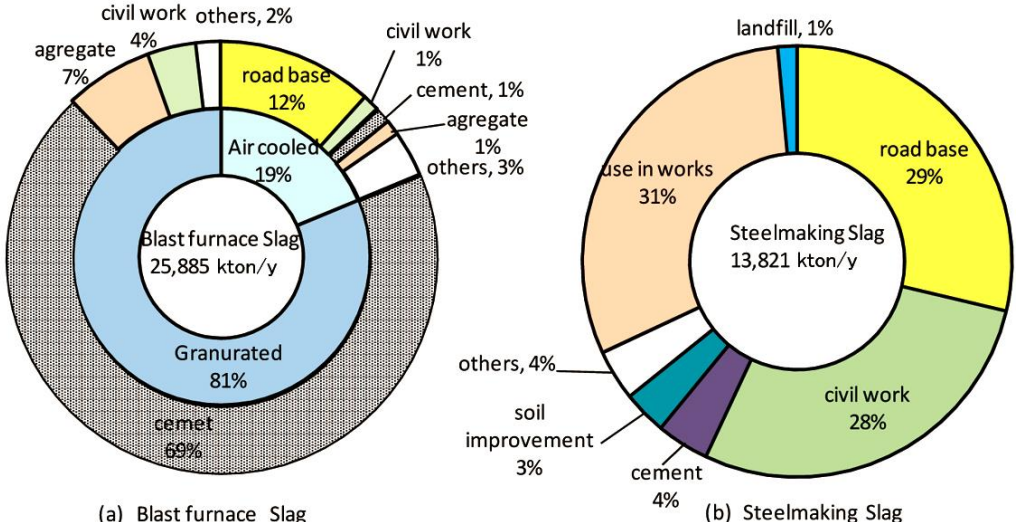

Figure 2- 5 Utilization of iron and steel slag in Japan in 2012

aggregate can be satisfactory in an express-highway construction.

Although steel slag can partially fulfill the demand of aggregate in road construction, studies above also indicate that steel slag cannot replace the role of limestone as a whole since steel slag may result in volumetric instability. There are limitations and strict technical criteria to use steel slag as aggregate in road construction. There is a trilogy of steel slag utilization: processing, testing and setting criteria (Wang, 2010). The expansion force and disruption test must be conducted to evaluate the expansive properties of steel slag aggregates prior to its utilization in

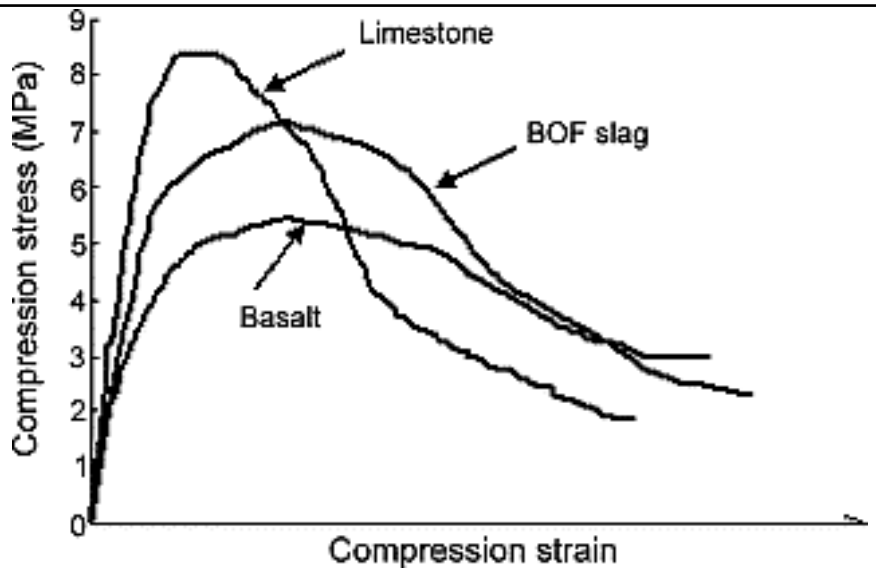

Figure 2- 6 Compressive strength of various common aggregate (Xue et al., 2006).

confined conditions. The autoclave disruption test is also necessary as an initial test to evaluate if the steel slag is suitable for confine matrices. It is imperative that slag must meet the special quality and design criteria. Often steel slag does not satisfy the criteria, thus, end up to be landfilled.

2.4.2 Steel slag in concrete structure

Steel slag is also comprehensively studied for its utilization in concrete fields. Maslehuddin et al (2003) compared the properties of steel slag and limestone in concrete mixtures. They reported that the physical properties of steel slag aggregates were superior to those of limestone; the unit weight of steel slag aggregate cement concrete was 17 % higher than that of crushed limestone. The compressive strength of steel slag aggregate was also reported higher than limestone. The initiation time of reinforcement corrosion and time to crack of the concrete specimen with steel slag aggregate was longer than the concrete with limestone. However, the replacement of steel slag as aggregate is limited to 50% to reduce the concrete weight.

One study found that steel slag beneficially affected the engineering properties of concrete mixtures (Abu-Eishah et al., 2012). Steel slag formed high crystalline mineralogy compounds which indicate low hydraulic reactivity and dimensional stability. With the steel slag addition, the ductility of concrete can be improved, and

the high strength can be achieved. They also indicate that the addition of other substances such as fly ash and silica fume can significantly improve the durability performance of steel slag concrete. Qasrawi et al., 2009 investigated the feasibility of unprocessed steel slag as fine aggregate in concrete. The studied steel slag had a low free lime and very low pozzolanic reaction. For sand replacement up to 30%, the compressive strength of concrete with fine steel slag was found to be increased 1.1-1.3 times of without steel slag. For 30%-50% sand replacement, the tensile strength of concrete increased 1.2-2.4 times of that without fine steel slag.

BOF slag has limited cementitious properties due to both a lack of tricalcium silicate (C_3S) and the presence of wustite solid solution (FeO) as the main mineral. There are several studies indicating that cementitious properties can be enhanced. Murphy et al. (1997) offered multiple ways of enhancing the cementitious product in steel slags such as FeO adjustment to Fe_2O_3 by an oxidation process and water quenching in the cooling process of steel slag. Montgomery and Wang (1991) reported the effect of adding instant-chilled slag (ICS) in concrete strength which gave greater indirect tensile and flexural strengths than those of corresponding control concrete containing limestone aggregate. Montgomery and Wang, (1991b) reviewed the feasibility of steel slag utilization in steel slag blended cement (SSBC). The studies results indicate that the steel slag exhibited a good hydraulic activity when blended with gypsum with or without ordinary portland cement (OPC). They further revealed that the OPC is necessarily added to stabilize the SSBC cement; a minimum 10% of OPC clinker and maximum 40% steel slag should be applied for a good stability concrete. Those concrete applications and treatments for enhancing the cementitious properties require additional procedures before steel slag could be fully utilized.

Studies have also been performed in knowing the possibility of adding steel slag in the raw meal of OPC clinker production. Although the utilization rate of BOF slag is not as high GBF slag, approximately 4% of total steel slag production in Japan was used in cement production (Horii et al., 2015). Tsakiridis et al. (2008) reported that the steel slag addition to an OPC production does not negatively affect the sintering and hydration process of OPC clinker production; the compressive strengths of OPC with steel slag were found to be at least as high as the OPC without steel slag. A specified steel slag, after various technical means, could overcome the low early strength and slow setting of steel slag cement (Dongxue et al., 1997). The pore

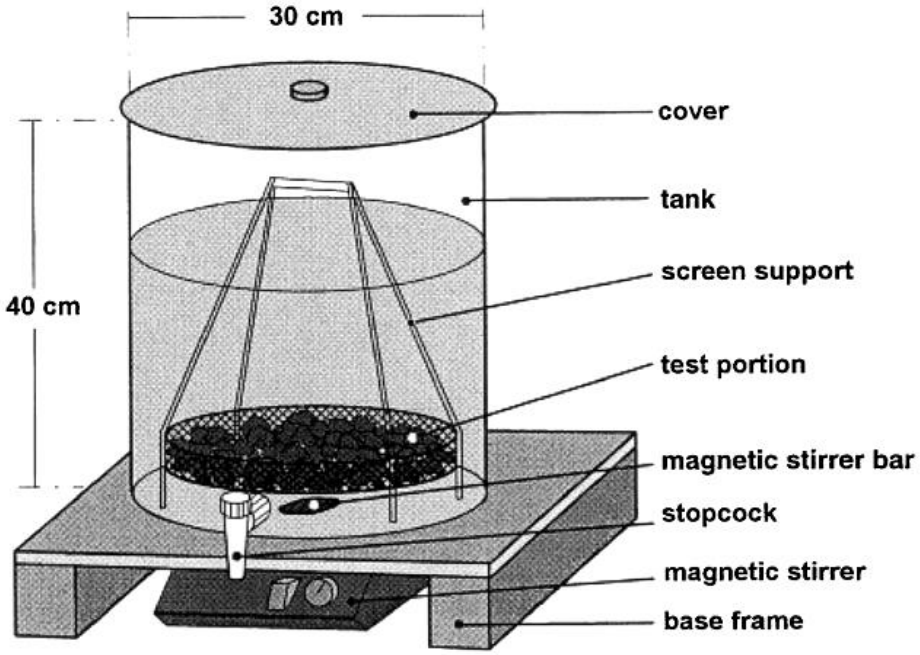

Figure 2- 7 Leaching Test Apparatus (Motz and Geiseler, 2001).

structure and strength of steel slag cement at 28 days are found to be similar to that of OPC, but the properties of steel slag cement are superior at later curing. The durability of steel slag cement is also better than OPC: better resistance to sulfate and carbonate and the reduction of alkali reaction.

2.5 BOF slag to environment

The use of steel slag for various purposes has been confirmed as safe for humans, and environmentally friendly. Proctor et al., 2000 showed BOF slag to be a non-hazardous material to human health and the environment by performing various tests: Analytical evaluation of minor metals, acidic and neural leaching test, and toxicity characteristic leaching procedure (TCLP) test. The tests were performed on various types of slags from different states in the U.S. Nevertheless, the avoidance of using various slag types and sources for a single purpose was suggested because it is easier to perform a risk assessment. There was potential for metals to leach from slag and migrate through the air because the larger particle size of steel slag would be exposed to weathering processes and become smaller particles. Such a phenomenon may only occur in an air-exposed application, but for other purposes such as fill, landscape, submerged fill and reducing the accessibility of slag for suspension, it will be sufficiently safe for the environment.

Motz and Geiseler (2001) also highlighted the non-hazardous potential from BOF slag for the environment because results from a leachate test showed no significant impact other than an increasing pH due to the partial solution of free lime. Using a leaching technique developed in Germany, leaching test of a hardened material such as steel slag can be successfully performed. Results showed that the chromium as a mineral compound could possibly be in higher amounts, but the concentrations in leachates are low since the chromiums are bound within stable crystalline phases. Also, other heavy metals are found very low and still under allowable criterion or not relevant under environmental aspects.

Table 2- 1 Comparison of the results of the TCLP slag leachage test to TCLP criteria (Proctor et al., 2000).

	TLCP screening criterion (mg/L)	90% UCL TCLP leachage of slag			Exceed criterion or not		
Metal		BF	BOF	EAF	BF	BOF	EAF
arsenic	5	0.0048	0.0054	0.011	no	no	no
barium	100	1.2	0.88	1.67	no	no	no
Cadmium	1	0.0054	0.01	0.037	no	no	no
Chromium (VI)	5	0.026	ND	0.018	no	no	no
Chromium (total)	5	0.22	0.04	1.0	no	no	no
lead	5	ND	0.015	0.063	no	no	no
mercury	0.2	ND	0.0005	0.00089	no	no	no
selenium	1	ND	ND	0.0073	no	no	no
silver	5	ND	0.029	0.027	no	no	no

ND= Not detected. The TCLP screening criteria was according to Method 1331 TCLP (Method 1311 TCLP, 1991).

2.6 Soil stabilization using steel slag

Despite having similar minerals and chemical compositions to that of OPC, the use of BOF slag in the area of soil stabilization has not been fully investigated and developed. A study conducted by Poh H. Y. et al. (2006) showed that BOF slag fines are able to improve the engineering properties of two types of soil in the U.K, English China clay and Mercia Mudstone. The study result indicated that the BOF slag fines addition (15%-20% by total dry mass) increased strength and durability, and reduced expansion of the two soils. For a better result, they recommend quicklime and sodium

metasilicate as an activator in soil stabilization using BOF slag fines. The main difference between the stabilization using BOF slag and OPC was that the predominant minerals in BOF slags fines were the slow hydrating and slow strength developing β-C_2S and the inert γ-C_2S while in OPC contained the fast hydrating minerals tricalcium silicate (C_3S).

2.6.1 Dredged-marine-clay stabilization using BOF slag

In Japan, comprehensive studies have been performed to allow the use of BOF slag in stabilizing dredged marine soils. The idea to simultaneously recycle both dredged marine soils and BOF slag in big scales are expected to produce a new geo-material for embankment constructions. Generally, the ultimate target is using the stabilized soils with BOF slag (SMSS) as an embankment fill where the high strength is not highly required. The most common addition rates used are 20% to 40% of the total solid volume.

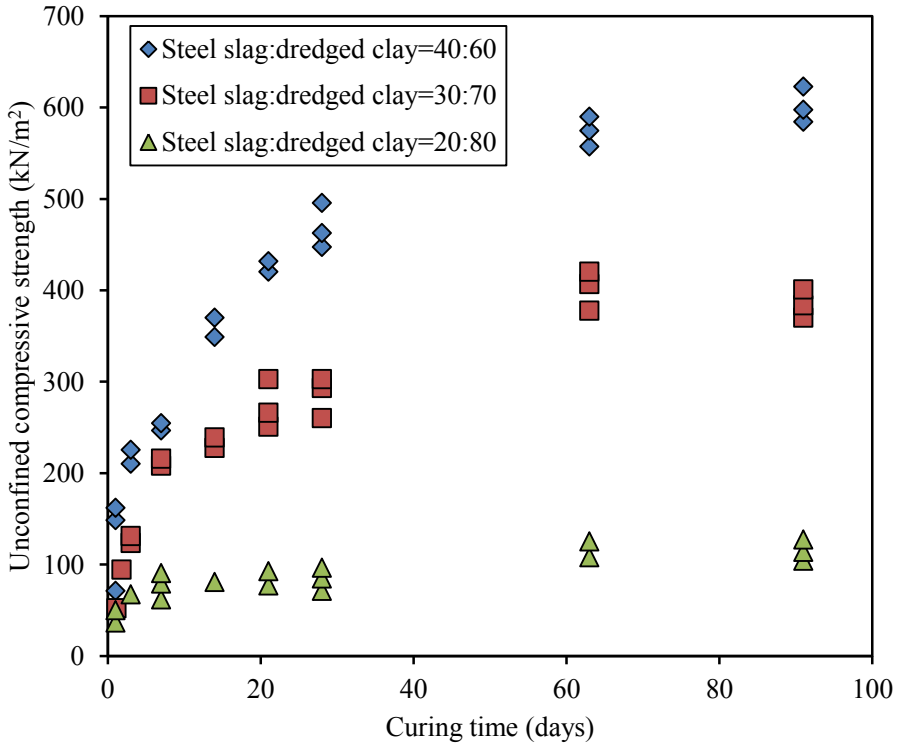

Figure 2- 8 Strength development of SMSS with various additions (Nagatome et al., 2008).

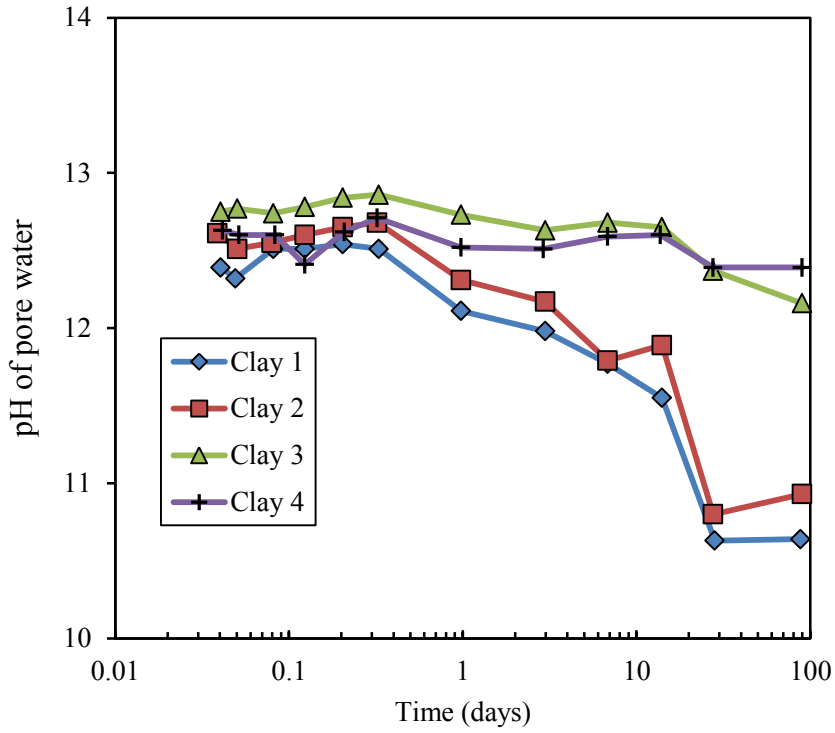

Figure 2- 9 pH variation of pore water around the SMSS with the elapsed time (Weerakoon et al., 2018)

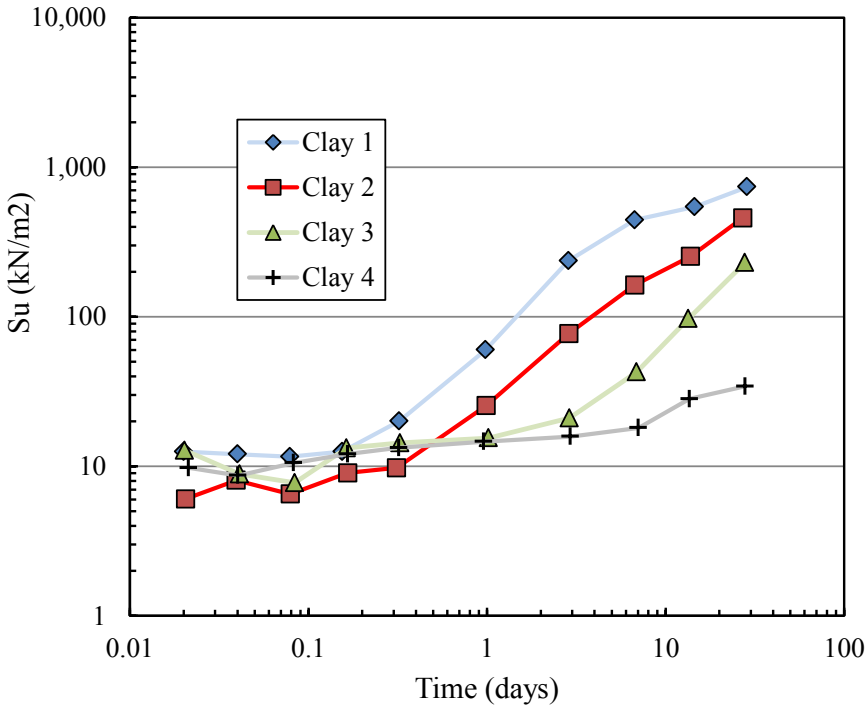

Figure 2- 10 Strength of SMSS with elapsed time.

Weerakoon et al. (2018) studied the feasibility of steel slag use in stabilizing various dredged soils in Japan. The studied dredged soils were taken from 4 different origins that varied from low to high plasticity clays. It is reported that the strength of SMSS developed significantly with time (Figure 2-9). There were significant decreases in pH of pore water from 12.8 to 10.6 with an elapsed time (Figure 21-0). The authors reported that the strength development of SMSS at the later stage was mainly affected by amorphous silica, of non-biogenic in particular. It is suggested that soils with low amorphous silica are hard to solidify and less affected by a BOF slag addition. It is also found that a correlation to predict the stiffness of stabilized dredged soils can be made based on its compressive strength.

2.6.2 Strength mobilization mechanism

The physical state of dredged marine drastically altered after mixing dredged marine clay with BOF slag (Figure 2-11). The dredged marine clay that once in the liquid state quickly change to a solid state with the addition of BOF slag. The air-dried steel slag absorbed the free water of dredged marine clay caused an instant decrease in the moisture content of dredged marine clay. It caused the soil mixture to rapidly gain significant strength.

The free lime content in BOF slag is considered to be potential to chemically improve the nature of dredged marine clay. As described above, when free lime meets water, it hydrates and produced Portlandite. Figure 2-12 shows the effect of different free lime content of BOF slag to the strength of the stabilized soils with BOF slag. It was reported that with the higher free lime content of the BOF slag, the higher strength of the stabilized soil. Another study studied the effect of aging of BOF slag in stabilizing soft soil. It is found that at the early stage of curing, both fresh and aged BOF slag could bring strength modification, however, at the later stage, the soils stabilization with aged BOF slag produced stagnant strength (Figure 2-13).

Shi (2004) reported that the presence of C_2S, C_4AF, and little C_3S in steel slag also endorsed the cementitious properties of steel slag. The existence of residual free lime produces portlandite ($Ca(OH)_2$) which can lead to a solidification of soft soils.

$$CaO + H_2O \rightarrow Ca(OH)_2 + heat \quad (2)$$

The additional water in soft soil is driven off through steam since the reaction produces heat. The hydration reaction substantially reduces the thickness of the

Figure 2- 11 Physical state of dredged marine soil before (left) and after (right) mixing with BOF slag (Yamagoshi et al., 2014a).

absorbed water layer, causing reduced susceptibility to water addition (Rogers and Roff, 1997). However, the hydration process of free lime in steel slag differs to that the burnt lime; the hydration speed of free lime in steel slag is relatively slower compared to that of burnt lime. This is due to the high calcining temperature (1700º C) involved in the furnace.

Later, the pozzolanic reaction occurs; the portlandite, silica, and alumina minerals from clay react to form calcium silicate hydrate (C-S-H) gel to further bind the soil skeleton together. The type of pozzolanic reaction owned by steel slag (Kiso et al., 2008) is expressed as follow:

$$Ca(OH)_2 + SiO_4 + nH_2O \rightarrow C\text{-}S\text{-}H \quad (3)$$

$$Ca^{2+} + AlO_2 + X^- + nH_2O \rightarrow Ca_4Al_2O_6X_2.nH_2O \quad (4)$$

Figure 2-5 shows the results of x-ray diffraction test on dredged marine clay and stabilized marine clay (Yamagoshi et al., 2014a). It further indicates the consumption of SiO_2 and AlO_2 minerals in dredged marine clay showed by the decrease in concentration due to the pozzolanic reaction.

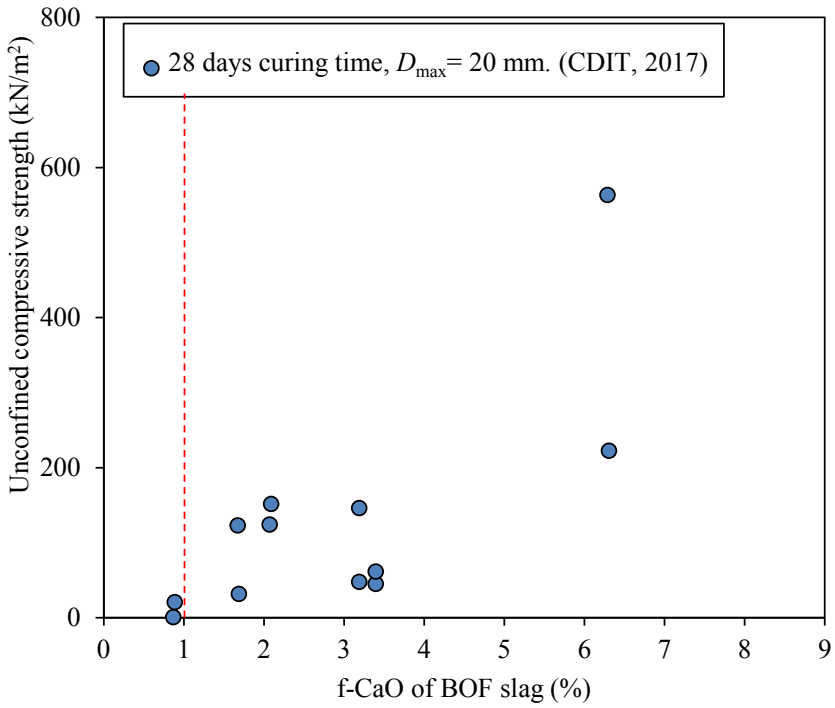

Figure 2- 12 Effect of different f-CaO content to the strength of stabilized soils with BOF slag.

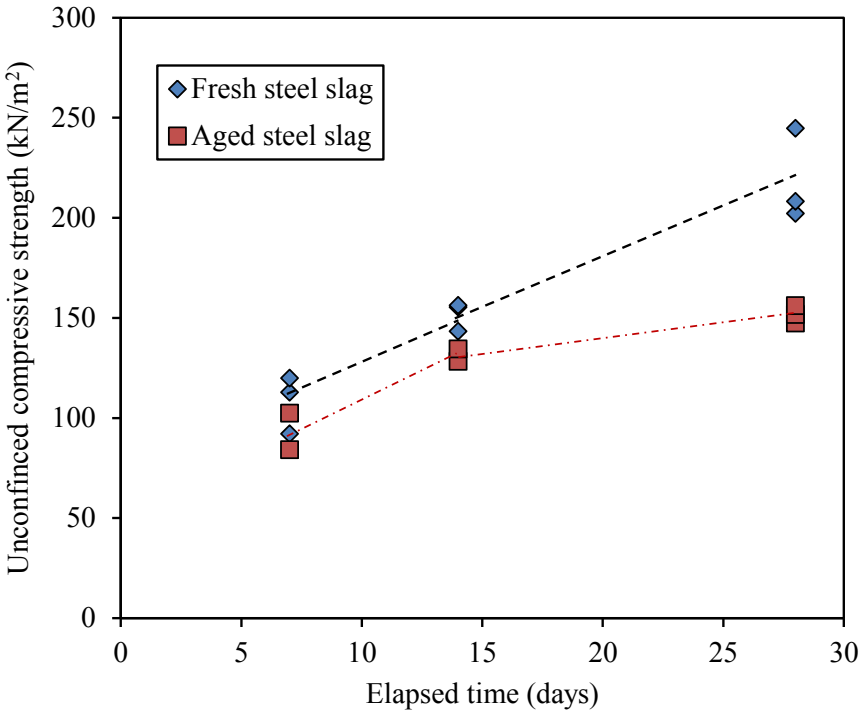

Figure 2- 13 Strength development of stabilized soils with fresh and aged BOF slag (Hirai et al., 2011).

Toda et al. (2018) reported that there are 3 key factors that affect the amount of C-S-H formation in the SMSS: (i) calcium ion supply from steel slag, (ii) pH of pore water surrounds the stabilized soil (iii) silica supply ions from soils. To form C-S-H, the dissolved Ca ions were mainly supplied by the portlandite in steel slag. There is a significant rise of pH in the stabilized soils with BOF slag; the dissolution of portlandite in BOF slag produces a hyper-alkaline condition in the water that will enhance the formation of C-S-H gel. They suggested that the amorphous silica of soils plays an important role in the strength-mobilization of the stabilized soils because the needed silica minerals in forming C-S-H mainly originate from the dissolution of amorphous silica.

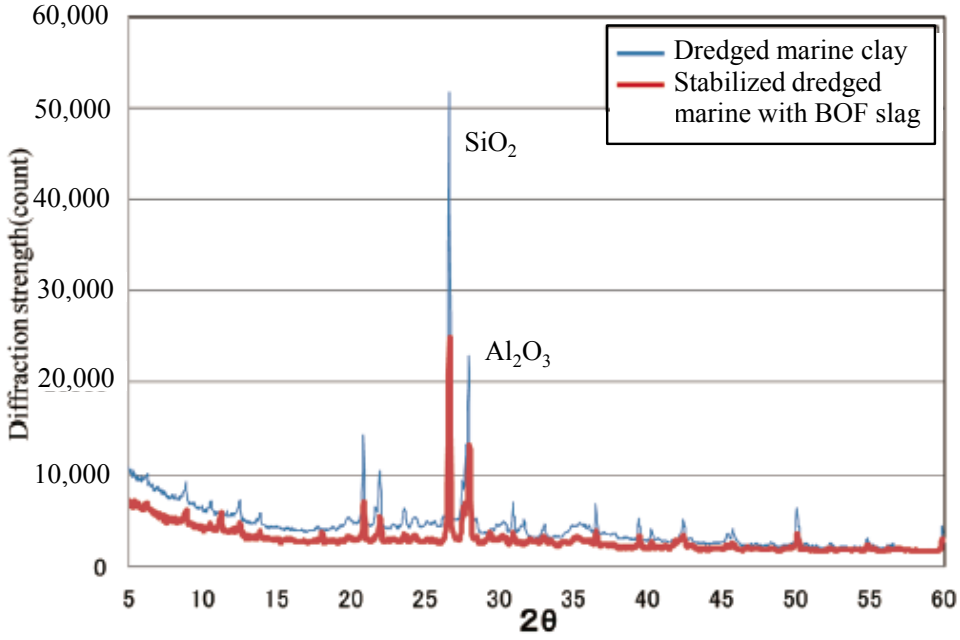

Figure 2- 14 Results of X-ray diffraction of dredged marine clay and SMSS (Yamagoshi et al., 2014a).

The addition of BOF slag to dredged soil can create hyper-alkaline pore water, however, the additional factor such as high content of organic in soils may affect the alkaline condition of the water (Kang et al., 2017; Tremblay et al., 2002). Often, dredged soils consist of a small amount of organic matter which affects the strength development of the SMSS. The effect may vary depending on the type of organic matters. The organic acids produce a pH lower than 9 in pore solution and bind with the dissolved Ca ions cause to limit the supply of Ca ion for the C-S-H formation. The organic/humic acid will further inhibit the crystal growth of calcite by forming

ligands with the calcite surface. The oil and non-miscible hydrocarbon type of organic content delay the hydration reaction by coating the cement particle.

Hirai et al. (2012) observed the strength mechanism of stabilized dredged marine soils with an electron probe micro-analyzer (EPMA) (Figure 2-6). The analysis using EPMA was performed to measure the distribution of substances concentrate in stabilized soils with BOF slag. Specimens were acquired from an actual fill of stabilized soils with BOF slag with cylindrical molds and divided into the lower and upper part. The lower part of each figure corresponds to the solidified part of the SMSS, and the upper part corresponds to the dredged soils. The high concentration of SiO_2, Al_2O_3, and CaO existed at the solidified part which is evidence of the existence of C-S-H formation in stabilized soils with BOF slag.

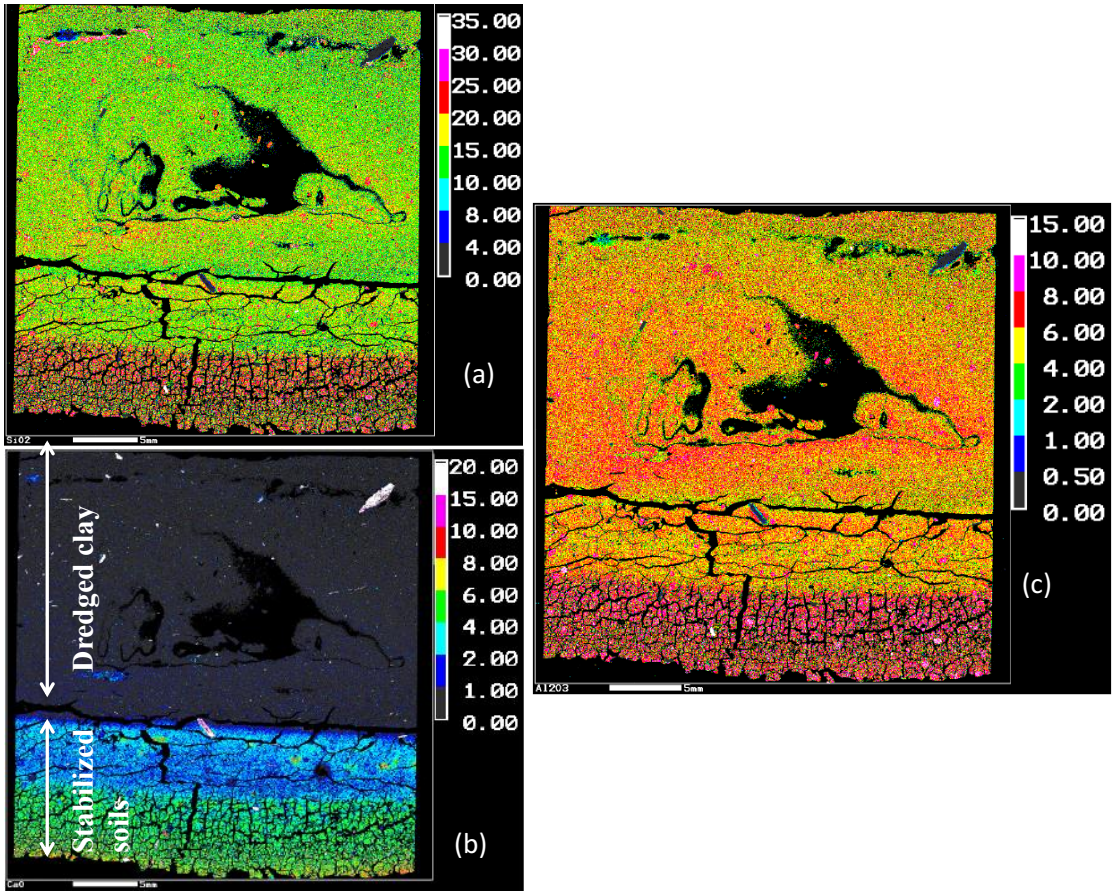

Figure 2- 15 EPMA test results of dredged clay and stabilized soils with BOF slag. a) concentration of SiO_2; b) concentration of CaO; c) concentration of Al_2O_3 (Hirai et al., 2012)

2.6.3 Field studies of Stabilized soils with BOF slag

For the last decade, various studies had been performed on the feasibility of stabilized soil with BOF slag as an embankment material. Yamada et al. (2013) investigated the feasibility of SMSS construction by performing a submerged model of stabilized soil with BOF slag above unimproved soft soil. The volumetric ratio of soils to BOF slag was 70 to 30. The authors reported that the slope gradient was 1:2.5 to 1:3 with specimen height 30 cm (Figure 2-16). Without any temporary support structure, the minimum slope gradient needed in actual construction is 1:2, thus, from these results, it can be said that the stabilized soil with BOF slag is satisfactory to the criteria. Honda et al. (2016) conducted multiple centrifuge tests to represent the actual construction of artificial tideland. The stabilized soil with BOF slag was used as a counterweight. It is verified that the stabilized soil with BOF slag is capable to exhibit high residual strength; under a load of 1.5 times of its compressive strength, there was no major deformation occurred. It was after a load of 2 times of its compressive strength, large deformations and subsidence occurred.

One study investigated the feasibility of reclamation of the stabilized soils with BOF slag using pipe-mixing method (Yamagoshi et al., 2014b). The authors reported that as general, the pipe-mixing method used for cement can be applied for BOF slag. The stabilized soils exhibited decent compressive strength, 60-140 kN/m^2 at 28-days curing. The consolidation settlement of the stabilized soil with BOF slag took a shorter time compared to that of sand. Another study conducted by Tanaka et al. (2014) investigated the feasibility of embankment construction made of the stabilized soils with BOF slag using both a free-fall fill method and a pipe-mixing fill method. It is reported that the pipe-mixing method could mix with 4000m3 per day. However, there was a significant decrease in the strength of SMSS since additional water is needed in the pipe-transportation system. It is also reported that the field strength investigation can be conducted using the cone penetration test (CPT) test.

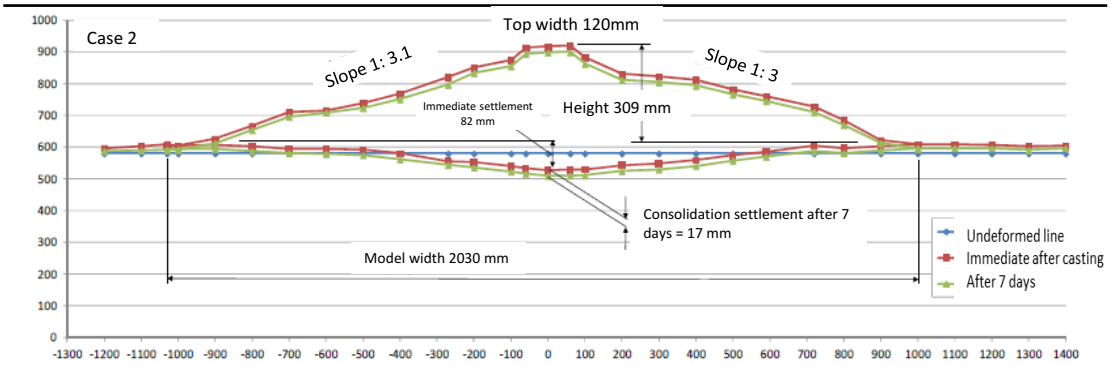

Figure 2- 16 A small-scale model of embankment using the stabilized soil with BOF slag.

Figure 2- 17 Reclamation of stabilized soils with BOF slag using the pipe-mixing

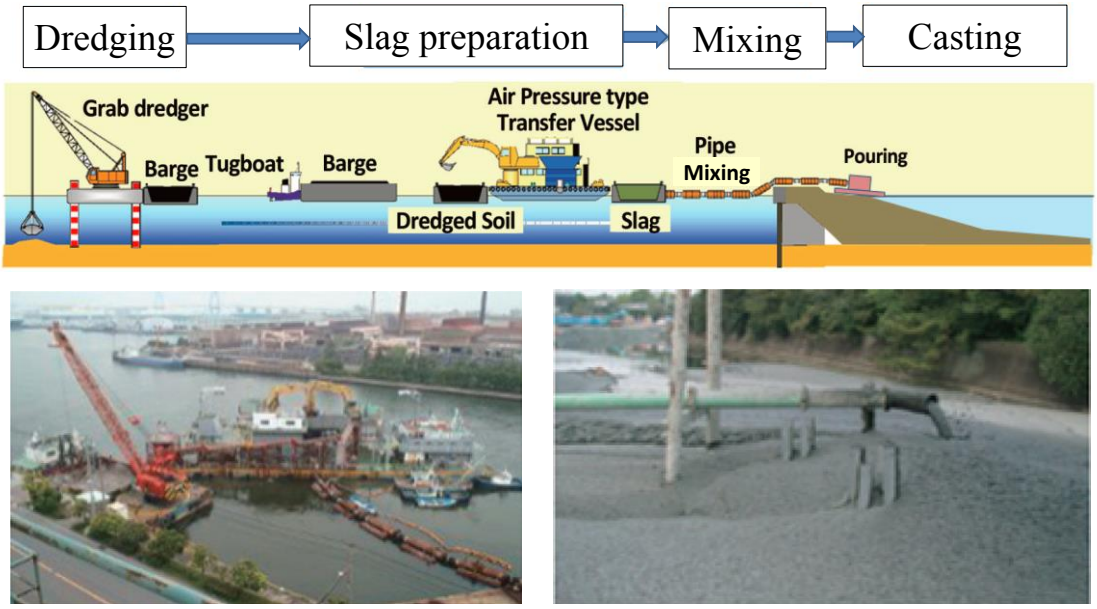

method (Yamagoshi et al., 2014b).

2.7 References

Abu-Eishah, S.I., El-Dieb, A.S., and Bedir, M.S. (2012). Performance of concrete mixtures made with electric arc furnace (EAF) steel slag aggregate produced in the Arabian Gulf region. Construction and Building Materials *34*, 249–256.

Ahmedzade, P., and Sengoz, B. (2009). Evaluation of steel slag coarse aggregate in hot mix asphalt concrete. J. Hazard. Mater. *165*, 300–305.

Amu, O.O., Fajobi, A.B., and Afekhuai, S.O. (2005). Stabilizing Potential of Cement and Fly Ash Mixture on Expansive Clay Soil. Journal of Applied Sciences *5*, 1669–1673.

Asi, I.M., Qasrawi, H.Y., and Shalabi, F.I. (2007). Use of steel slag aggregate in asphalt concrete mixes. Can. J. Civ. Eng. *34*, 902–911.

Bartos, M.J. (1977a). Classification and Engineering Properties of Dredged Material. (ARMY ENGINEER WATERWAYS EXPERIMENT STATION VICKSBURG MISS).

Bartos, M.J. (1977b). Use of Dredged Material in Solid Waste Management. (ARMY ENGINEER WATERWAYS EXPERIMENT STATION VICKSBURG MISS).

Brandt, D.A., and Warner, J.C. (Jairus C.) (1999). Metallurgy fundamentals (Tinley Park, Ill. : Goodheart-Willcox).

Chiu, C.F., Zhu, W., and Zhang, C.L. (2009). Yielding and shear behaviour of cement-treated dredged materials. Engineering Geology *103*, 1–12.

Collins, R.J., and Ciesielski, S.K. (1994). RECYCLING AND USE OF WASTE MATERIALS AND BY-PRODUCTS IN HIGHWAY CONSTRUCTION. NCHRP Synthesis of Highway Practice.

Delimi, R., Ghorab, M.F., Chtcherbakov, V., and Messadi, D. (1991). Physico-Chemical Studies of the CaO-Ethylene Glycol System. Determination of free lime in industrial products. Journal Für Praktische Chemie *333*, 593–600.

Dongxue, L., Xinhua, F., Xuequan, W., and Mingshu, T. (1997). DURABILITY STUDY OF STEEL SLAG CEMENT. Cement and Concrete Research *27*, 983–987.

Federico, A., Vitone, C., and Murianni, A. (2015). On the mechanical behaviour of dredged submarine clayey sediments stabilized with lime or cement. Can. Geotech. J. *52*, 2030–2040.

Geiseler, J. (1996). Use of steelworks slag in Europe. Waste Management *16*, 59–63.

Goto, H., and Kakita, Y. (1955). Determination of Free Lime in Slag. Science Reports of Research Institute, Tohoku University. Ser. A, Physisc, Chemistry and Metallurgy *7*, 135–139.

Hirai, S., Mizutani, T., Kikuchi, Y., Nakashima, S., and Iguchi, K. (2011). Study on effect of mixing condition on strength of mixture of dredged soil and steel slag. The 9th Environtmental and Geotechnical Symposium 103–110.

Hirai, S., Mizutani, T., Kikuchi, Y., and Kawabata, Y. (2012). Study on the Efffect of Mixing Condition on Mechanical properties of Mixture of dredged Soil and Steel Slag (Report of The Port and Airport Research Institute).

Hiroki, T., Susumu, I., and Kazuaki, wagatsuma (2019). Detection of free-lime in steelmaking slag by Cathodoluminescence Method. 鉄と鋼 *105*, 522–529.

Honda, H., Tsuchida, T., Tanishiki, K., Hayashi, M., Yamada, K., Kumagai, T., Yanagihashi, T., and Makino, T. (2016). Development if the artificial tide land using improved dredged soil by the steelmaking slag. Japanese Society of civil engineering B3 *72*, I_443-I_448.

Horii, K., Kitano, Y., Tsutsumi, N., and Kato, T. (2013). Processing and Reusing Technologies for Steelmaking Slag. 123–129.

Horii, K., Kato, T., Sugahara, K., Tsutsumi, N., and Kitano, Y. (2015). Overview of Iron/Steel Slag Application and Development of New Utilization Technologies. Nippon Steel and Sumitomo Metal Technical Bulletin *109*, 5–11.

Ingles, O.G., and Metcalf, J.B. (1972). SOIL STABILIZATION PRINCIPLES AND PRACTICE. *11*.

Inoue, R., and Suito, H. (1995). Hydration of Crystallized Lime in BOF Slags. ISIJ International *35*, 272–279.

Javellana, M.P., and Jawed, I. (1982). Extraction of free lime in portland cement and clinker by ethylene glycol. Cement and Concrete Research *12*, 399–403.

JSCE (2017). Technical manual steelmaking slag treated soil for harbor, airport, and coastal construction projects (Japan society of civil engineering).

Juckes, L.M. (2003). The volume stability of modern steelmaking slags. Mineral Processing and Extractive Metallurgy *112*, 177–197.

Kandhal, P., and Hoffman, G. (1997). Evaluation of Steel Slag Fine Aggregate in Hot-Mix Asphalt Mixtures. Transportation Research Record: Journal of the Transportation Research Board *1583*, 28–36.

Kang, G., Tsuchida, T., and Athapaththu, A.M.R.G. (2015). Strength mobilization of cement-treated dredged clay during the early stages of curing. Soils and Foundations *55*, 375–392.

Kang, G., Tsuchida Takashi, Kim Young-sang, and Baek Won-jin (2017). Influence of Humic Acid on the Strength Behavior of Cement-Treated Clay during Various Curing Stages. Journal of Materials in Civil Engineering *29*, 04017057.

Kato, M., Hari, T., Saito, S., and Shibukawa, M. (2014). Determination of Free Lime in Steelmaking Slags by Use of Ethylene Glycol Extraction/ICP-AES and Thermogravimetry. Tetsu-to-Hagane *100*, 340–345.

MacPherson, D.R., and Forbrich, L.R. (1937). Determination of Uncombined Lime in Portland Cement: The Ethylene Glycol Method. Ind. Eng. Chem. Anal. Ed. *9*, 451–453.

Maslehuddin, M., Sharif, A.M., Shameem, M., Ibrahim, M., and Barry, M.S. (2003). Comparison of properties of steel slag and crushed limestone aggregate concretes. Construction and Building Materials *17*, 105–112.

Method 1311 TCLP (1991). METHOD 1311TOXICITY CHARACTERISTIC LEACHING PROCEDURE.

Montgomery, D.G., and Wang, G. (1991a). Instant-chilled steel slag aggregate in concrete - strength related properties. Cement and Concrete Research *21*, 1083–1091.

Montgomery, D.G., and Wang, G. (1991b). Preliminary laboratory study of steel slag for blended cement manufacture. Materials Forum Journal *15*, 374–382.

Motz, H., and Geiseler, J. (2001). Products of steel slags an opportunity to save natural resources. Waste Manag *21*, 285–293.

Murphy, J.N., Meadowcroft, T.R., and Barr, P.V. (1997). Enhancement of the cementitious properties of steelmaking slag. Canadian Metallurgical Quarterly *36*, 315–331.

Nagatome, T., Gomyo, M., Nozaki, I., Takeda, M., Kiso, E., and Tsuji, M. (2008). Effect of strength improvement of dredged soil with converter slag. The 43rd Geotechnical Engineering Conference (Hiroshima) 539–540.

Oss, H.G. van (2012). Slag-iron and steel, annual review 2006. 2012 Mineral Industry Surveys, U.S Geological Survey, Reston, VA.

Paria, S., and Yuet, P.K. (2006). Solidification–stabilization of organic and inorganic contaminants using portland cement: a literature review. Environ. Rev. *14*, 217–255.

Pasetto, M., and Baldo, N. (2010). Experimental evaluation of high performance base course and road base asphalt concrete with electric arc furnace steel slags. J. Hazard. Mater. *181*, 938–948.

Poh H. Y., Ghataora Gurmel S., and Ghazireh Nizar (2006). Soil Stabilization Using Basic Oxygen Steel Slag Fines. Journal of Materials in Civil Engineering *18*, 229–240.

Proctor, D.M., Fehling, K.A., Shay, E.C., Wittenborn, J.L., Green, J.J., Avent, C., Bigham, R.D., Connolly, M., Lee, B., Shepker, T.O., et al. (2000). Physical and Chemical Characteristics of Blast Furnace, Basic Oxygen Furnace, and Electric Arc Furnace Steel Industry Slags. Environ. Sci. Technol. *34*, 1576–1582.

Qasrawi, H., Shalabi, F., and Asi, I. (2009). Use of low CaO unprocessed steel slag in concrete as fine aggregate. Construction and Building Materials *23*, 1118–1125.

Ramachandran, V.S., Sereda, P.J., and Feldman, R.F. (1964). Mechanism of Hydration of Calcium Oxide. Nature *201*, 288.

Rogers, C.D.F., and Roff, T.E.J. (1997). Lime modification of clay soils for construction expediency. Proceedings of the Institution of Civil Engineers - Geotechnical Engineering *125*, 242–249.

Sasanian, S., and Newson, T.A. (2014). Basic parameters governing the behaviour of cement-treated clays. Soils and Foundations *54*, 209–224.

Shi, C. (2004). Steel Slag—Its Production, Processing, Characteristics, and Cementitious Properties. Journal of Materials in Civil Engineering *16*, 230–236.

Sorlini, S., Sanzeni, A., and Rondi, L. (2012). Reuse of steel slag in bituminous paving mixtures. J. Hazard. Mater. *209–210*, 84–91.

Tanaka, Y., Ko, C., Imamura, T., Shibuya, T., Yamagoshi, Y., Akashi, Y., Kitano, Y., and Kanno, H. (2014). Reclamation of the artificial ground made of dredged soil and converter slag. Japanese Society of Civil Engineering B3 *70*, I_888-I_893.

Tang, Y.X., Miyazaki, Y., and Tsuchida, T. (2001). Practice of Reused Dredgings by Cement Treatment. Soils and Foundations *41*, 129–143.

Terashi, M., and Katagiri, M. (2005). Key issues in the application of vertical drains to sea reclamation by extremely soft clay slurry. Elsevier Geo-Engineering Book Series *3*, 119–143.

Toda, K., Sato, H., Weerakoon, N., Otake, T., Nishimura, S., and Sato, T. (2018). Key Factors Affecting Strength Development of Steel Slag-Dredged Soil Mixtures. Minerals *8*, 174.

Tremblay, H., Duchesne, J., Locat, J., and Leroueil, S. (2002). Influence of the nature of organic compounds on fine soil stabilization with cement. Can. Geotech. J. *39*, 535–546.

Tsakiridis, P.E., Papadimitriou, G.D., Tsivilis, S., and Koroneos, C. (2008). Utilization of steel slag for Portland cement clinker production. Journal of Hazardous Materials *152*, 805–811.

Vakili, A.H., Selamat, M.R., and Moayedi, H. (2013). Effects of Using Pozzolan and Portland Cement in the Treatment of Dispersive Clay. ScientificWorldJournal *2013*.

Van Leussen, W., and Nieuwenhuis, J.D. (1984). Soil mechanics aspects of dredging. Géotechnique *34*, 359–381.

Vaverka, J., and Sakurai, K. (2014). Quantitative Determination of Free Lime Amount in Steelmaking Slag by X-ray Diffraction. ISIJ International *54*, 1334–1337.

Verhasselt, A., and Choquet, F. (1989). 24 - Steel slags as unbound aggregate in road construction: problems and recommendations. In Unbound Aggregates in Roads, R.H. Jones, and A.R. Dawson, eds. (Butterworth-Heinemann), pp. 204–211.

Wachsmuth, F., Geiseler, J., Fix, W., Koch, K., and Schwerdtfeger, K. (1981). Contribution to the Structure of BOF-Slags and its Influence on Their Volume Stability. Canadian Metallurgical Quarterly *20*, 279–284.

Wang, G. (2010). Determination of the expansion force of coarse steel slag aggregate. Construction and Building Materials *24*, 1961–1966.

Wang, G., Wang, Y., and Gao, Z. (2010). Use of steel slag as a granular material: volume expansion prediction and usability criteria. J. Hazard. Mater. *184*, 555–560.

Wang, J., Ni, J., Cai, Y., Fu, H., and Wang, P. (2017). Combination of vacuum preloading and lime treatment for improvement of dredged fill. Engineering Geology *227*, 149–158.

Weerakoon, N.R., Nishimura, S., Sato, H., Toda, K., Sato, T., and Arai, Y. (2018). Stiffness and strength mobilisation in steel-slag-mixed dredged clays in early curing. Proceedings of the Institution of Civil Engineers - Ground Improvement 1–17.

de Wit, P. (2005). Optimising maintenance dredging. In 2nd International Conference on Maintenance Dredging, (Thomas Telford Publishing), pp. 65–71.

Xue, Y., Wu, S., Hou, H., and Zha, J. (2006). Experimental investigation of basic oxygen furnace slag used as aggregate in asphalt mixture. J Hazard Mater *138*, 261–268.

Yamada, K., Tsuji, T., Watabe, Y., Mizutani, T., Morikawa, Y., and Ukai, A. (2013). Experiment and examination about submerged mound made of mixture of dredged soil and converter slag on the soft ground. Japanese Society of civil engineering B3 *69*, I_1048-I_1053.

Yamagoshi, Y., Akashi, Y., Kitano, Y., Kiso, E., Kosugi, C., Miki, O., Nakagawa, M., and Hata, K. (2014a). Basic Characteristic of CaO-improved soil. Nippon Steel and Sumitomo Metal Technical Bulletin *No. 399*, 51–58.

Yamagoshi, Y., Akashi, Y., Kanno, H., Nobuhiro, T., and Tanaka, Y. (2014b). Reclamation by CaO improved soil. Nippon Steel and Sumitomo Metal Technical Bulletin *399*, 65–72.

Yildirim, I., and Prezzi, M. (2009). Use of Steel Slag in Subgrade Applications. JTRP Technical Reports.

Yildirim, I.Z., and Prezzi, M. (2011). Chemical, Mineralogical, and Morphological Properties of Steel Slag.

(2012). Ground Improvement (Boca Raton: CRC Press).

Coastal Development Institute of Technology (CDIT). 2015. Technical Manual of Dredged soil and Converter slag for Port, Airport, and Coast Facilities. Appendix 2. Influence factor on the strength of dredged soil and converter slag.

Emery, J.J. (1974). A simple test procedure for evaluating the potential expansion of steel slag. Proc. Of the 1974 Annual Conference, Roads and Transportation Association of Canada, Toronto, Ontario, 90-103.

Kiso, E., Tsujii, M., Ito, K., Nakagawa, M., Gomyo, M., Nagatome, T. 2008. Method of dredged soil improvement by mixing with converter steel-making slag. Kaiyo Kaihatsu Ronbunshu 2008, 24, p 327-332. (In Japanese).

Nippon Slag Association (NSA). 2010. Environmental Materials, Iron and Steel Slag.

Japanese standards association: 'Iron and steel slag for road construction (English translation)', JIS A 5015, 1992, Tokyo, Japanese Standard Association.

Chapter 3

Strength Development and Microstructural Characteristics of Soft Dredged Clay with Basic Oxygen Furnace Steel Slag

TABLE OF CONTENTS

3.1 Introduction

In maintaining ports and securing navigable waterways, a large amount of soft clayey soils at the sea bottom is dredged annually. As certain difficulties and economic issues exist in securing suitable disposal sites for dredged deposits, alternative green and economical approaches for recycling and applying dredged clay have become a major research topic. In general, dredged soil exhibits extremely low shear strength, high fine content, high compressibility, and a natural water content that is commonly higher than its liquid limit (Kitazume and Terashi, 2013). As a result, dredged clayey soils may not be able to be used as raw materials without any special treatment. Dredged clays stabilized with binders such as ordinary Portland cement and lime have been studied extensively studied and implemented as construction materials, filling and reclamation materials, artificial barrier layers, and submerged embankments in ports and airport areas (Tang et al., 2001; Tsuchida et al., 2007; Watabe and Noguchi, 2011).

Steel slag is a by-product material generated during steelmaking and refining operations in the steel manufacturing process. Steel slags can be classified into two types, namely basic oxygen furnace (BOF) slag and electric arc furnace (EFA) slag. Previous studies have demonstrated that steel slag exhibits superior engineering characteristics, such as a high friction angle, low water absorption, high stiffness, abrasion resistance, and high compactibility. These properties are the main reason for its extensive utilization in road construction, ground improvement (sand compaction pile methods), and asphalt mixtures as aggregate materials (Asi, 2007; Xue et al., 2006). However, it is well known that the steel slag contains inactive materials referred to as free-CaO and free-MaO, which can hydrate and nearly double their volume through hydration, and their expansion potential with time causes slag cracking (Shen et al., 2009a; Horii et al., 2013). An aging treatment process is subsequently required to prevent volume expansion prior to utilization as aggregate materials.

BOF consists of dicalcium silicate (C_2S), the rhombohedral to orthorhombic (R-O) phase (solid solution of CaO, FeO, MgO, and MnO), tricalcium silicate (C_3S), tetracalcium aluminoferrite (C4AF), dicalcium ferrite (C2F), free-lime (f-CaO), olivine, and merwinite, and its chemical and mineralogy properties are similar to

those of Portland cement (Mahieux et al., 2009; Belhadj et al., 2012; Qiang et al., 2016; Deng et al., 2017). BOF has been referred to as a weak Portland cement, owing to its low C_3S and C_2S contents (Lee 1974; Shi and Qian, 2000; Poh et al., 2006). According to the BOF mineral components, it can be used as a stabilizer with or without an activator to solidify soils instead of other binders, as well as an aggregate in civil engineering works. Recently, in Japan, dredged clayey soils stabilized with BOF have been used as various geo-materials requiring relatively low strength, such as the filling material in quay walls, submerged embankments, and breakwater (Guidebook for Oceanographic Application of Converter Slag, 2008). Moreover, the environmental impact was confirmed, in order to successfully reuse BOF as a soil stabilizer and filling material. The safety assessment for environmental impact was divided into two categories; 1) safety against harmful substances, such as heavy metals and toxic substances, and 2) safety against pH value. The safety evaluation for harmful substances was conducted following the Act on the Prevention of Marine Pollution and Marine Accidents in Japan. The pH effect of environmental safety was determined by means of a test method for the pH of suspended soils (JGS 0211, 2009), whereby the pH value was monitored on the site and compared to the results of laboratory experiments. According to the results, the BOF-treated dredged clay met all of the criteria for stability against environmental impact, and also reaffirmed the environmental impact stability by means of monitoring and testing in the actual field (Guidebook for Oceanographic Application of Converter Slag, 2008). This application method may provide an environmentally friendly manner of recycling dredged clayey soils as construction materials, and expanding the use of steel slag as a binder on behalf of cement that emits anthropogenic CO_2. Over the past several decades, the majority of the research regarding steel slag has focused on road base course material (Shen et al., 2009b), ground improvement material (Takahashi et al., 2011; Kinoshita et al., 2012), aggregates in asphalt mixtures (Ahmedzade and Sengoz, 2009; Pasetto and Baldo, 2010), concrete aggregates (Arribas et al., 2014; Rondi et al., 2016), and cement additives (Liu et al., 2014; Qiang et al., 2016). Based on the literature review, the study of BOF commonly focuses on its applicability as an aggregate material in diverse fields. Consequently, studies investigating the utilization of BOF for soft dredged clay stabilization are very scares in countries other than Japan (Poh et al., 2006; Deng et al., 2017). Furthermore, the mechanism of the

strength mobilization of dredged clay treated with BOF over the curing time immediately following mixing has also not yet been clarified.

The main objective of this study is to investigate the strength development of dredged clay stabilized by BOF at various curing times in order for it to be used as a geo-material in geotechnical applications, while considering its microstructural and mineralogical properties. In order to evaluate the stabilized dredged clay strength development, a series of laboratory vane shear (LVS) and unconfined compression (UC) tests were carried out on specimens prepared with different BOF contents, as well as the water content at various curing times immediately following mixing, ranging from 0.5 h to 90 d. Moreover, the microstructural properties of the dredged clay stabilized by BOF were analyzed by means of a scanning electron microscope (SEM) and energy dispersive spectroscopy (EDS) analysis.

.

3.2 Experimental program

3.2.1 Material

Marine clay dredged at the Tokuyama Port, Yamaguchi prefecture, Japan, was used as the base clay in this experiment. The geotechnical properties of the dredged marine clay are summarized in Table 1. The liquid and plastic limits were 107.15% and 38.64%, respectively. This soil exhibits a high plasticity, with a plastic index of 68.50%. The ignition loss was 8.17%, while the specific gravity was 2.65. The marine dredged clay was composed of 9.98% coarse-grained soils (> 75 μm) and 90.02% fine-grained soils (< 2 μm). Based on the Unified Soil Classification System (USCS), the dredged clay used in this study was classified as an inorganic clay of high plasticity, or organic clay of medium to high plasticity (CH-OH).

The BOF used in this experiment was a product of the Fukuyama steel plant of the JFE Steel Corporation, and its physical properties are listed in Table 2. The BOF particle sizes were less than 5 mm, and the BOF contained a 6.48% moisture content of its air-dried mass. The saturated surface and absolute dry densities of the BOF were 3.15 and 3.02, respectively, while the water absorption rate was 4.18%. The BOF free-CaO content was determined to dissolve an ethylene glycol among CaO using phenol extraction and atomic absorption analysis, and its value was 4.27%. The

particle-size distribution curves for the Tokuyama dredged clay and BOF are plotted together in Fig. 3-1.

The chemical composition percentages of the BOF obtained by X-ray fluorescence analysis and comparisons with the chemical composition ranges for different BOF types obtained from the literature are provided in Table 3. In the BOF used in this study, calcium, iron, and silicon oxides accounted for more than 87%, and the chemical composition ranges were very similar to those of the literature (Shi, 2004; Belhadj et al., 2012). Furthermore, Belhadj et al. (2012) reported that the BOF composition agrees with that of clinker, except for the high iron content. However, it should be noted that the BOF composition is highly variable depending on the raw materials, steel type, manufacturing process, and furnace conditions, among others.

Table 3- 1 Physical properties of dredged clay at Tokuyama Port

Property	Value
Liquid limit, w_{LL} (%)	107.15
Plastic limit, w_{PL} (%)	38.64
Plasticity index, w_{PI} (%)	68.50
Ignition loss, L_i (%)	8.17
Specific gravity, G_s (g/cm^3)	2.65
Coarse-grained soil (%)	9.98
Fine-grained soil (%)	90.02
Unified Soil Classification System (USCS)	CH-OH
pH	7.2

Table 3- 2 Basic properties of BOF slag

Property	Value
Saturated surface-dry density (g/cm^3)	3.15
Absolute dry density (g/cm^3)	3.02
Water absorption rate (%)	4.18
Initial water content (%)	6.48
Particle size (mm)	Less than 5 mm
Coarse-grained soil (%)	99.50
Fine-grained soil (%)	0.50
Free Calcium, F-CaO (%)	4.27

In order to obtain a comprehensive understanding the mechanical and microstructural properties of the dredged marine clay stabilized with BOF, a series of laboratory tests were carried out on specimens with different water and BOF proportions, as presented in Tables 4 and 5, and preparation procedure of sample was followed by the Guidebook for Oceanographic Application of Converter Slag (2008). The initial clay water content, w_0, was determined based on the clay liquid limit, w_{LL}, and the sample conditions in this study were set as 1.2, 1.5, 1.7, and 2.0 times the liquid limit, considering the initial water contents of cement-treated soil used in construction projects in coastal areas (Tang et al., 2001; Tsuchida et al., 2007; Watabe and Noguchi, 2011). The ratio of the BOF volume to the total volumes of soil mixture, R_{BOF} (%), is defined in Equation 1:

$$R_{BOF} = \frac{V_{BOF}}{V_{soil} + V_{water} + V_{BOF}} \times 100 \quad (\%) \quad , \qquad (1)$$

where V_{soil} and V_{water} are the dried soil and water volumes, respectively, and V_{BOF} is the BOF volume.

The Tokuyama dredged clay was filtered through a 2 mm sieve to remove coarse particles or other impurities. The BOF was air-dried at a room temperature of 20 ± 3°C for 1 d to dry only the moisture of slag surface, i.e., the surface dry density condition. The BOF water content following air-drying was 1.12%. Artificial seawater

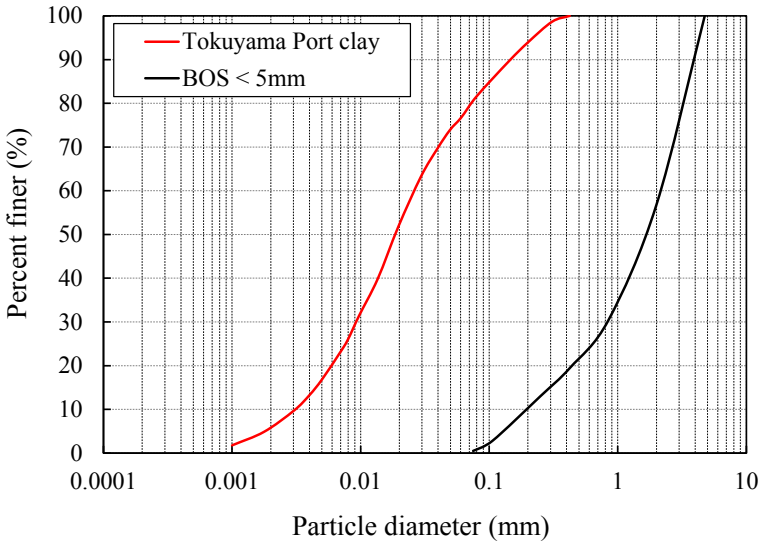

Figure 3- 1 Particle-size distribution of Tokuyama clay and BOF slag.

with a 3.5% salinity was prepared as additional water used in the desired water content of the experimental samples in order to create identical conditions to those of marine clay in coastal areas. The slurry obtained after adding BOF and additional water to the marine dredged clay was fully mixed for 5 min using a hand mixer.

LVS and UC tests were adopted to evaluate the strength development at the early and later curing stages, respectively. A cylindrical mold of 60 mm in diameter and 60 mm in height was prepared for the LVS test. A cylindrical tinplate mold with a diameter of 50 mm and height of 100 mm was employed for the UC test. The mixture was poured into the molds by dividing the three layers, and lightly tapped to remove the void of air bubbles in the molds. The cylindrical molds were covered with polythene wrap and cured under atmospheric pressure at a temperature of 20 ± 3°C, while the cylindrical tinplate molds of the UC test were cured in distilled water at room temperature. The specimen preparation for this procedure required approximately 30 min. Accordingly, the curing starting time of curing was determined as 30 min following mixing.

For the sample preparation for the SEM and EDS, the stabilized specimens listed in Table 3 were trimmed into small fragments prior to drying in order to implement freeze-drying with ease. The prepared fragments were frozen instantly by means of immersion in liquid nitrogen of approximately −195°C for 30 min. The frozen samples were then evacuated at a pressure of −0.5 Pa at −40°C for 1 d using vacuum drying apparatus. The freeze-dried samples were broken up by finger pressure into pieces of approximately 6 mm in diameter and 6 mm in height. The undisturbed surfaces of the broken samples were positioned upwards on an aluminum stub, and fixed using carbon bond and tape. Finally, the samples on the aluminum stub were coated with gold in order to obtain a high-quality image from the SEM and EDS tests.

3.2.2 Tests performed

In this study, all of the laboratory tests were conducted on dredged marine clay stabilized with BOF to investigate the geotechnical properties, strength development, and microstructural and mineralogical properties. A flow test was carried out on all specimens immediately following mixing to determine the mixture workability. The LVS test was conducted on samples during the early curing stage (0.5 to 10 h), while the UC test was carried out on samples during the later curing stages (10 h to 90 d).

The SEM and EDS analyses were conducted on eight samples and one sample, respectively, in order to examine the reaction products of the stabilized dredged marine clay, and SEM was additionally carried out on two cement-treated clay samples and compared to that of ordinary Portland cement.

3.2.2.1 Flow test

A flow test was carried out following the cylinder method of the Japan Highway Public Corporation (JHS A 313, 1992) in order to obtain the flow value as a significant parameter in evaluating the fluidity and workability for stabilized marine dredged clay. An open-end cylindrical acrylic mold with a diameter and height of 80 mm was initially placed on a metalized plastic plate and then filled with the mixture up to the cylinder upper end so as to prevent overflowing from the cylinder. The cylinder mold was lightly tapped on the cylinder side with a finger so that the mixture surface was horizontal and coincided with the cylinder upper end. The cylinder was lifted vertically, allowing for the mixture to spread freely on the plate, and the spread diameters in two perpendicular directions were measured after 1 min. Finally, the flow value was determined by the average value of spread diameters.

3.2.2.2 LVS and UC tests

The LVS test was performed to measure samples with comparatively low strengths and very early curing times, ranging from 0.5 to 10 h, when the samples could not stand on their own. The vane diameter and height were both 20 mm, and a vane height/diameter ratio (H/D=1) was used. The rotation speed of the laboratory vane was set at 6°/min, and the vane was rotated until 60°. Moreover, the torque peaks in the mixtures were reached within 60° in all experiments conducted.

The UC test was conducted following the Japan Industrial Standard JIS A 1216 (2008) on the remaining samples at a later curing stage, namely 10 h to 90 d, which could stand with sufficient strength after completing the LVS test. A linear variable differential transformer was used to measure the local internal strain, and the compression strain rate was 1% per minute.

In this study, the undrained shear strength (s_u) obtained from the LVS test was calculated using the equation $q_u = 2s_u$. The strength of the marine dredged clay stabilized with BOF was expressed as either q_u or $2s_u$ with the curing time.

Table 3- 3 Chemical composition of BOF

Chemical	BOF (%) of this study	BOF (%)[a]	BOF (%)[b]
SiO_2	14	8–20	8.6–13.1
Al_2O_3	2.7	1–6	1.7–2.1
FeO	33	10–35	28.3–32
CaO	40	30–55	40.1–45
MgO	2.3	5–15	4.5–7.5
MnO	4.1	2–8	2.0–4.1
TiO_2	0.49	0.4–2	0.5–0.9
S	0.029	0.05–0.15	0.4–1.2
P	3.1	0.2–2	1.4–2.4
Cr	0.19	0.1–0.5	N/A[c]

[a]Shi (2004)
[b]Belhadj et al. (2012)
[c]Not available

Table 3- 4 Type and condition of tests conducted in laboratory

Type of test	Normalized initial water content, w_0/w_{LL}	BOF content, BOF_{Vol} (%)	Curing time
LVS and UC*	1.2, 1.5, 1.7, 2.0	20, 30	0.5, 2, 5, 7, 10, 15 (hours) 1, 2, 3, 7, 28, 90 (days)
SEM	1.5, 2.0	20, 30	28, 90 (days)
EDS	2.0	20	28 (days)

*LVS: laboratory vane shear test; UC: unconfined compression test

3.2.2.3 SEM and EDS analysis

In order to investigate the changes in the matrix microstructure of the stabilized clay qualitatively, SEM and EDS analyses for a mineralogical study were carried out using a JEOL JSM - IT300 SEM, operating at 30 kV. The SEM was fitted with an energy-dispersive X-ray spectrometer. By means of EDS, the specimen chemical compositions were analyzed. Micrographs were obtained using the EDS2000 software.

3.3 Results

3.3.1 Physical properties of BOF-treated dredged clay

3.3.1.1 Stress-strain curve

Figure 3-2 illustrates the stress-strain curves from 15 h to 90 d of curing, obtained from the UC test on the samples with a BOF content of 30% and $w_0 = 1.5\ w_{LL}$. As

indicated in Fig. 3-2, the stress-strain curve behavior changed significantly with the curing time. The 15 h curing curve exhibited a failure strain of approximately 2% and was generally similar to the stress-strain property of general soft clay. In the stress-strain curve after 7 d of curing, the axial strain at failure was decreased, and was less than 2%. The axial strain at failure in the sample with the longest curing period of 90 d was approximately 0.8%. These values are very similar to those determined for cement-treated clay (Miura et al., 2001; Lorenzo and Bergado, 2004; Horpibulsk et al., 2011).

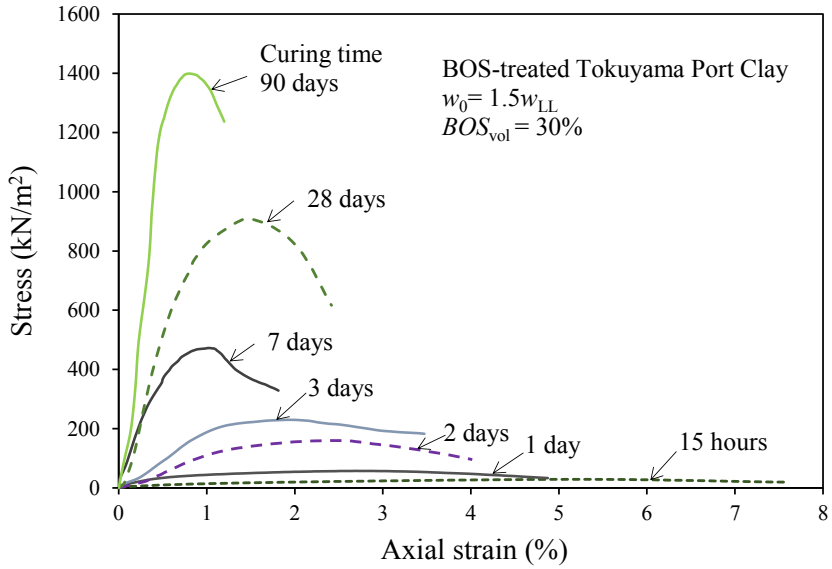

Figure 3- 2 Stress-strain curves for BOF-treated Tokuyama Port clay (e.g. BOF_{vol}=30% and w_0=1.5w_{LL})

3.3.1.2 Flowability

Cement-treated and BOF-treated dredged clay can be utilized as backfill, embankment, and sealing materials. These materials have a specific layer thickness and gradient when placed in the construction site. Moreover, the layer thickness and gradient are determined by the construction conditions (Tang et al., 2001). Therefore, the flowability of a mixture immediately following mixing with a binder is a very significant indicator for reflecting the workability at construction. Furthermore, the target flow value varies according to the construction method and material application purpose. Figure 3-3 illustrates the variation in flowability (*FA*) with an increase in the initial water content (w_0/w_{LL}) for all BOF mixtures in this experiment. The flow value ranged from 80 to 98 mm, and the flowability exhibited an increase with an increase in the initial water content and a decrease with an increase in the BOF content. It was

Table 3- 5 Mix proportion calculation.

No.	Volumetric BOF addition rate, R_{BOF}	Tokuyama Port clay						BOF	BOF-treated soil	Density of BOF-treated soil (g/cm^3)
		Density (g/cm^3)	Soil particle	Water	Added water	Total water	Total mass and volume	Normalized water content, w_0/w_{LL}	Particle density = 3.15 g/cm^3	
			2.646	1.03*	1.03*	1.03*				
Case 1	20%	Mass (g)	2,372	2,541	509	3,050	5,422	1.2	3,038	8,459	1.75
		Volume (mL)	896	2,467	494	2,961	3,857		964	4,822	
Case 2	20%	Mass (g)	2,042	2,560	722	3,282	5,323	1.5	3,117	8,440	1.69
		Volume (mL)	772	2485	701	3,186	3,958		989	4,947	
Case 3	20%	Mass (g)	1,907	2,394	1,080	3,474	5,382	1.7	3,224	8,606	1.66
		Volume (mL)	721	2,325	1,049	3,373	4,094		1,023	5,117	
Case 4	20%	Mass (g)	1,725	2,239	1,458	3,697	5,422	2.0	3,340	8,761	1.63
		Volume (mL)	652	2,173	1,416	3,589	4,241		1,060	5,301	
Case 5	30%	Mass (g)	1,939	2,310	183	2,493	4,433	1.2	4,257	8,690	1.91
		Volume (mL)	733	2,243	178	2,421	3,154		1,352	4,505	
Case 6	30%	Mass (g)	1,701	2,114	620	2,734	4,435	1.5	4,451	8,886	1.88
		Volume (mL)	643	2,052	602	2,654	3,297		1,413	4,710	
Case 7	30%	Mass (g)	1,565	2,051	799	2,850	4,415	1.7	4,534	8,949	1.87
		Volume (mL)	591	1,991	776	2,767	3,359		1,439	4,798	
Case 8	30%	Mass (g)	1,413	1,869	1,159	3,028	4,441	2.0	4,690	9,131	1.85
		Volume (mL)	534	1,815	1,125	2,940	3,474		1,489	4,963	

found that the flowability increase rate between the initial water contents of 1.2 and 2.0 w_0/w_{LL} demonstrated an approximately 18% increase, irrespective of the BOF content. Moreover, the flowability decrease rate according to an increase in the BOF content at the same initial water content ranged from 1.24 to 3.98%. These phenomena are predominantly owing to the changes in the free-water content; that is, the free-water content increases with an increase in the initial water content, and decreases with an increase in fine aggregates of air-dried BOF, which absorb the free-water content because of the increased specific surface.

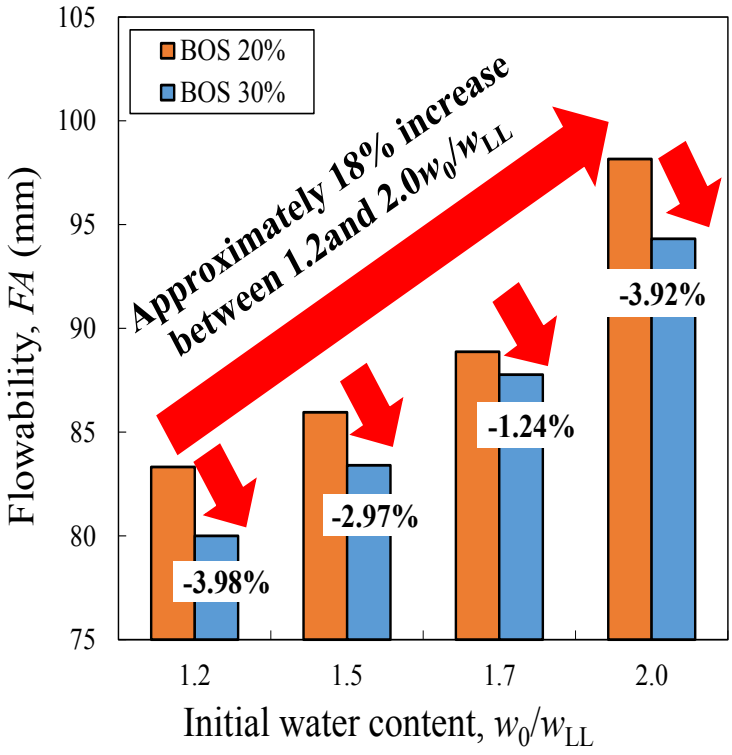

Figure 3- 3 Variation in flowability with initial water content for each BOF content.

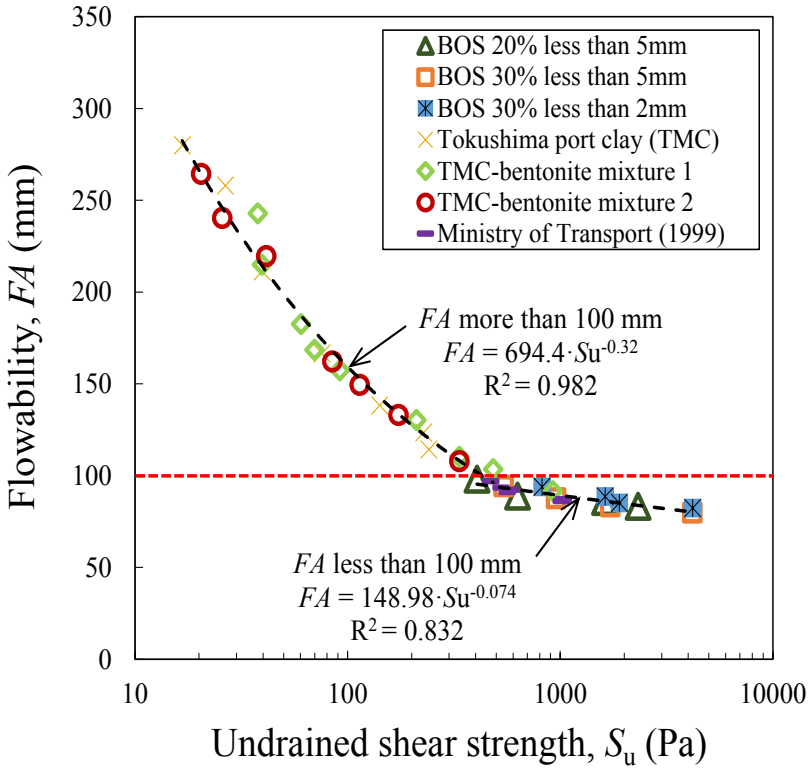

Figure 3- 4 Relationship between flowability and undrained shear strength

Figure 3-4 presents the relationship between the flowability and undrained shear strength. Additional flow tests were carried out for a mixture stabilized with BOF, where the R_{BOF} of less than 2 mm diameter was 30%, untreated Tokuyama port clay (TPC), and TPC-bentonite mixtures, and several data collected from the literature (Ministry of Transport, Fifth District Port Construction Bureau, 1999) in order to assess the relationships between flowability and undrained shear strength accurately over a wide range. These values are primarily governed by the specific surface area, as well as the adsorption ability and void ratio related to the inter-particle contact. For example, a large amount of cement-treated dredged clay produced by the pre-mix vessels method have frequently been used as construction material for back filling or reclamation, and its flow value has conventionally been controlled to be within the range of 100 to 150 mm, depending on the construction conditions (Technical Manual of Pre-mix Vessels Method, 2013). Therefore, in this study, two ranges for the relationship between the flowability and undrained shear strength were proposed: a flow values above and below 100 mm. The range of flow values less than 100 mm was 80 to 98 mm, with the undrained shear strength ranging from 406 to 4193 Pa. The flow values above 100 mm ranged from 103 to 280 mm, corresponding to undrained

shear strengths of 17 to 924 Pa. As illustrated in Fig. 3-4, the flowability in the range of more than 100 mm decreased considerably with an increase in the undrained shear strength. For less than 100 mm, the flowability decreased gently with the undrained shear strength. Two equations can be expressed with high determination coefficients (more than 100 mm: $R^2 = 0.98$ and less than 100 mm: $R^2 = 0.83$), as follows:

$$FA = 694.4 \cdot S_u^{-0.32} \text{ (More than 100mm)} \quad (2)$$

$$FA = 149.0 \cdot S_u^{-0.074} \text{ (Less than 100mm)} \quad (3)$$

It is established that the undrained shear stress may be a significant variable related to the flowability, which can be determined using the proposed equations.

3.3.2 Strength development characteristics with curing time

A series of LVS and UC tests were carried out to examine the strength development characteristics of the dredged clay stabilized with different BOF and initial water contents, from immediately following mixing to long-term curing times varying from 0.5 h to 90 d; the relationship between strength and curing time is plotted in Fig. 3-5. The stabilized dredged clay strength development generally exhibited an increase with an increase in the BOF and decrease in the initial water content of the dredged clay. The strength development was changed at a specific curing time with different strength increment rates, which is the gradient for the relation of the strength and curing time in the log-log scale graph. It was observed that the strength development increased marginally up to 5 h of curing time up to 5 h of curing time. The strength development exhibited a reduction between 0.5 and 2 h of curing, even though the curing time was passed, except for three samples, namely $BOF_{Vol} = 30\%$, and $w_0 = 1.2$, 1.5, and 2.0 w_{LL}. Moreover, the strength increments of the excluded samples increased very slightly with an increase in strength against the elapsed curing time. This means that the strength did not develop within the range of 0.5 to 2 h, and this period is known as a “dormant period” in the concrete engineering field. Seng and Tanaka (2011) reported that the dormant period of marine clay treated with ordinary Portland cement (OPC) is approximately 30 min immediately following mixing. It was found that the setting time at which the strength development begins of dredged clay stabilized with BOF is significantly longer than that of OPC; that is, the rate of the hydration reaction increasing the stabilized dredged clay strength is very slow at the

very early curing stage (within 5 h) compared to OPC.

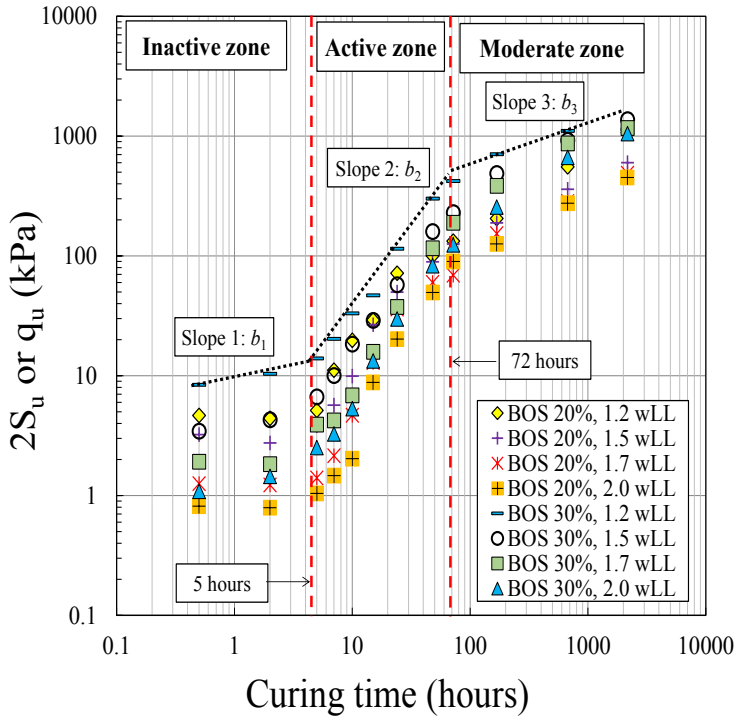

Figure 3- 5 Strength development of SMSS on log-log scale

Figure 3-6 presents the X-ray diffraction patterns of the BOF provided in this study. The main minerals of BOF include calcium hydroxide ($Ca(OH)_2$), calcite ($CaCO_3$), CaO, C_2S, and wüstite (FeO). The presence of FeO, srebrodolskite ($Ca_2Fe_2O_5$), and fayalite (Fe_2SiO_4) indicates a higher iron oxide condition in BOF. In these X-ray diffraction patterns, the C_2S identified in the BOF was the major mineral, in the form

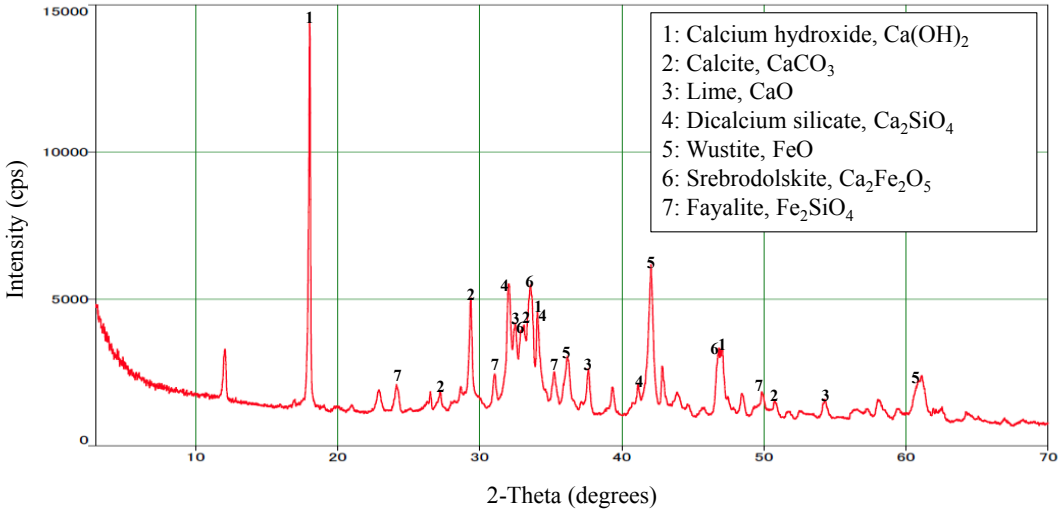

Figure 3- 6 X-ray diffraction patterns of BOF used

of β-C_2S, which is present in cement, and this mineral can be hydrated and gain strength owing to the hydration reaction. Based on the results, it suggested that the stabilizing mechanisms of the BOF-treated dredged clay are the hydration reaction of the C_2S and the pozzolanic reaction of the $Ca(OH)_2$ and Si/Al obtained in the clay. Hence, possible reasons for the slow hydration rate are the deficiency of certain minerals (C_3A or C_4AF) that create a high hydration rate in very early curing, and the lack and low activity of C_2S and C_3S in the BOF compared to OPC (Poh et al., 2006; Qiang et al., 2016). Wang et al. (2010) mentioned another reason, namely that, owing to the structure of the free lime in BOF being denser than that of burnt lime and the decreased ability of moisture to react with the free lime, the hydration reaction of free lime in the BOF is slow compared to burnt lime, in which the hydration can be completed within 30 min. I considered that this finding may be useful in predicting or controlling the fluidity and the workability of BOF-treated clay, depending on the construction conditions. Moreover, after 5 h of curing, the strength development was sharply increased with a high strength increment rate up to 3 d of curing governed in the hydration reaction. Thereafter, moderation with curing periods (from 3 to 90 d) dominated by the pozzolanic reaction was predominant, with a gentle slope, relative to a low strength increment rate. Based on this behavior, I suggest that the strength development can be divided into three zones in the log-log scale graph: 1) inactive zone (0.5 to 5 h), 2) active zone (5 h to 3 d), and 3) moderate zone (3 to 90 d). Figure 3-7 illustrates the strength development comparison between the BOF-treated Tokuyama clay and cement-treated Tokuyama clay obtained in the literature (Kang et al., 2016, 2017a, 2017b). Data of the cement-treated Tokuyama clay were obtained from samples of 10 and 20% cement content determined by the mass ratio, $c^*=m_{cement}/(m_{clay}+m_{cement})$. It has previously been reported that the strength development of cement-treated clay increases linearly from immediately following mixing and changes before and after 3 d of curing with different strength increment rates. The strength values of the cement-treated clay before 3 d of curing were higher than those of the BOF-treated clay, while after 3 d of curing, the strength magnitudes of the BOF-treated clay were larger or smaller than those of the cement-treated clay. Hence, it is noted that the strength increment rate with curing time may differ depending on the binder type.

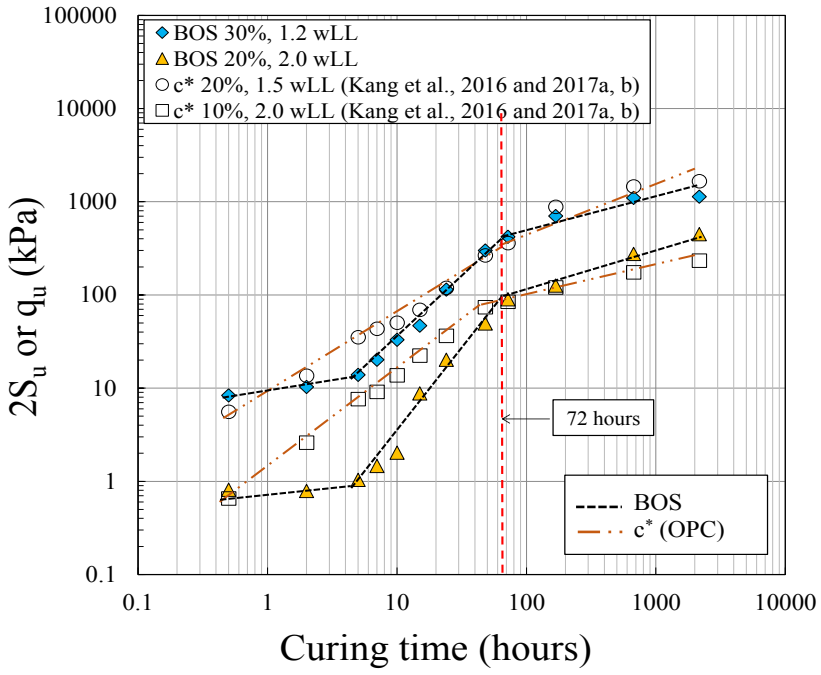

Figure 3- 7 Strength comparison between SMSS and cement-treated clay.

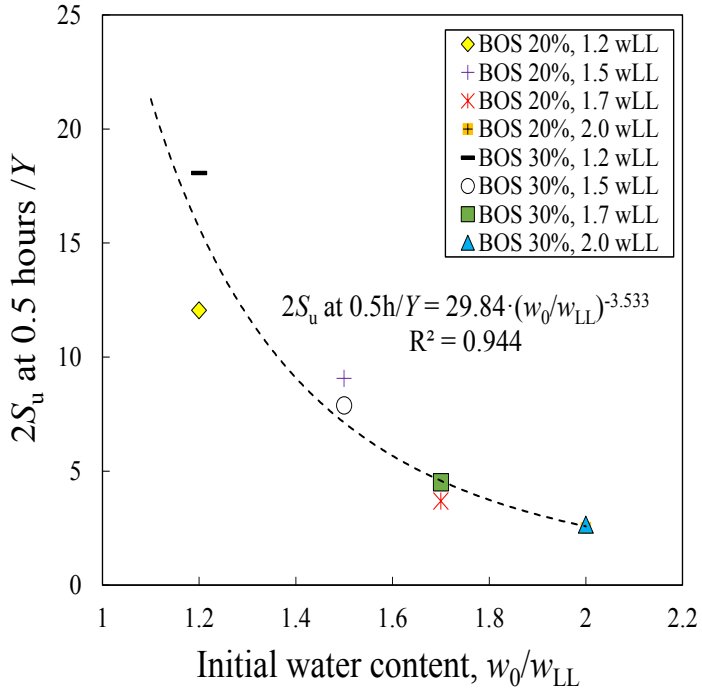

Figure 3- 8 Strength at curing 0.5 h, normalized by volumetric soild content, and initial water content.

3.3.2.1 Proposed strength estimation equations for each zone and its microstructure properties

As mentioned previously, the strength development was classified into three zones, namely the inactive zone (0.5 to 5 h), active zone (5 h to 3 d), and moderate zone (3 to 90 d), in accordance with the strength increment rate. Consequently, equations for each zone were proposed with various indices.

3.3.2.2 Strength estimation equation for inactive zone (0.5 to 5 h)

The strength at 0.5 h of curing and the strength increment rate were used to propose the strength estimation equation for the inactive zone. The strength at 0.5 h of curing was correlated with the volumetric solid content, Y, which is defined as follows:

$$Y = \frac{V_{\mathrm{BOF}} + V_{\mathrm{Soil}}}{V_{\mathrm{BOF}} + V_{\mathrm{Soil}} + V_{\mathrm{Water}}}, \tag{4}$$

where V_{BOF}, V_{Soil}, and V_{Water} are the BOF, soil, and water volumes, respectively.

The strength increment rate (gradient for the relationship between the strength and curing time within 5 h), b_1, obtained in relation to the curing time strength and logarithm, was associated with a BOF mass ratio. The BOF ratio is defined as the ratio of the BOF mass to the mass of solid particles, as per Eq. (5):

$$BOF_{\mathrm{mass}} = \frac{m_{\mathrm{BOF}}}{m_{\mathrm{BOF}} + m_{\mathrm{soil}}}, \tag{5}$$

where m_{BOF} and m_{soil} are the BOF mass and soil dry mass, respectively.

Figure 3-8 demonstrates the relationship between the strength at a curing time of 0.5 h, normalized by the volumetric solid and initial water contents. This relation exhibited a strong correlation with the high determination coefficient, $R^2 = 0.944$, and can be expressed by a single line of a power function form. This relation means that the factor governing the strength increase at curing of 0.5 h is not a chemical effect such as hydration or pozzolanic reactions, but rather physical effects owing to a change in the amount of free water and the void ratio. Based on the relationship illustrated in Fig. 3-7, the equation for estimating the strength at curing of 0.5 h can be obtained, as per Eq. (6):

$$2S_{u0.5h} = A(w_0/w_{LL})^{-B} \cdot Y$$
$$2S_{u0.5h} = 29.84(w_0/w_{LL})^{-3.53} \cdot Y \quad , \tag{6}$$

where $2S_{u0.5h}$ is the strength at curing of 0.5 h, w_0/w_{LL} is the initial water content, and A and B are the parameters related to the volumetric solid and initial water contents, respectively.

Figure 3-9 illustrates the relationship between the strength increment coefficient in the inactive zone, b_1, and the BOF mass ratio, BOF_{mass}. The b_1 value generally increased with an increase in the BOF_{mass} except in the sample with BOF_{Vol} = 20% and w_0/w_{LL} = 1.7. Moreover, it can be observed that the values of b_1 in the BOF of 20% were smaller than those of the BOF of 30%. This relationship can be reasonably represented as a single line by the following polynomial function:

$$b_1 = b_a \cdot BOF_{mass}^2 - b_b \cdot BOF_{mass} + b_c$$
$$b_1 = 12.186 \cdot BOF_{mass}^2 - 13.654 \cdot BOF_{mass} + 3.853 \tag{7}$$

where b_1 is the strength increment coefficient in the inactive zone, and b_a, b_b, and b_c are the parameters depending on BOF_{mass}.

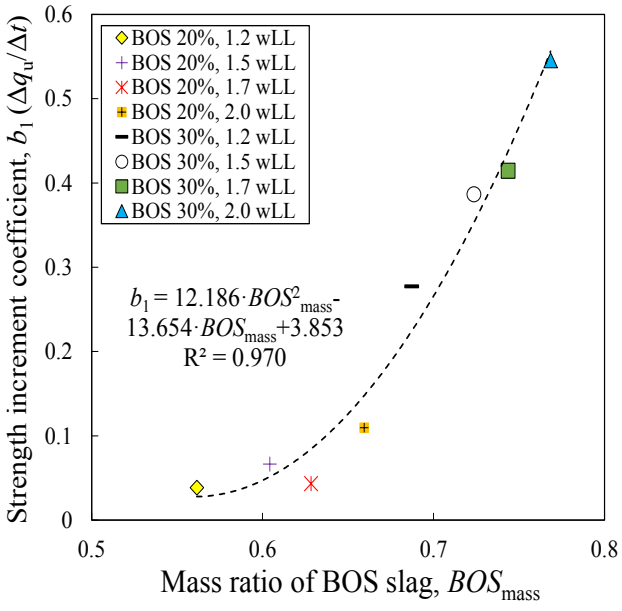

Figure 3- 9. Relation of strength increment coefficient in inactive zone and *BOFmass*.

An empirical equation for predicting the strength in the inactive zone was proposed based on Eqs. (6) and (7), as follows:

$$2S_{\mathrm{u}}\ (\text{Inactive zone}) = A(w_0 / w_{\mathrm{LL}})^{-B} \cdot Y\left[1 + b_1\, ln\,(t / 0.5h)\right] \quad (8)$$

It should be noted that Eq. (8), composed using the volumetric solid content and BOF mass ratio, could be estimated for the strength in the inactive zone, ranging from 0.5 to 5 h.

3.3.2.3 Strength estimation equation for active zone (5 h to 3 d)

Kang et al. (2016, and 2017a and b) suggested two equations that can estimate the strength of cement-treated marine clay during early and later curing times, based on the concept of changing the strength before and after 3 d of curing in the log-log scale graph. The proposed equations were composed of the strength at 1 h of curing and strength increment coefficients (slope for the relationship between the strength and curing time), and the 1 h of curing and strength coefficients could be determined by the specific volume ratio and cement content. In this study, the strength estimation equations for the BOF-treated dredged clay in the active and moderate zones were also proposed based on the strength at 1 h of curing and strength increment coefficients.

Referring to Fig. 3-5, the strength development increased linearly with the curing time on the log-log scale, and its relation can be placed into a linear model by a power function for predicting the strength of BOF-treated dredged clay in the active zone, for 5 h to 3 d of curing, as expressed in Eq. (9):

$$\begin{aligned} &\ln(q_u \text{or } 2S_{\mathrm{u}}) = \ln a_1 + b_2 \ln(t) \\ &\exp\{\ln(q_u \text{or } 2S_{\mathrm{u}})\} = \exp\{\ln a_1 + b_2 \ln(t)\} \\ &q_u or\ 2S_u = a_1 \cdot \exp\{b_2 \cdot \ln(t)\} \\ &q_u or\ 2S_u (\text{active zone}) = a_1 \cdot t^{b2} \end{aligned} \quad , \quad (9)$$

where q_{u} or $2S_{\mathrm{u}}$ are the strengths obtained by the UC and LVS tests, respectively, a_1 is the strength at 1 h of curing, and b_2 is the strength increment coefficient, which represents the slope for the strength and curing time relation in the active zone.

After determining the strength parameter, a_1, using regression analysis on the relationship between the strength and curing time in the log-log scale, a_1 was

associated with a specific volume ratio (v'/v_{LL}), which is the specific volume of the BOF-treated clay normalized by that at the dredged clay liquid limit. The definitions for the indices used are as follows:

$$v'(\text{BOS - treated clay}) = \frac{V_{\text{Soil}} + V_{\text{Water}} + V_{\text{BOS}}}{V_{\text{Soil}} + V_{BOS}},\ v_{\text{LL}}(\text{Dredged clay}) = \frac{V_{\text{Soil}} + V_{\text{Water}}}{V_{\text{Soil}}}. \quad (10)$$

Figure 3-10 illustrates the relationship between the logarithms of a_1 and those of the specific volume ratio, $\ln v'/\ln v_{LL}$, and compares this with the result of the cement-treated Tokuyama clay obtained from Kang et al. (2017a). The a_1 value exhibited a reduction with an increase in the specific volume ratio for each BOF content, which means an increase in the water content, and increased with an increase in the BOF content. It was found that the a_1 value of the BOF-treated dredged clay was smaller than that of the cement-treated dredged clay. The $\ln(a_1)$ and $\ln v'/\ln v_{LL}$ values exhibited strong correlations with the high determination coefficients, and could be divided into two lines depending on the BOF contents. The correlations were presented as expressed in Eq. (11):

$$\begin{aligned} &\ln(a_1) = c_1 - c_2\left(\ln v'/\ln v_{\text{LL}}\right) \\ &\text{or} \\ &a_1 = \exp(c_1)\, v'^{-c_2/\ln v_{\text{LL}}} \end{aligned}, \quad (11)$$

where c_1 is the strength when the specific volume ratio is 0: $\ln v'/\ln v_{LL} = 0$. Parameter c_2 represents the strength increment rate with the specific volume ratio (gradient of the relationship between the logarithm of strength and the logarithm of the specific volume ratio). The c_1 and c_2 values for each BOF content used were determined as illustrated in Eq. (11).

$$\begin{aligned} &BOF_{\text{vol}} = 20\%: \quad a_1 = \exp(16.91)\, v'^{-23.12/\ln v_{\text{LL}}} \\ &BOF_{\text{vol}} = 30\%: \quad a_1 = \exp(14.55)\, v'^{-24.13/\ln v_{\text{LL}}} \end{aligned}. \quad (11)'$$

Based on the results for the relation of a_1 and $\ln v'/\ln v_{LL}$, it was observed that a_1 can successfully be determined by the specific volume ratio.

The strength increment coefficient, b_2, in the active zone, obtained from the graph for the relationship between the strength and curing time in the log-log scale, exhibits a correlation with the BOF mass ratio. The b_2 data of the cement-treated clay calculated by the cement mass ratio, $m_{\text{cement}}/m_{\text{soil}}+m_{\text{cement}}$, obtained from Kang et al.

(2017a) were added to the graph for comparison of the strength increment rate according to the binder type. Figure 3-11 illustrates the relationship between the strength increment coefficient in the active zone, b_2, and the BOF mass ratio with the cement-treated clay data. It was found that the b_2 of the BOF-treated dredged clay was increased significantly with an increase in the binder mass ratio. Moreover, the b_2 values of the BOF of 20% exhibited a wide range, in accordance with an increase in the binder mass ratio, compared to that of the BOF of 30%. In the case of cement, b_2 exhibited a slight increase or constant value with an increase in the binder mass ratio, irrespective of the cement and water contents. It can be observed that the b_2 of the BOF-treated clay was greater than that of the cement-treated clay. Based on the results, it is implied that the strength increment behavior owing to the hydration reaction that increases the strength in the active zone may differ in accordance with the binder type. Therefore, the correlation between b_2 and the BOF mass ratio can be classified into BOF contents and expressed as per Eq. (12):

$$\begin{aligned} & b_2 = d_1 \cdot BOF_{\text{mass}} - d_2 \\ BOF_{\text{vol}} = 20\%: \quad & b_2 = 4.53 \cdot BOF_{\text{mass}} - 1.35 \\ BOF_{\text{vol}} = 30\%: \quad & b_2 = 3.31 \cdot BOF_{\text{mass}} - 0.96 \end{aligned} \quad , \tag{12}$$

where d_1 is the strength increment rate with the BOF mass ratio and d_2 is the strength increment coefficient when $m_{\text{BOF}}/(m_{\text{soil}}+m_{\text{BOF}})$ is 0.

By substituting Eq. (11), determining the strength at 1 h of curing, and Eq. (12), predicting the strength increment coefficient in the active zone, into Eq. (9) regarding the strength estimation model of the active zone, the empirical equation for estimating the strength of the BOF-treated dredged clay in the active zone can be developed as follows:

$$q_u or\ 2S_u(\text{active zone}) = \exp(c_1)\, v'^{-c_2/\ln v_{\text{LL}}} \cdot t^{(d_1 \cdot BOS_{\text{mass}} - d_2)} \tag{13}$$

The proposed Eq. (13) can estimate the strength in the active zone, at 5 h to 3 d, using the specific volume ratio and BOF mass ratio.

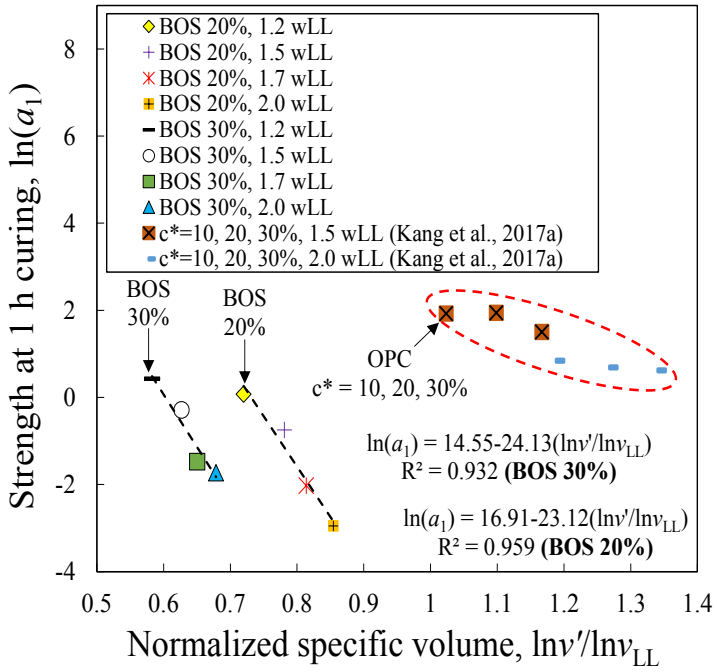

Figure 3- 10 Relationship between logarithms of a_1 and logarithms of specific volume ratio, $\ln v'/\ln v_{LL}$, and comparison with results of cement-treated Tokuyama clay

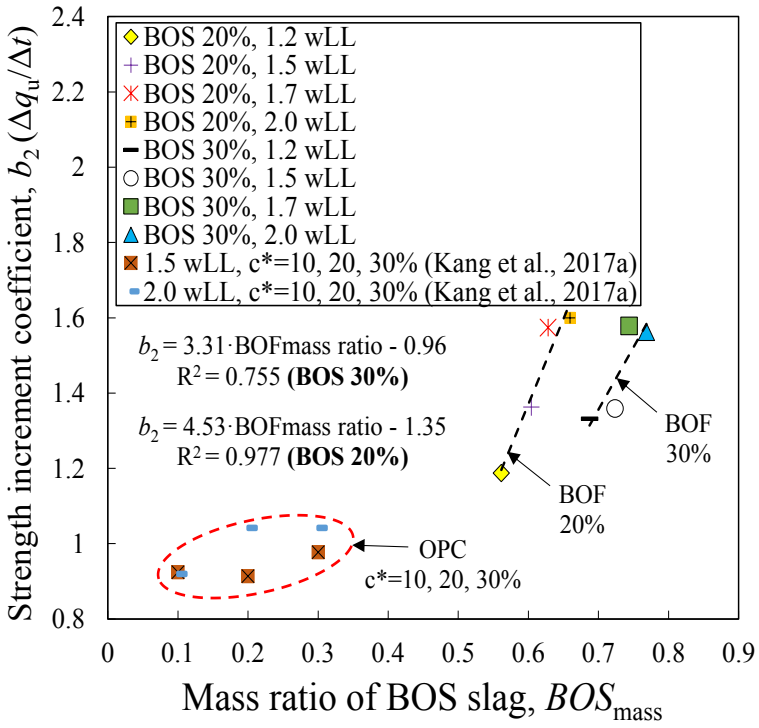

Figure 3- 11 Relationship between strength increment coefficient in active zone and BOS mass ratio with data of cement-treated Tokuyama clay

3.3.2.4 Strength estimation equation for moderate zone (3 to 90 d)

For the moderate zone (3 to 90 d), I propose the strength estimation model as per Eq. (14):

$$q_u(\text{moderate zone}) = q_{u(3\text{days})}\left\{1 + b_3 \ln(t/t_{3\text{days}})\right\}, \tag{14}$$

where q_u (moderate zone) is the strength, b_3 is the strength increment coefficient in the moderate zone, which is the gradient for the relationship between the strength and curing time, and t and $t_{3\text{days}}$ are the curing time and 3 d of curing time, respectively.

The b_3 value was determined by means of regression analysis for the relationship between the strength and curing time logarithm in the semi-log scale graph, and correlated by the BOF mass ratio. Figure 3-12 illustrates the relation of the b_3 and BOF mass ratio, and a comparison with that of Portland cement obtained from the literature (Kang et al., 2017a). It was revealed that the b_3 value of the BOF of 30% increased marginally with an increase in the BOF mass ratio, while the b_3 of the BOF of 20% was very slight with a variation in the BOF mass ratio. This behavior means that, for the BOF of 20%, the strength development rate owing to pozzolanic reaction at the long-term curing time was insignificant. However, the b_3 of the cement-treated clay increased linearly with the cement mass ratio, except for $c^* = 30\%$ and $1.5w_{LL}$. It was found that the b_3 of the cement content of 10% was smaller than that of the BOF of 20% and 30%, while the cement-treated clay range was wider than that of the BOF. Based on the results, the correlation of b_3 and the BOF mass ratio can be expressed by a linear function, as expressed in Eq. (15):

$$\begin{aligned} & & b_3 &= e_1 \cdot BOF_{mass} + e_2 \\ BOF_{\text{vol}} = 20\%: & & b_3 &= 0.99 \cdot BOF_{mass} + 0.53 \\ BOF_{\text{vol}} = 30\%) & & b_3 &= 8.33 \cdot BOF_{\text{mass}} - 4.64 \end{aligned} \tag{15}$$

where e_1 is the strength increment rate with the BOF mass ratio and e_2 is the strength increment coefficient when $m_{BOF}/(m_{soil}+m_{BOF})$ is 0.

By substituting the strength estimation equation for the active zone, Eq. (13), and the strength increment coefficient for the moderate zone, Eq. (15), into the proposed Eq. (14), the equation for predicting the strength in the moderate zone was proposed, as follows:

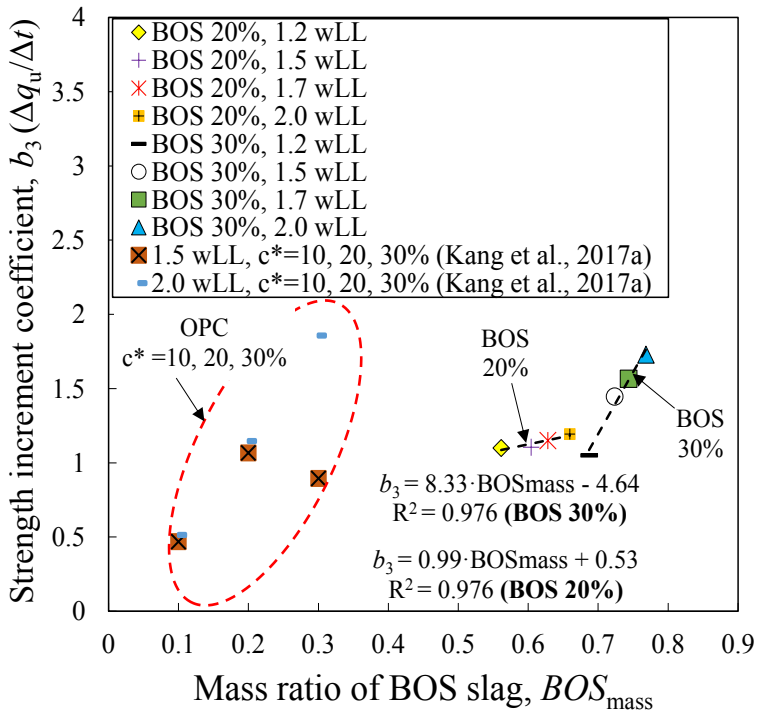

Figure 3- 12 Relationship between strength increment coefficient in moderate zone and BOS mass ratio with data of cement-treated Tokuyama Port clay

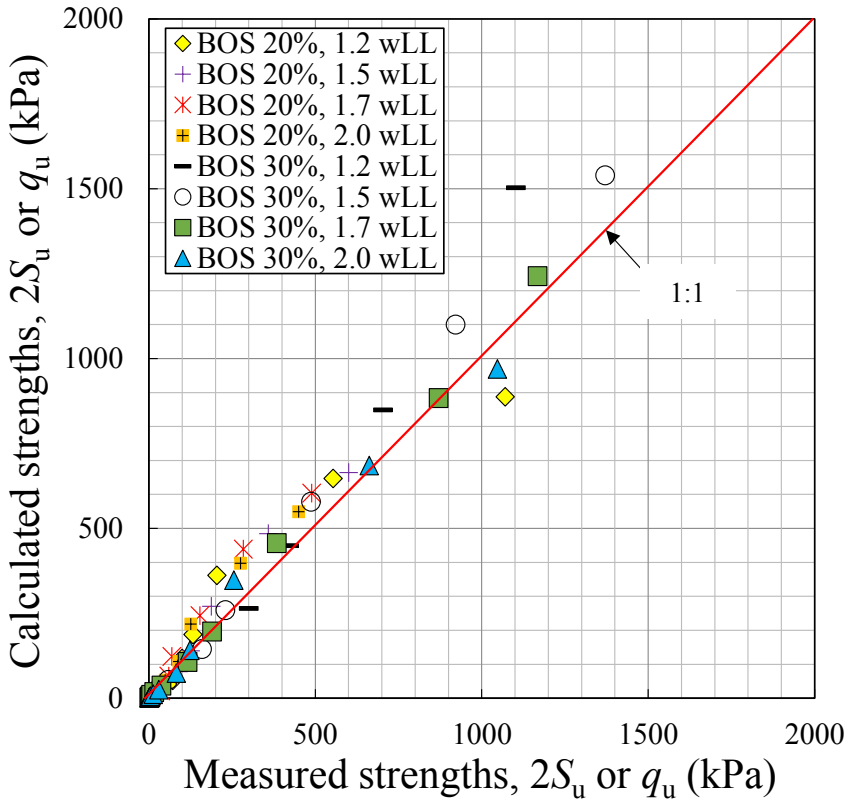

Figure 3- 13 Comparison of calculated and measured strengths

$$q_u(\text{moderate zone}) = \exp(c_1)\, v'^{-c_2/\ln v_{LL}} \cdot t_{3\text{days}}^{d_1 \cdot (BOS_{\text{mass}}) - d_2} \cdot \left[1 + b_3 \ln(t/t_{3\text{days}})\right]. \quad (16)$$

Figure 3-13 provides a comparison of the measured strengths and those calculated by the empirical equations proposed in this study. The measured and calculated values agreed strongly with the overall data.

It should be noted that this study was focused on understanding the characteristics of the strength behavior of BOF-treated dredged clay at the very early and later curing times, and a comparison with that of Portland cement-treated dredged clay. However, the strength behavior of the BOF-treated dredged clay may be affected by the BOF size, free-CaO content, and soil types, among other factors. Therefore, it is essential to investigate the parameter variations of the proposed equation with various considerations, such as the BOF properties and soil types.

3.3.3 SEM and EDS analysis

In general, the cement stabilization process involves the growth of newly formed phases within soil textiles by means of the hydration reaction of clinker and pozzolanic reactions in calcium hydroxide ($Ca(OH)_2$) and silica/alumina from soil. New cementitious compounds in the soil fabric result in hardening occurring, owing to binding to the soil microstructure, thereby increasing the inter-particle contacts and filling the pore spaces in the mixture. Furthermore, the geotechnical characteristics such as permeability, strength, and stiffness can be modified by the stabilization reaction. Hence, the factors affecting the formation of cementitious compounds, such as the clinker amount, degree of alkaline dissolution of the alumina and silica in soil, pozzolanic sources, diffusion, and surficial aqueous complexation, are significant in the stabilization process (Scrivener, 1991; Wilkinson et al., 2010). It is considered that the stabilization mechanisms of the BOF-treated clay are the hydration and pozzolanic reactions, because BOF also contains mineral compounds similar to those of Portland cement and free lime (F-CaO), which cause the hydration and pozzolanic reactions to occur. Figure 3-14 presents the microstructural aspects of the Tokuyama clay stabilized with BOF contents of 20 and 30%, and initial water contents of 1.5 and 2.0w_{LL}, following 28 and 90 d of curing. The reticulation structure of the amorphous C-S-H gel and platy AFm phases on all samples were observed with intergrowths of

rod-like ettringite within the flat clay structure and flocculated clay-BOF cluster. The degree of cementitious compounds, reticulation of C-S-H gel, AFm phases, ettringite, and flocculated clay-BOF clusters were more apparent with an increase in the BOF content and curing time. In Figs. 3-14 (c) and (d), it can be observed that the BOF particles were wrapped by C-S-H gels, AFm, and flocculated clay-BOF clusters. In Fig. 3-14 (c), it can be observed that the BOF particles retained their smooth surfaces, which means that the hydration reaction was rarely developed. However, in Fig. 3-14 (e), it can be observed that a dense matting of amorphous C-S-H gel and small particles covered the BOF surface. This means that the hydration reaction occurred from the BOF. From the micrographs in Fig. 3-14 (e), it was determined that the BOF is a highly reactive material that has the potential to undergo hydraulic reactions with clay clusters. Figure 3-15 illustrates the SEM micrograph of the cement-treated Tokuyama Port clay. The C-S-H and AFm forms are commonly observed with long needle-type ettringite in the cement-treated sample. The sample of cement content of 10% exhibited C-S-H gel and ettringite with large openings, and the void among the cementitious compounds was significantly larger than those of the BOF-treated clay. In case of the cement content of 20%, it can be seen that the reticulation structure of the C-S-H gel and platy AFm phases became more evident with an increase in the cement content, and denser than those of the BOF-treated clay. Figure 3-16 presents the typical EDS analysis with the identified chemical elements of the small particles in the activated BOF of Fig. 3-14 (e). From the EDS analysis results in the yellow area of the SEM micrographs, magnified 10000 times, the dominant chemical elements are oxygen (O) and calcium (Ca). Therefore, it is considered that the small particles on the BOF surface were calcium oxide (CaO), which was found to exist around the BOF.

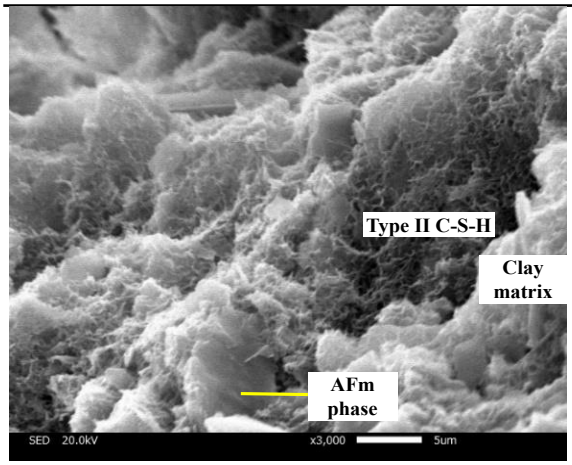

(a) $w' = 1.5w_{LL}$, $BOF_{Vol.} = 20\%$, $T = 28$days

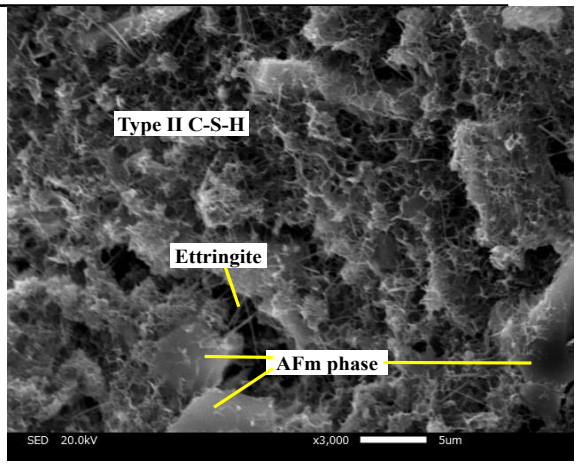

(b) $w' = 1.5w_{LL}$, $BOF_{Vol.} = 20\%$, $T = 90$days

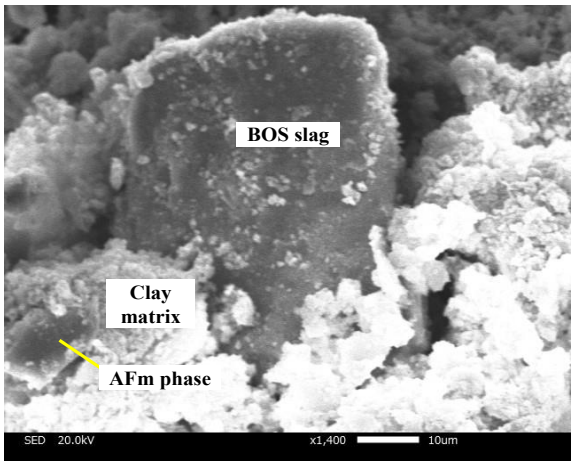

(c) $w' = 1.5w_{LL}$, $BOF_{Vol.} = 30\%$, $T = 28$days

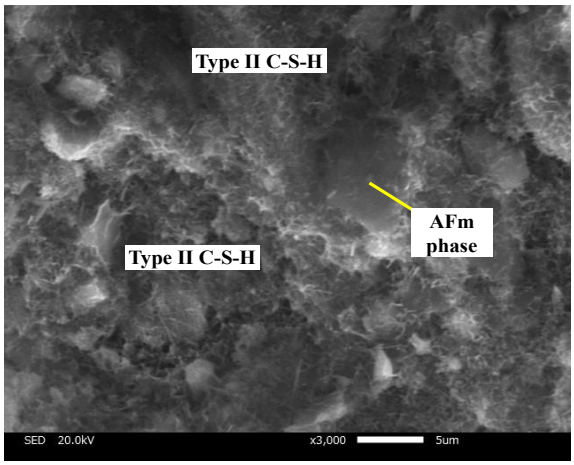

(d) $w' = 1.5w_{LL}$, $BOF_{Vol.} = 30\%$, $T = 90$days

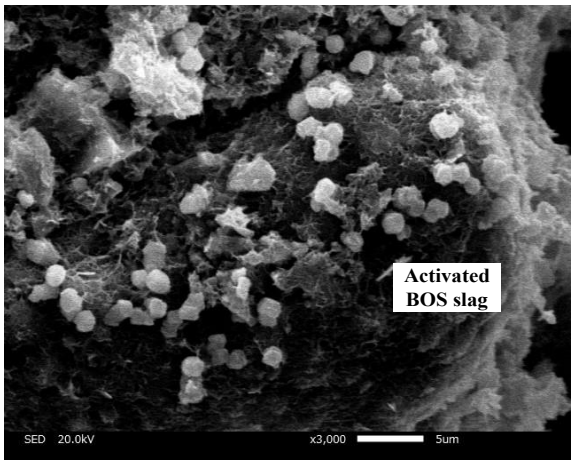

(e) $w' = 2.0w_{LL}$, $BOF_{Vol.} = 20\%$, $T = 28$days

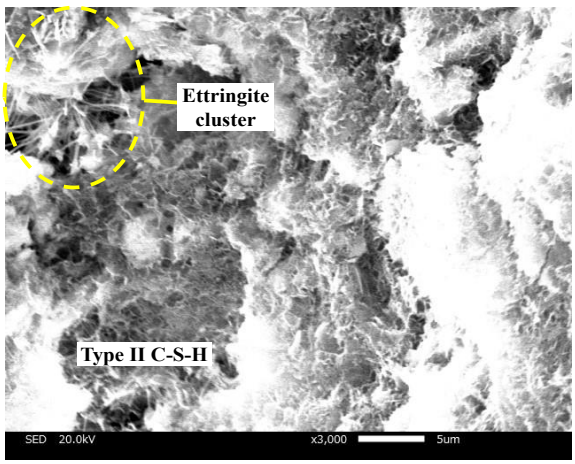

(f) $w' = 2.0w_{LL}$, $BOF_{Vol.} = 20\%$, $T = 90$days

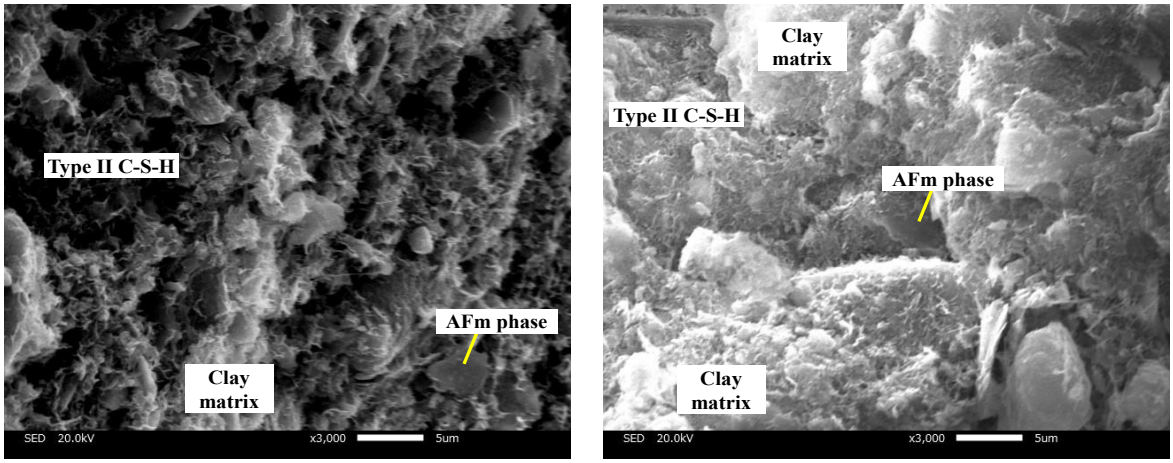

(g) $w' = 2.0w_{LL}$, $BOF_{Vol.} = 30\%$, $T = 28$days (h) $w' = 2.0w_{LL}$, $BOF_{Vol.} = 30\%$, $T = 90$days

Figure 3- 14SEM micrographs representatives of SMSS.

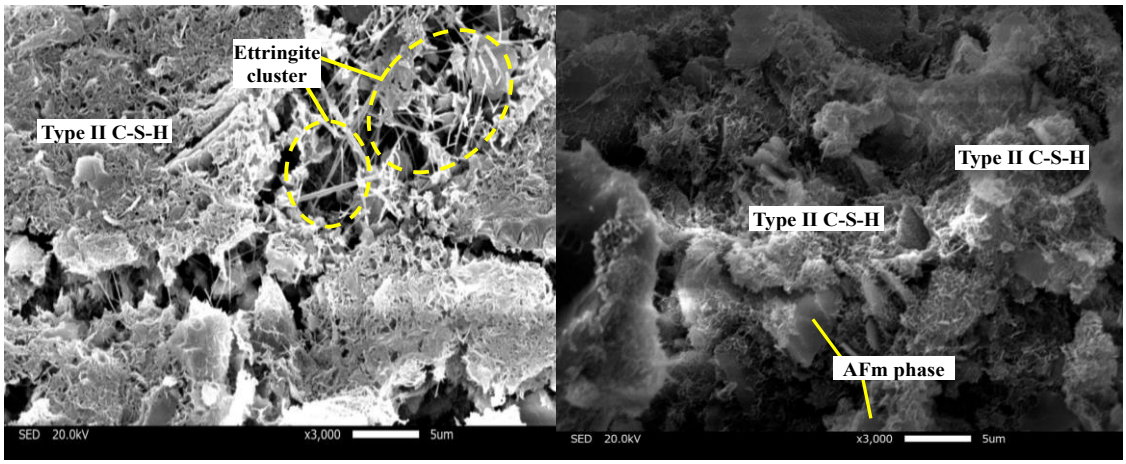

(a) $w' = 1.5w_{LL}$, cement content = 10%, $T = 28$days (b) $w' = 1.5w_{LL}$, cement content = 20%, $T = 28$days

Figure 3- 15 SEM micrographs of cement-treated Tokuyama Port clay

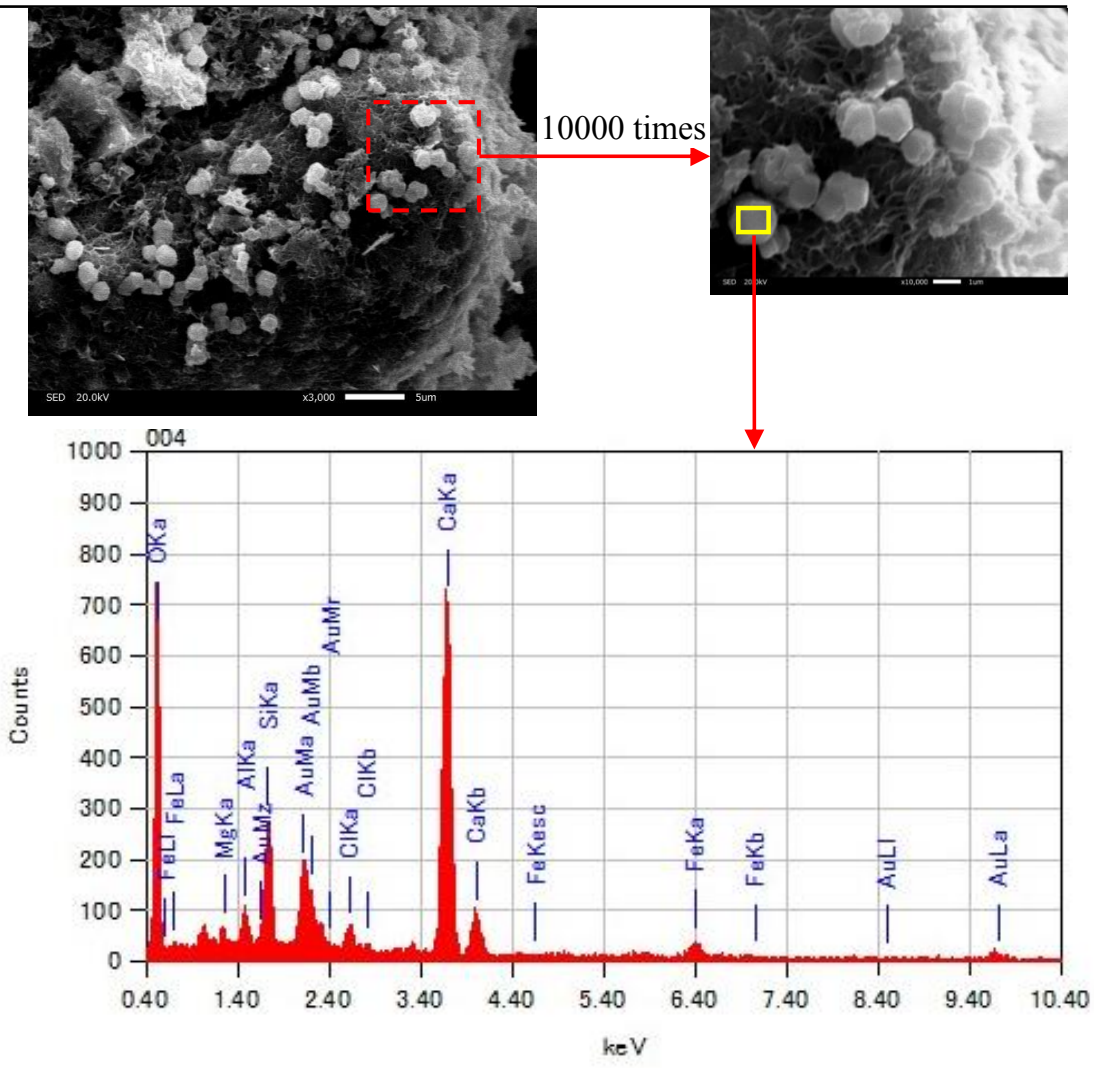

Figure 3- 16 EDS analysis of small particles on BOF

3.4 Conclusions

An investigation into the strength development and microstructural properties of BOF-treated dredged clay had been presented in this paper. Based on the results of the strength and SEM micrograph analyses in this study, the following conclusions are summarized:

1. The flow value exhibited a strong correlation with the undrained shear strength of the stabilized soils, which may be a significant variable for determining the flowability of the stabilized dredged clay with BOF slag.
2. A dormant period was observed, in which the strength of the stabilized soil with BOF slag do not increase between the 0.5 and 2 h curing times. The strength

development can be classified into three zones, according to the strength increment rates; 1) inactive zone (0.5 to 5 h), 2) active zone (5 h to 3 d), and 3) moderate zone (after 3 days).

3. For the inactive zone, the equation for estimating the strength was proposed according to the volumetric solid content, initial water content, and strength increment rate. The strength in the active and moderate zones could be estimated based on the equation consisting of the normalized specific volume (v'/v_{LL}) and strength increment rates for each of the active and moderate zones.
4. The rate of strength increment of the stabilized soil changed according to the active and moderate zones. Moreover, the value and range of the strength increment rate varied with the type of binder, BOF, and cement. For the active zone, the increment rate of the BOF strength increased significantly with an increase in the BOF mass due to the hydration reaction. The rate of strength increment in the moderate zones differed with the change in the BOF slag content. Based on this result, the effect of the pozzolanic reaction in increasing the strength at the long-term curing time can be changed with the R_{BOF} content.
5. The reticulation structures of the amorphous C-S-H gel and platy AFm phases on all samples were observed with rod-like intergrowths. The degree of cementitious compounds became more evident with an increase in the R_{BOF} content and curing time. The C-S-H gel and ettringite with large openings, and the voids among the cementitious compounds of the BOF-treated clay, differed compared to cement-treated clay.

3.5 References

Act on the Prevention of Marine Pollution and Marine Accidents in Article 5, Section 1. 1973. (in Japanese).

Ahmedzade, P., Sengoz, B., 2009. Evaluation of steel slag coarse aggregate in hot mix asphalt concrete. Journal of Hazardous Materials. 165, 300–305.

Arribas, I., Vegas, I., San-Jose, J. T., Manso, J. M., 2014. Durability studies on steelmaking slag concretes. Materials and Design. 63, 168–176.

Asi, I. M., 2007. Evaluating skid resistance of different asphalt concrete mixes. Build. Environ. 42, 325–329.

Belhadj, E., Diliberto, C., Lecomte, A., 2012. Characterization and activation of Basic Oxygen Furnace slag. Cement & Concrete Composites. 34, 34–40.

Deng, Y. F., Zhang, T. W., Zhao, Y., Liu, Q. W., Wang, Q., 2017. Mechanical behavior and microstructure of steel slag-based composite and its application for soft clay stabilization. European Journal of Environmental and Civil Engineering. 21, 1–16.

Guidebook for Oceanographic Application of Converter Slag, 2008 (in Japanese).

Horpibulsk, S., Rachan, R., Suddeepong, A., Chinkulkijniwat, A., 2011. Strength development in cement admixed Bongkok clay: laboratory and field investigations. 51 (2), 239–251.

Horii, K., Tsutsumi, N., Kitano, Y., Kato, T., 2013. Processing and reusing technologies for steelmaking slag. Nippon Steel Technical Report. 104, 123–129.

JGS 0211 2009. Test method for pH of suspended soils (in Japanese).

JHS A 313 1992. Cylinder method for consistency test, Japan Road Association (in Japanese).

JIS A 1216 2008. Method for Unconfined Compression Test of Soils (in Japanese).

Kang, G-O., Tsuchida, T., Athapaththu, A. M. R. G., 2016. Engineering behavior of cement-treated marine dredged clay during early and later stages of curing. Engineering Geology. 209, 163–174.

Kang, G-O., Tsuchida, T., Kim, Y-S., 2017. Strength and stiffness of cement-treated marine dredged clay at various curing stages. Construction and Building Materials. 132, 71–84.

Kang, G-O., Tsuchida, T., Kim, Y-S., Baek, W-J., 2017. Influence of humic acid on the strength Behavior of cement-Treated clay during various curing stages. Journal of Materials in Civil Engineering. 29 (8), 8 pages.

Kinoshita, H., Ichii, K., Morikawa, H., Takahashi, H., Shinozaki, H., Takahashi, Y., 2012. Characteristics and assessment of seismic behavior of improved ground by sand compaction pile method using iron and steel slag as base of gravity caisson structure. Japanese Geotechnical Journal. 7 (1), 323–337 (in Japanese).

Kitazume, M., Terashi, M., 2013. The deep mixing method. CRC press Taylor & Francis Group, London, UK.

Lee, A. R., 1974. Blastfurnace and steel slag: Production, properties and uses, Edward Arnold, London.

Liu, S., Wang, Z., Li, X., 2014. Long-term properties of concrete containing ground granulated blast furnace slag and steel slag. Magazine of concrete Research. 66 (21), 1095–1103.

Lorenzo, G. A., Bergado, D., 2004. Fundamental parameters of cement-admixed clay–new approach. Journal of Geotechnical and Geoenvironmental Engineering. 130 (10), 1041–1050.

Mahieux, P. Y., Aubert, J. E., Escadeillas, G., 2009. Utilization of weathered basic oxygen furnace slag in the production of hydraulic road binders. Construction and Building Materials. 23, 742–747.

Miura, N., Horpibulsk, S., Nagaraj, T. S., 2001. Engineering behavior of cement stabilized clay at high water content. Soils and Foundation. 41 (5), 33–45.

Ministry of Transport, The Fifth District Port Construction Bureau, 1999. Pneumatic flow mixing method (in Japanese).

Pasetto, M., Baldo, N., 2010. Experimental evaluation of high performance base course and road base asphalt concrete with electric arc furnace steel slags. Journal of Hazardous Materials. 181, 938–948.

Poh, H. Y., Ghataora, G. S., Chazireh, N., 2006. Soil stabilization using basic oxygen steel slag fines. Journal of Materials in Civil Engineering. 18 (2), 229–240.

Qiang, W., Mengxiao, S., Jun, Y., 2016. Influence of classified steel slag with particle sizes smaller than 20 μm on the properties of cement and concrete. Construction and Building Materials. 123, 601–610.

Rondi, L., Bregoli, G., Sorlini, S., Cominoli, L., Collivignarelli, C., Plizzari, G., 2016. Concrete with EAF steel slag as aggregate: A comprehensive technical and environmental characterization. Composites Part B. 90, 195–202.

Scrivener K. L., 1991. The microstructure of concrete. Materials Science and Concrete (Skalny JP (ed.)). American Ceramic Society, Westerville, OH, USA, 127–161.

Seng, S., Tanaka, H., 2011. Properties of cement-treated soils during initial curing stages. Soils and Foundations. 51 (5), 775–784.

Shen, D. H., Wu, C. M., Du, J. C., 2009a. Laboratory investigation of basic oxygen furnace slag for substitution of aggregate in porous asphalt mixture. Construction and Building Materials. 23, 453–461.

Shen, W. G., Zhou, M. K., Ma, W., Hu, J. Q., Cai, Z., 2009b. Investigation on the application of steel slag–fly ash–phosphogypsum solidified material as road base material. Journal of Hazardous Materials. 164 (1), 99–104.

Shi, C. J., Qian, J. S., 2000. High performance cementing materials from industrial slags–A review. Resources, Conservation Recycling. 29, 195–207.

Shi, C., 2004. Steel slag–its production, processing, characteristics, and cementitious properties. Journal of Material in Civil Engineering, ASCE. 16, 230–236.

Tang, Y. X., Miyazaki, Y., Tsuchida, T., 2001. Practices of reused dredging by cement treatment. Soils and Foundations. 41 (5), 129–143.

Takahashi, H., Morikawa, Y., Shinozaki, H., Kinoshita, H., Maruyama, K., 2011. Ground stability against backfill loading of SCP improved ground using solidified iron–and–steel slag. Japanese Geotechnical Journal. 6 (1), 81–95 (in Japanese).

Technical Manual of Pre-Mix Vessels Method, 2013. Association of Pre-Mix Vessels Method (in Japanese).

The Japan Iron and Steel Federation: Guidebook for Oceanographic Application of Converter Slag. 2008 (in Japanese).

Tsuchida, T., Tang, Y. X., Watabe. Y., 2007. Mechanical properties of lightweight treated soil cured in water pressure. Soils and Foundations. 47 (4), 731–748.

Wang, G., Wang, Y., Gao, Z., 2010. Use of steel slag as a granular material: Volume expansion prediction and usability criteria. Journal of Hazardous Materials. 184, 555–560.

Watabe, Y., Noguchi, T., 2011. Site-investigation and geotechnical design of D-runway construction in Tokyo Haneda Airport. Soils and Foundations. 51 (6),

1003–1018.

Wilkinson, A., Haque, A., Kodikara, J., 2010. Stabilisation of clayey soils with industrial by-products: part A. Ground Improvement. 163 (G13), 149–163.

Xue, Y., Wu, S., Hou, H., Zha, J., 2006. Experimental investigation of basic oxygen furnace slag used as aggregate in asphalt mixture. Journal of Hazardous Materials. 138 (16), 261–268.

Chapter 4

Particle Size Effect of Basic Oxygen Furnace Steel Slag in Stabilization of Dredged Marine Clay

TABLE OF CONTENTS

4.1 Introduction

A large body of research shows that Portland cement assures the quality and durability of the stabilization of dredged marine clay. However, Rubenstein (2012) claimed that not only did the manufacture of Portland cement consume energy and resources, but its production and usage were responsible for five percent of total carbon monoxide emitted around the world. Therefore, a sustainable stabilizer such as basic oxygen furnace (BOF) slag is proposed to replace Portland cement in treating the dredged marine clay.

Steel slag is generally considered to be a by-product and is classified into two types based on its processing flow. These are BOF slag from an iron-to-steel conversion and electric arc furnace (EAC) slag, from the melting of scrap in steel manufacturing (Shi, 2004). Studies have shown that BOF slag constituent minerals such as free-lime (f-CaO) or free-periclase (f-MgO) could cause volume instability and have lower cementitious properties (Wachsmuth et al., 1981; Wang et al., 2010; Yildirim and Prezzi, 2011). Most applications of BOF slag in civil works were intended to diminish the free lime content or add an activator rather than to benefit from it.

BOF slag has limited cementitious properties due to both a lack of tricalcium silicate (C_3S) and the presence of wustite solid solution (FeO) as the main mineral. Murphy et al. (1997) offered multiple ways of enhancing the cementitious product in steel slags such as FeO adjustment to Fe_2O_3 by an oxidation process and water quenching in the cooling process of steel slag. Montgomery and Wang (1991) reported the effect of adding instant-chilled slag (ICS) in concrete strength which gave greater indirect tensile and flexural strengths than those of corresponding control concrete containing limestone aggregate. Those treatments for enhancing the cementitious properties caused additional procedures before steel slag could be utilized.

Ahmedzade and Sengoz (2009) studied the influence of steel slag on the mechanical properties and electrical conductivity of asphalt concrete mixtures. It was found that steel slag as a road construction aggregate produced a better resistance to permanent deformation and greater stiffness in hot mixed asphalt (HMA) concrete than limestone. Kandhal and Hoffman (1997), however, suggested that steel slag

could only replace either fine or coarse aggregates and that encouraging a 100% replacement would cause over-asphalting and in-service traffic compaction, resulting in flushing. Previous studies (Kandhal and Hoffman, 1997; Wang et al., 2010) indicated that it is quite difficult to use BOF slag aggregate since various treatment are required prior to its usage to diminish the volume instability (long-term expansion). For concreting purposes, the replacement of limestone with steel slag gave a significantly longer time for concrete to initiate reinforcement corrosion and to crack, however the steel slag could only replace up to 50% of the function of limestone due to its large bulk density (1.4 times higher than limestone). Thus, the application of BOF slag as an aggregate in road construction and concrete still requires supplementary sources such as limestone.

The use of steel slag for various purposes has been confirmed as safe for humans, and environmentally friendly. Proctor et al. (2000) showed BOF slag to be a non-hazardous material to human health and the environment by performing various tests. Nevertheless, the avoidance of using various slag types and sources for a single purpose was suggested because it is easier to perform a risk assessment. There was potential for metals to leach from slag and migrate through the air because the larger particle size of steel slag would be exposed to weathering processes and become smaller particles. Such a phenomenon may only occur in an air-exposed application, but for other purposes such as fill, landscape, submerged fill and reducing the accessibility of slag for suspension, it will be sufficiently safe for the environment. Motz and Geiseler (2001) also highlighted the non-hazardous potential from BOF slag for the environment because results from a leachate test showed no significant impact other than an increasing pH due to the partial solution of free lime.

Little attention has been paid to the selection of BOF slag as a stabilizer for high moisture content soil without prior free lime reduction. Other research of BOF slag, such as on road material (Shen et al., 2009a; Shen et al., 2009b) and hydraulic structure “armourstones” (Motz and Geiseler, 2001) found it an advantageous method to recycle the steel slag prior to its weathering process. Mahieux et al. (2009) and Poh et al. (2006) focused on BOF slag in a study using compaction and optimum water content or less moisture content, which are inappropriate for dredged marine clay stabilization purposes.

In Japan, the significant difference between laboratory results and actual field investigations was one of the most common problems in soft soil stabilization using

BOF slag. There are no standards for correlating the strength obtained from laboratory and field test results. Despite the same quantity of addition, the same free-lime content, or characteristics of BOF slag used in both laboratory and field investigations, often the maximum grain-size used in field construction was much larger than in the laboratory. The reasons for this practice were the time-consuming nature of the tests, and limited resources, including the absence of large-scale strength apparatus, and limited clay and BOF slag samples for large-size samples.

The present study provides a set of general characteristics of the dredged marine clay, the BOF slag, the stabilized dredged marine clay, and the strength development of stabilized dredged marine clay using various maximum grain-sizes of BOF slag. The effects of a different maximum grain-size of BOF slag on the strength development of stabilized dredged marine clay was also studied. This is helpful for accurately predicting the strength development of BOF slag treated clay in field constructions using laboratory-strength-test results. Previous studies based on field construction investigations were also compared with this study to further understand the factors that significantly affect the strength development of the stabilized dredged marine clay with BOF slag.

4.2 Experimental design

The experiment was conducted in two stages. The physical properties of Tokuyama Port dredged marine clay and BOF slag were initially characterized. The primary aim of the experiment was to measure the strength development of stabilized soils by conducting a number of shear strength tests; a laboratory vane shear (LVS) test and an unconfined compressive (UC) test. These were performed as described below. Flow value tests were also conducted for each different mix proportion.

4.2.1 Materials

The dredged marine clay used for this investigation was drawn from the sea bottom of Tokuyama Port, Yamaguchi prefecture, Japan. Tokuyama Port marine clay had an initial moisture content, w_n, equal to 0.9–1.0 of its liquid limit, w_L. Using a grab-type dredger, the moisture content of the marine clay increased 1.2 to 1.3 times (Terashi and Katagiri, 2005). The dredged marine clay was highly plastic, with a liquid limit of 107.2% and a plastic limit of 38.6%. It had 90.0% fines content and a specific gravity

of (G_s) 2.65. The measured average organic matter was 8.2%, and salinity was 3.5%. The laboratory results of Tokuyama marine clay are summarized in Table 1.

Figure 4- 1 BOF slag with maximum grain-size <37.5 mm.

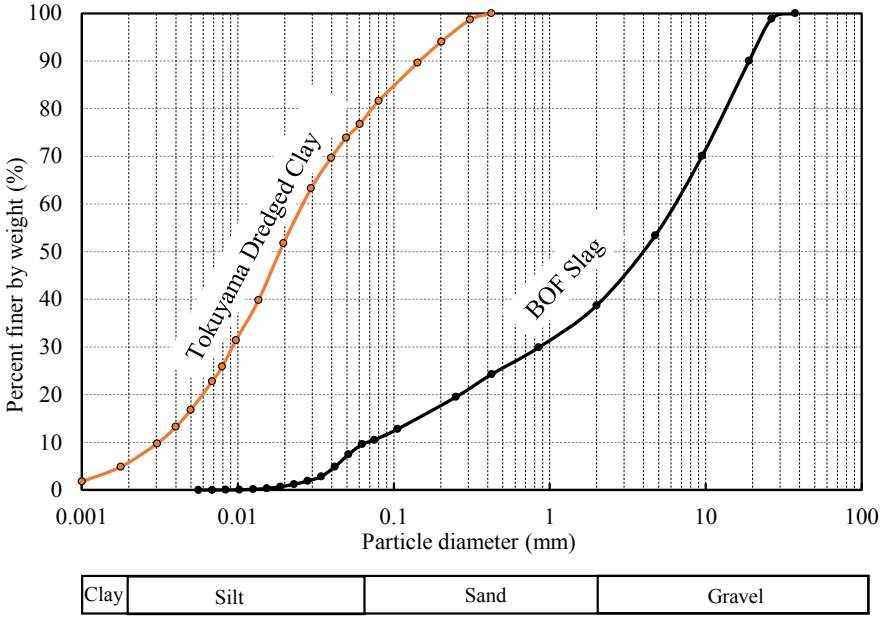

Figure 4- 2 Grain-size distribution of Tokuyama port clay and the BOF slag.

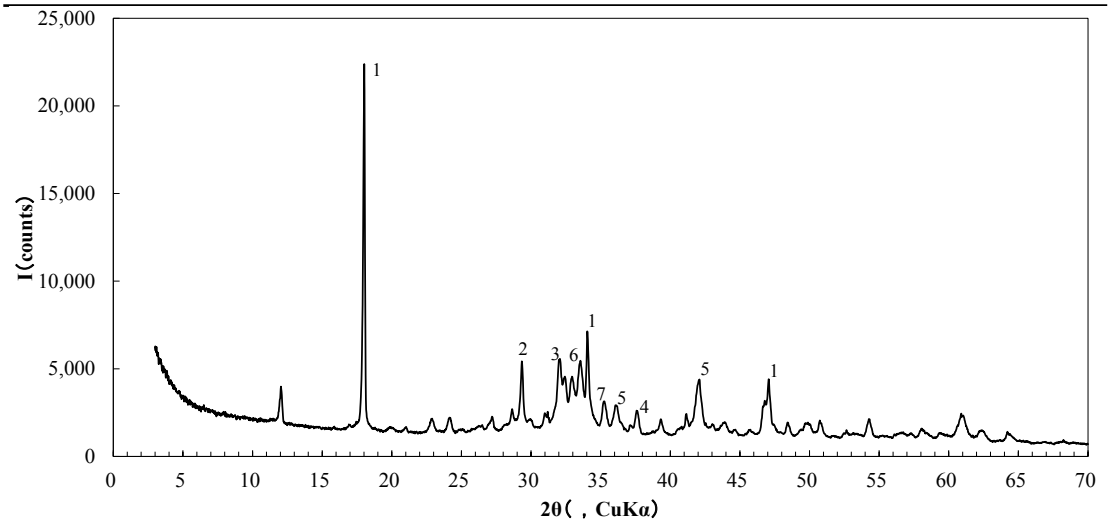

Figure 4- 3 X-ray diffraction result of BOF slag. [1]Portlandite; [2]Calcite; [3] Larnite; [4]Lime; [5]Wustite; [6]Srebodolskite; [7]Magnetite.

Fresh BOF slag was acquired from a single batch and supplied by the Fukuyama Facility of JFE Steel Corporation. The BOF slag was ground from its natural size to a grain-size distribution shown in Figure 4-1. No chemical pre-treatment was applied to the BOF slag. Its physical properties are listed in Table 2. Each sealed pack contained granular material with a maximum particle size of less than 37.5 mm and with 8.4% initial average moisture content. The grain-size distribution of BOF slag consisted of 10.5% fine particles (Figure 4-2). The BOF slag had a 3.19 g/cm^3 surface dry density and a 3.08 g/cm^3 absolute dry density. The water absorption rates of BOF slag were 4.6% and 2.5% for coarse aggregate and fine aggregate, respectively. An ethylene glycol method was performed to determine 8.49% of free lime.

X-ray fluorescence and X-ray diffraction tests were conducted to acquire the elemental composition and crystalline components of BOF slag, and compare the results with other types of BOF slag from previous studies (Murphy et al., 1997; Shi, 2004) (Table 3). In this study, the total amount of main elements determined, such as calcium oxide, iron, and silicon oxides were similar to those reported in previous studies. The crystalline components of BOF slag (Figure 4-3) also exhibited a similar composition, for example Portlandite ($Ca(OH)_2$), Srebrodolskite (Ca_2FeO_5), Calcite ($CaCO_3$), Larnite (Ca_2SiO_4), Lime (CaO), Wustite (FeO) and magnetite (Fe_3O_4). It is notable that the chemical constituents of BOF slag may be highly variable depending on the raw materials and manufacturing process.

Table 4- 1 Geotechnical and physical properties of Tokuyama Port Clay.

Property	Value
Liquid limit, (w_L) %	107.2
Plastic limit, (w_P) %	38.6
Plastic index, (*PI*) %	68.5
Particle density, (*Gs*) g/cm^3	2.65
Coarse-grained Soil (>75 μm), %	9.9
Fine-grained size (<75 μm), %	90.0
Unified Soil Classification System (USCS)	CH-OH
pH	7.2
Ignition loss, (*LOI*) %	8.2

Table 4- 2 Physical properties of Basic Oxygen Furnace slag.

Property	Value
Initial moisture content, %	8.4
Average of specific gravity, g/cm^3	3.15
Specific gravity of coarse aggregate <4.75 mm	2.96
Specific gravity of fine aggregate <4.75 mm	3.23
Absolute dry density, g/cm^3	3.02
Water Absorption rate of coarse aggregate, %	4.6
Water Absorption rate of fine aggregate, %	2.5
Maximum size of aggregate, mm	37.5
Coarse-grained size (>75 μm), %	89.5
Fine-grained size (<75 μm), %	10.5
Free CaO, (f-CaO), %	8.49

Table 4- 3 BOF slag composition (weight, %)

Chemical	BOF slag in this study	BOF slag[a]	BOF slag[b]
SiO_2	14	8–20	15
Al_2O_3	2.6	1–6	5
Fe_2O_3	33	10–35	29
CaO	41	30–55	38
MgO	2.3	5–15	6.5
MnO	3	2–8	5
TiO_2	0.41	0.4–2	1
S	0.031	0.05–0.15	n/a
P	3	0.2–2	0.5
Cr	0.12	0.1–0.5	n/a

[a]shi et.al (2004)
[b]Murphy et.al (1997)

4.2.2 Sample preparation and curing

To begin the sample preparation, the dredged marine clay was thoroughly separated from coarse particles such as coral reef and shells using a 2 mm sieve. Filtered clay was then hermetically stored in a box to avoid redundant moisture change prior to sample mixture. Before it could be sifted using various sieves to acquire different maximum grain-sizes, the BOF slag was air dried for 24 h at 20 ± 2 °C in a room at 60% humidity. The designed-grain-size BOF slag was then wrapped in a plastic bag to avoid free-lime loss due to contact with the air (Yildirim and Prezzi, 2015). Pre-cooled artificial seawater with 3.5% salinity was added to the dredged clay to achieve initial a setting water content of $w_0 = 1.5\ w_L$. The dredged marine clay and BOF slag with specific mix proportions (Table 4) were then blended for five minutes using a heavy-duty hand mixer, to produce a uniform soil-mixture. The particle segregation was not seen after the mixing process. Katayama and Tsuchida (2015) reported that the significant segregation do not occur in soil mixture (soil slurry and BOF slag) if the grain-size of BOF slag is less than 25.5 mm.

Immediately after mixing, the sample was gradually poured into the molds by applying light tapping for every three layers to eliminate trapped-air inside the soil mixture. The BOF slag addition (R_{BOF}) was determined by volumetric ratio calculated using Equation 1:

$$R_{BOF} = \frac{V_{BOF}}{V_{soil} + V_{water} + V_{BOF}} \times 100 \qquad (\%) \qquad (1)$$

where V_{BOF} is the solid volume of BOF slag, V_{soil} is the solid volume of soil, and V_{water} is the volume of water. To verify a delicate mixture, the sample unit weight in the mold was compared with its calculated unit weight.

For the strength tests in this study, two types of acrylic cylindrical molds and two types of tinplate molds were utilized (Table 5). Two different sizes of acrylic molds, ø60 mm × 60 mm for BOF slag < 10 mm and ø140 mm × 80 mm for BOF slag < 37.5 mm were adopted for the LVS test and placed in a room at 20 ± 2 °C and 60% relative humidity. Two different sizes of tinplate molds were utilized for the UC test which were ø50 mm × 100 mm for BOF slag < 10 mm and ø100 mm × 200 mm for

BOF slag < 37.5 mm. The samples in the tinplate molds were submerged with both top and bottom ends exposed to distilled water at 20 ± 2 °C.

4.2.3 Tests Performed

4.2.3.1 Flow test

The flow value test was originally a standard test in Japan (JHS A 313) to determine the workability of concrete, but recently it has also been utilized to understand the workability and flowability of stabilized material for the pipe-transportation purpose in embankment construction. The flow value test is a simple measurement of the spreading diameter of slumped soil mixture. Soil mixture was poured into the acrylic mold (⌀80 mm × 80 mm) that had been previously lubricated with a thin-layer of oil, then during the filling process, bubbles were carefully removed by applying a light tapping at the side of the mold. The excessive mixture was trimmed. Finally, the cylindrical mold was lifted, and after one minute, the average diameters at both perpendicular axes were measured to obtain the flow value.

4.2.3.2 Laboratory vane shear test

The LVS test, a scaled-down version of the field vane shear test (JGS 1441-2012) was adapted to measure a low strength sample (Figure 4-4). Samples that had been pre-cured for 0.5 to 15 h in the acrylic molds (Figure 4-5) were tested using six degrees/minutes of rotation speed. A rectangular vane was attached where the height × diameter varied from 20 × 20 mm to 40 × 60 mm, with a thickness of 0.8 mm (Table 5). Tests were constantly terminated after the vane had rotated 60 degrees or when the sample had reached the peak of measured torque. From the measured torque, undrained shear strength, S_u was obtained using the following equation:

$$S_{uVane} = \frac{M}{\pi\left\{\left(D^3/6\right)+\left(HD^2/2\right)-\left(d^3/12\right)+\left(d^2La/2\right)\right\}} \quad (2)$$

where M is torque produced by the vane blade and D is the diameter of the vane, H is the height of the vane, d is the diameter of the shaft, L is the contacted length of the vane shaft, and a is the friction coefficient of the shaft, the value is 1. In this equation, it is assumed that the friction between the vane shaft and the soil is equal to the shear strength, S_{uvane}.

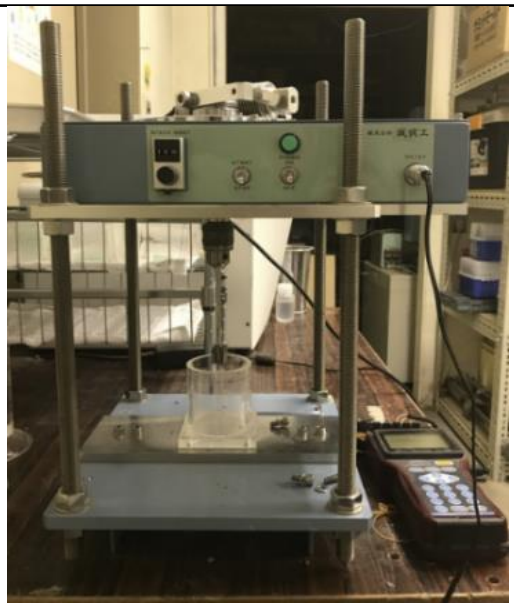

Figure 4- 4 Laboratory vane shear test apparatus.

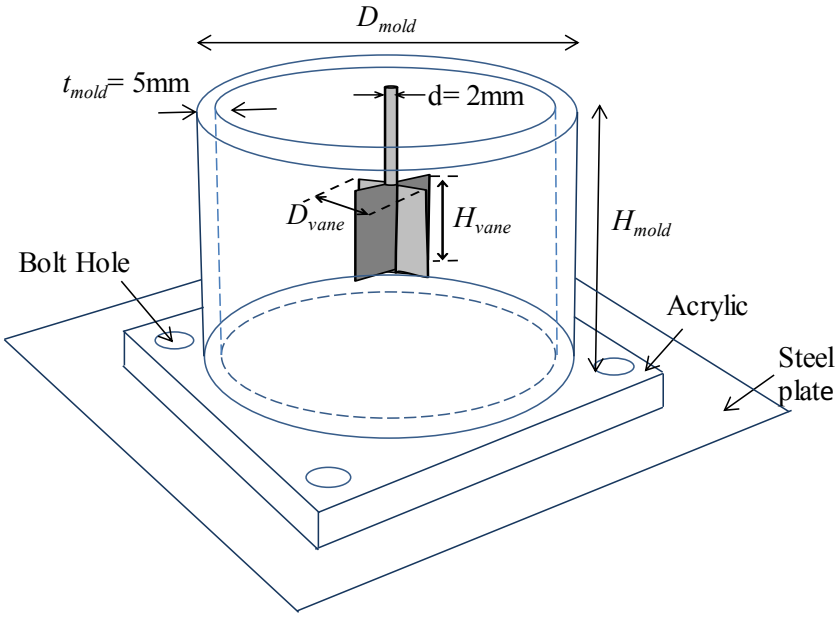

Figure 4- 5 Mold dimension of laboratory vane shear test.

An oversized correction was applied to the specimens with particle sizes of 9.5–37.5 mm to avoid any additional strength caused by the contact between large particles and the vane blade because the diameter of the vane blade was limited to 60 mm. The material retained on the 19 mm sieve was discarded and replaced with an equal amount of material passing 19 mm and retained at 9.5 mm.

Table 4- 4 Mix proportion and curing time of the stabilized soils with BOF slag.

Normalized clay water content (w/w_L)	R_{BOF} (%)	Maximum particle size	Curing Time
1.5 (160.72%)	20, 30	<0.89mm, <2mm, <4.75mm, <9.5mm	0.5h, 2, 5, 7, 10, 15 (hours) 1, 2, 3, 7, 28, 90 (days)
1.5 (160.72%)	20, 30	<37.5mm	0.5h, 2, 5, 7, 10, 15 (hours) 1, 2, 3, 5, 7, 14, 28, 90 (days)
1.5 (160.72%)	30	0.85-9.5mm, 2-9.5mm, 4.5-9.5mm 9.5-37.5mm	1, 3, 7, 28, 90 (days)

Table 4- 5 Samples mold size for LVS test and UC test, and Vane Blade size.

BOF slag addition Maximum Particle Size (mm)	Size LVS sample Diameter (mm) x Height (mm)	Size UC sample Diameter (mm) x Height (mm)	Size of Vane Blade Diameter (mm) x Height (mm)
<0.89 <2.00 <4.75 <9.5	60 x60	50x100	20x20
<37.5	140x80	100x200	40x60
0.85-9.5 2-9.5 4.75-9.5	n/a	50x100	n/a
9.5-37.5	n/a	100x200	n/a

4.2.3.3 Unconfined Compressive test

The UC test, which is a common test to measure the soil shear strength, was selected in this experiment due to its effortlessness, economy, and less time-consuming features. The UC test was accurately performed as per the Japanese code (JGS 0511-2014). An automatic loading machine with load cell capacities of 2 kN, 5 kN, and 20 kN and a linear variable differential transformer (LVDT) were vertically attached to measure stress-strain of the samples. Both ends of the sample surfaces were carefully trimmed and aligned to a ±1 mm tolerance before the testing proceeded.

To retain the maximum ratio of particle size to diameter = 1/6 (ASTM D2166-16), a larger mold ⌀100 mm × 200 mm was used for the sample, with a maximum

particle size of BOF slag of less than 37.5 mm. Constant strain rate = 0.5–1% per min was accounted for in performing the UC test on every three samples of the 15 h to 90 d curing time. For the acceptance criteria, the standard deviation between two specimens with the same mix proportion should not exceed 10% of the mean strength.

4.3 Results and Discussions

4.3.1 Unit weight

Figure 4-6 provides an overview of the unit weight of stabilized soils as a function of the 20–30% addition rate of BOF slag at identical initial water content 1.5 w_L. In soil mixtures with the grain-size 0–2 mm, the 20–30% addition rate increased the unit weight to 16.36–18.04 kN/m^3. For soil mixtures mixed with 0–4.75 mm and 0–9.5 mm of maximum grain size, the 20–30% addition rate increased the unit weight to 16.56–18.35 kN/m^3, and 16.78–18.68 kN/m^3, respectively. Soil mixtures with grain-size 0–37.5 mm produced 16.84–18.72 kN/m^3 of unit weight. From the results, it is clear that the 10% difference rate of BOF slag addition produced approximately 1.1 times higher unit weight at any particle size.

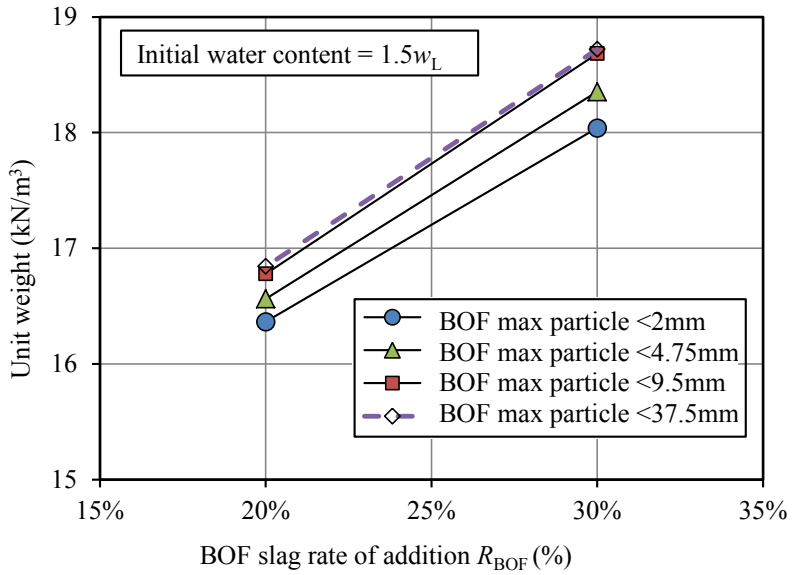

Figure 4- 6 The measured unit weight of the stabilized soils with BOF slag.

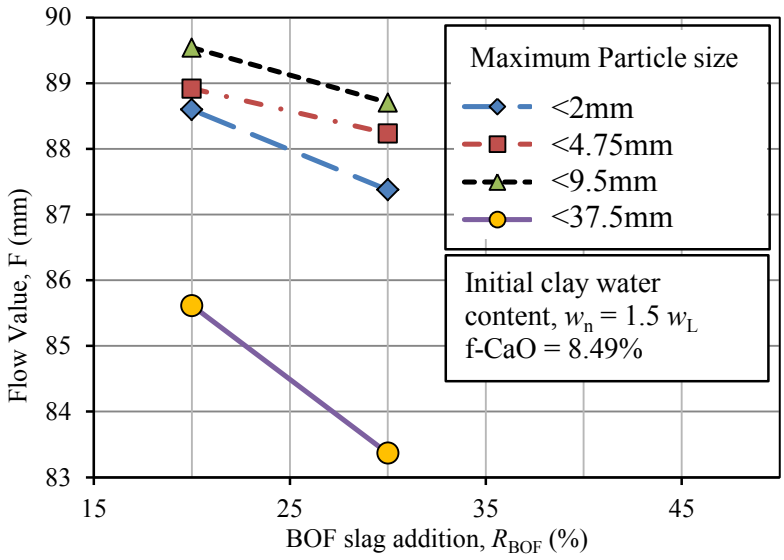

Figure 4- 7 Flow value of the stabilized dredged marine clay with different BOF slag rate of addition and maximum particle size.

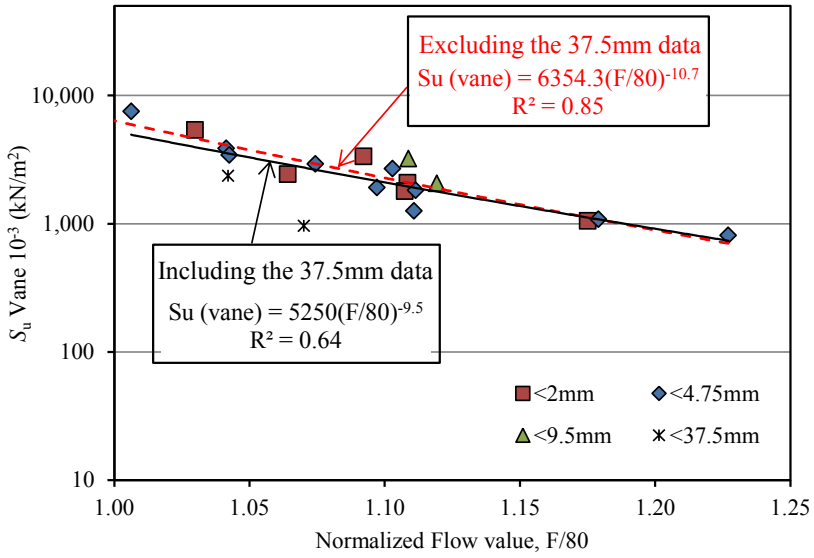

Figure 4- 8 Normalized flow value to vane shear strength at immediate curing time of the stabilized clay using BOF slag.

Despite the same addition rate and initial water content, a larger maximum grain-size of BOF slag produced a larger unit weight value. This increased unit weight was due to the different initial dry density of BOF slag. A 0–4.75 mm grain-size had 2.96 g/cm^3 and a 4.75–37.5 mm grain-size had 3.23 g/cm^3 of dry density. The stabilized soils with large unit weights would be advantageous as a counterweight element in filling construction.

4.3.2 Flow Value

Figure 4-7 shows the result of the flow value test as a function of BOF slag addition at various maximum grain-sizes with the same initial clay water content $w_n = 1.5\ w_L$. It indicates that the larger maximum particle size tends to produce a larger flow value of stabilized soils at the same initial moisture content, except for BOF slag with 37.5 mm maximum grain-size. The larger flowability is related to a larger dry density of BOF slag, which produces a higher self-weight of mixtures. It is believed that the different particle size of BOF slag will significantly affect the flow value. This causes the pipe-distribution to be more difficult due to a lower flowability. Therefore, in adopting the larger particle size of BOF slag, the appropriate amount of addition rate and initial water content should be taken into consideration to reach a delicate flow value.

There is a significant relationship between the flow value and immediate shear strength of the stabilized soils using BOF slag (Figure 4-8). However, this result did not agree with the data of BOF slag which included the particle size larger than 37.5 mm (Figure 4-8). This is likely due to a small cylinder 80 mm × 80 mm of flow test which has an unsuitable ratio due to the large particle size of 37.5 mm. As a result, the flow value test is not a suitable test to determine the flow value of the granular material with the over-sized particle.

4.3.3 Stress-Strain Curve

The stress-strain curve of the stabilized soils using BOF Slag from 1-90 d curing time of sampling with maximum particle size 2 mm and 37.5 mm, $R_{BOF} = 30\%$ and $w_0 = 1.5\ w_L$ is shown in Figure 4-9. The strengths produced by these two types of maximum size were distinct, with the strength produced by 2 mm at 28 d being approximately 3.5 times higher than by 37.5 mm.

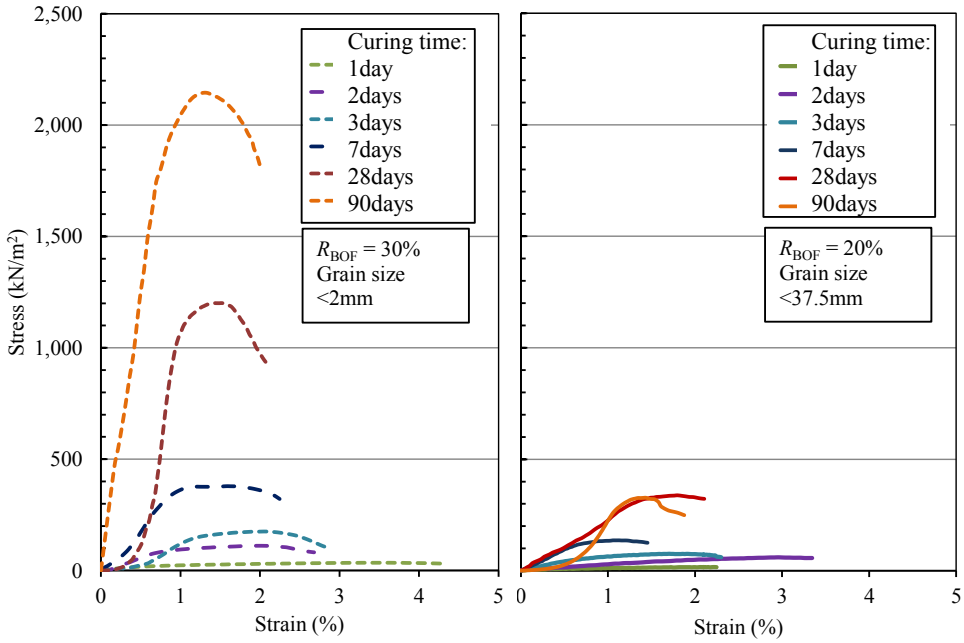

Figure 4- 9 UC test result of the stabilized soils using BOF slag with maximum particle size 2 mm and 37.5 mm.

The nature of the clay changes due to a longer curing time and becomes stronger but brittle as the BOF slag with a smaller particle size is added, is indicated by the stress-strain curve behavior (Figure 4-9). The strain at failure of smaller maximum particle size changed due to curing time. This could be divided into two types: 1) for early curing time of up to 3 d, the strain at failure was 2% or more which was similar to soft soil, and 2) for later curing time, the strain at failure was 1.2%, which was similar to stiff soil.

Unlike stabilized soils using a 2 mm particle size with greatly varied stress-strain curve shapes, the stress-strain curve shape formed by stabilized soils using a 37.5 mm particle size showed no significant shape-alteration with the change of curing time. The strain at failure of larger grain-sizes showed greater values of 1.5–2.5%, which was generally similar to soft clay.

4.3.4 Time-Strength Mobilization

Basic oxygen furnace slag is a chemically-active material. Shi (2004) reported that the presence of C_3S, C_2S, C_4AF in steel slag endorsed the cementitious properties of steel slag. Based on the components of BOF slag, it was suggested that the strength mechanism of dredged clay stabilized with BOF slag is a hydration reaction due to the

presence of mineral components such as C_2S, C_3S, C_4AF, and the pozzolanic reaction obtained between the portlandite ($Ca(OH)_2$) and silica and alumina minerals resolved in clay.

Importantly, in this study, the free lime content in the stabilized soils was recorded to be very high, being 8.49%. According to Shi (2004), and Yildirim and Prezzi (2011), free lime is the undissolved lime in a steel refining process coming from two sources; precipitated and residual lime. Without access to water from fractures or pores, for example, the residual lime may not be able to hydrate. Wachsmuth et al. (1981) reported that precipitated lime is limited to 4%, meaning that approximately 5.49% or more line in this study was residual which acted similarly to quicklime. Due to the grinding process, the residual lime can be exposed to water. The existence of free lime will produce portlandite ($Ca(OH)_2$) which can lead to a solidification of soft soils.

$$CaO + H_2O \rightarrow Ca(OH)_2 + heat \quad (3)$$

The additional water in soft soil is driven off through steam since the reaction produces heat. The hydration reaction substantially reduces the thickness of absorbed water layer, causing a reduced susceptibility to water addition. Later, the pozzolanic reaction occurs; the portlandite, silica, and alumina minerals from clay react to form calcium silicate hydrate (C-S-H) gel to further bind the soil skeleton together (Rogers and Roff, 1997). The chemical equation reported by Kiso et. al (2008) and further studied by Toda et al. (2018) can be expressed in Equations 4 and 5 :

$$Ca(OH)_2 + SiO_4 + nH_2O \rightarrow C\text{-}S\text{-}H \quad (4)$$

$$Ca^{2+} + AlO_2 + X^- + nH_2O \rightarrow Ca_4Al_2O_6X_2.nH_2O \quad (5)$$

Toda et. al (2018) reported that there was a significant rise of pH in the stabilized soils with BOF slag. The dissolution of portlandite in BOF slag can produce a hyper-alkaline condition in the water that will enhance the formation of C-S-H gel. The effect of humic acid on the alkaline condition of water was fully considered. However, the loss of ignition *(LOI)* 8.2% in this study was relatively low. Kang et al. (2017) studied the effect of various humic acid contents to the strength development of cement treated clay, and it was reported that humic acid less than 10% barely give significant effect to the strength development of stabilized soils.

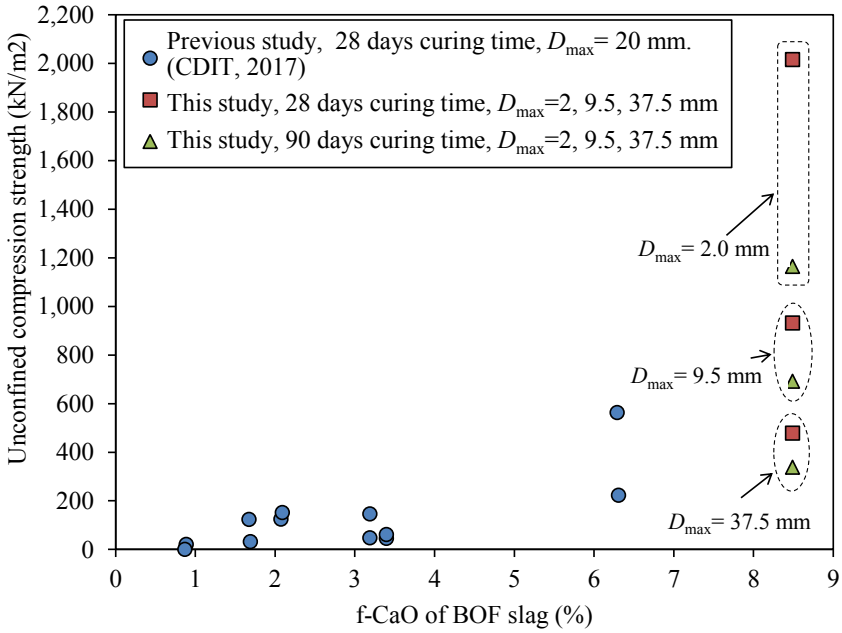

Figure 4- 10 Unconfined compressive strength of stabilized soil using BOF slag with various free lime content.

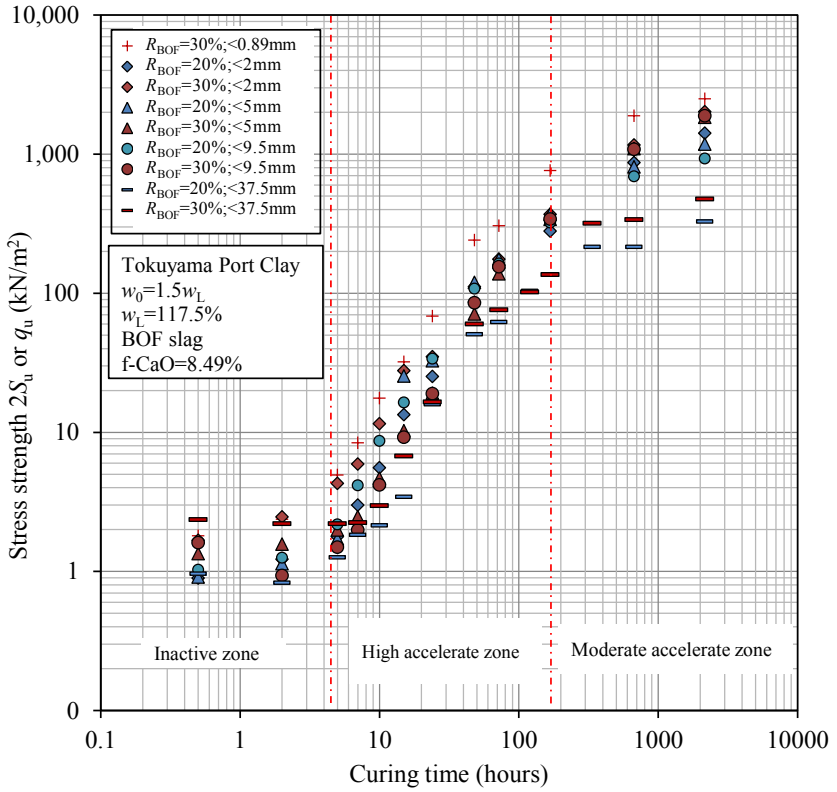

Figure 4- 11 Time-strength mobilization of stabilized soils using BOF Slag.

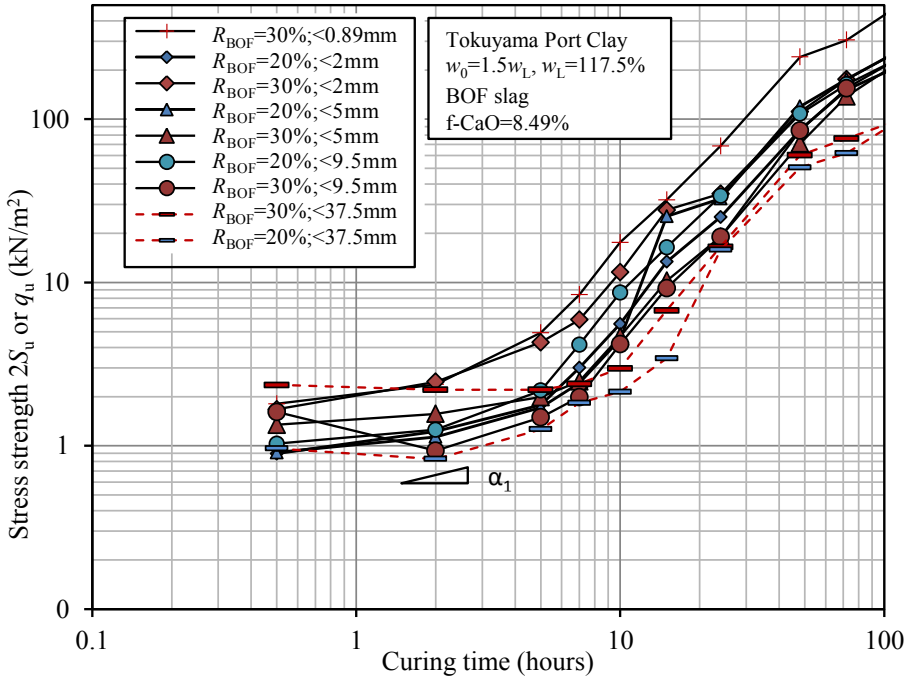

Figure 4- 12 Strength development of stabilized soils at early curing time.

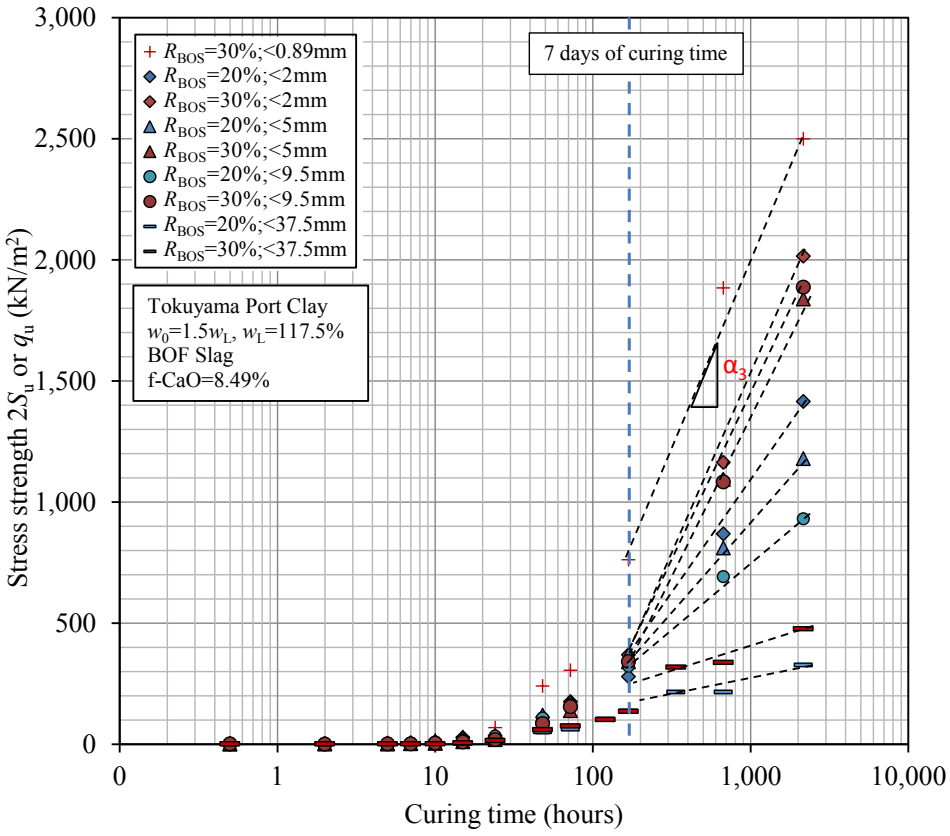

Figure 4- 13 Time-strength mobilization of the stabilized soils using BOF slag in semi-logarithmic scale.

Figure 4-10 illustrates the unconfined compressive strength of stabilized soils using BOF slag with different free lime content from various studies (Coastal Development Institute of Technology, 2017). It is clearly seen that the strength of stabilized soils was mainly affected by free lime content as well as the grain sizes of BOF slag.

Although the UC test is a beneficial test for measuring the strength test q_u of most stabilized soils, this type of strength test to measure soil samples is limited because of an undrained shear strength of less than 2.5 kN/m^2. Therefore, another simple strength test, the LVS test was adopted to measure samples with low undrained shear strength S_u. In this study, the measured undrained shear strength, q_u obtained from the UC test was determined as 2 times the value of undrained shear strength, S_u obtained from the LVS test; $q_u = 2S_u$.

The results of the tests showed that the strength development of stabilized soils using BOF slag of different maximum particle sizes varied considerably with various curing times. Figure 4-11 demonstrates the mean collected values from the LVS and UC tests performed on samples stabilized with BOF slag with a 20–30% ratio of addition and different maximum particle sizes. Generally, in soil stabilization using BOF slag, the strength development of stabilized soils showed three different stages which were an inactive zone, a high acceleration zone, and a moderate acceleration zone. These results were similar to previous research (Sato et al., 2016; Kang et al., 2019).

4.3.5 Strength at early-stage of curing time

The strength development of stabilized soils at the early stage of curing time was significantly affected by the grain-size of the BOF slag. The inactive zone or no strength gain period was characterized by relatively constant strength, until a certain curing time was clearly seen between the smaller maximum grain-size (< 9.5 mm) and the larger grain-size (< 37.5 mm) (Figure 4-12). The soil mixture with a less than 9.5 mm maximum grain-size exhibited up to 5 h of dormancy, while with a larger maximum grain-size of > 37.5 mm it had no significant strength gain for up to 10 h.

Although the strength increment of the larger particle size was insignificant at the early stage of curing time, the immediate strength (0.5 h of curing time) of the larger particles showed a considerably higher value than the smaller particles. The

stabilized soils using BOF slag with a 37.5 mm maximum particle size produced approximately 2.5 kN/m^2 of unconfined compressive strength (Figure 4-12). This indicated that at immediate curing time, the strength was largely affected by the particle size and later, the size effect was neutralized by the amount of free lime it contained.

4.3.6 Strength at later-stage of curing time

In the semi-log scale of the relationship between the strength of stabilized soils and curing time, it is clear that the strength development changed to linear lines after 7 d (Figure 4-13). The later strength mobilization was also largely affected by the particle size. In the same free-lime content and initial clay water content, the smaller particle size produced a higher strength increment, which is likely due to a larger contact surface between free lime and soil skeleton.

4.3.7 Strength increment of stabilized soils

The different particle size also affected the strength increment of the early strength of stabilized soils. The coefficient of strength increment of the stabilized soils was divided into three parts based on the different strength development that was previously explained. It therefore ranged from 0.5–5 h to 5–72 h for the early stage of curing time and 3–90 d for the later stage of curing time. Figure 4-14 illustrates the relationship between various maximum grain-sizes and the strength increment coefficient, α1, α2 and α3 (illustrated in Figures 4-12 and 4-13) which are calculated as follows:

$$\alpha_1 = \frac{\Delta(\log q_u)}{\Delta(\log t)} \quad \text{for inactive zone} \tag{6a}$$

$$\alpha_2 = \frac{\Delta(\log q_u)}{\Delta(\log t)} \quad \text{for high acceleration zone} \tag{6b}$$

$$\alpha_3 = \frac{\Delta q_u}{\Delta(\log t)} \quad \text{for moderate acceleration zone} \tag{6c}$$

From Figure 14a, it can be seen that the coefficient of strength increment shows a distinct increment with the smaller maximum particle size. Moreover, the

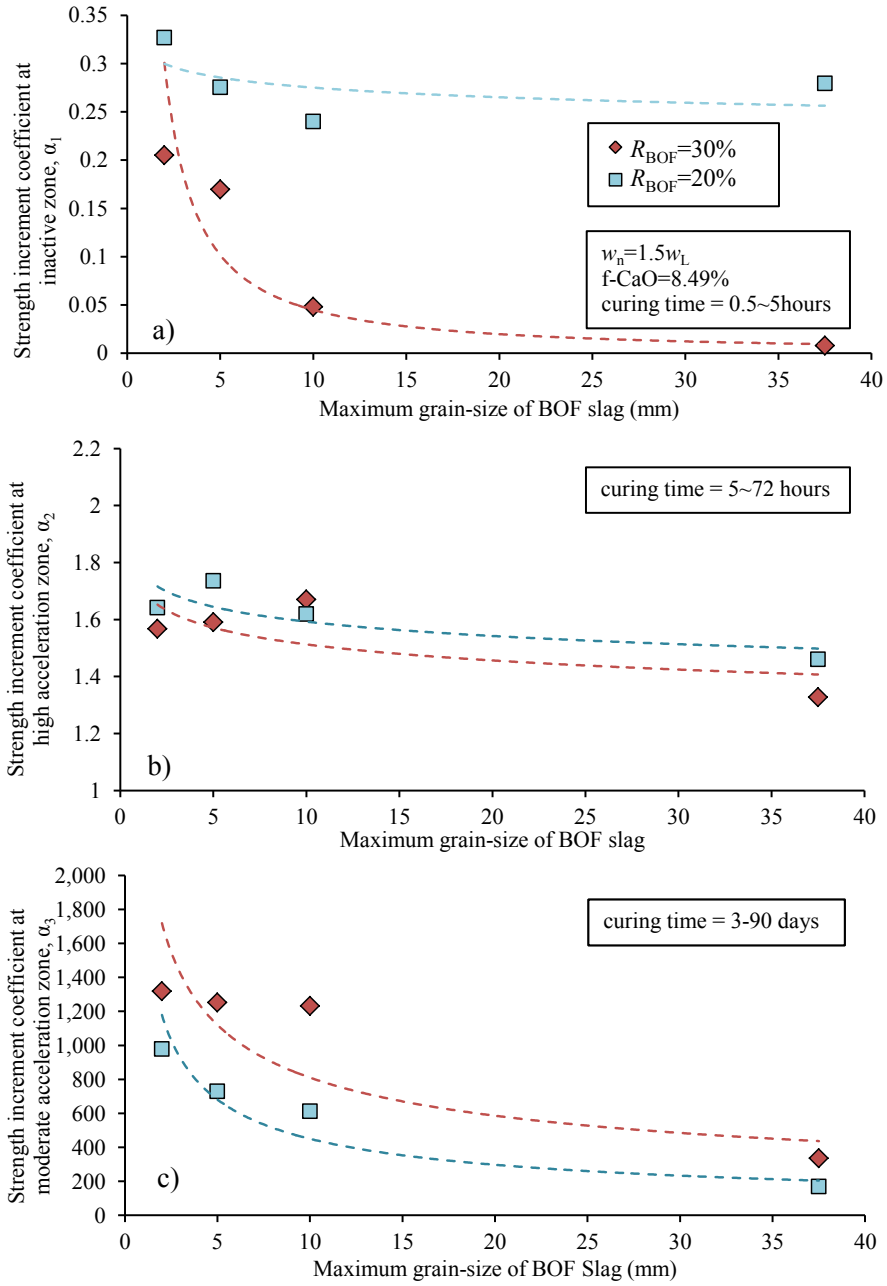

Figure 4- 14 Strength increment coefficient of the stabilized soils at: a) 0.5-5 h b) 5-72 h c) 3-90 d.

larger the addition rate of BOF slag, the wider the strength increment differs between the different maximum grain-size.

Figure 4-14b indicates the strength increment coefficient, α_2 of the stabilized soils from 5–72 h of curing time. The strength increment shown by a 30% rate of addition produced a lower value than the 20% rate of addition. This is due to the different initial strength exhibited by the two different rates of addition. The strength increment coefficient for this period of curing time ranged from 1.35 to 1.75, which

indicated a significant difference in strength increment from the previous curing time of 0.5–5 h α_1.

Figure 14c indicates the strength increment coefficient of the stabilized soils at the later stage of curing time, ranging from 3 to 90 d of curing time. It is assured that the rate of addition significantly affected the strength development of the stabilized soils in this period of time. Unlike the α_1 and α_2, the strength increment at the later stage of curing time, α_3 is significantly higher with the 30% addition rate than the 20% addition rate.

4.3.8 Secant Modulus

Secant modulus, E_{50}, of the stabilized soils was determined from the slope of the obtained stress-strain curve from the UC test. The collected secant modulus from this study and a previous study conducted by Kang et al. (2019) are shown in Figure 4-15, indicating that the secant modulus of the stabilized soils can be estimated to be 88.5–120 q_u, where q_u is the unconfined compressive strength of the stabilized soils.

From the combined data, it appears that the correlation of secant modulus from the unconfined stress strength was not significantly affected by the different

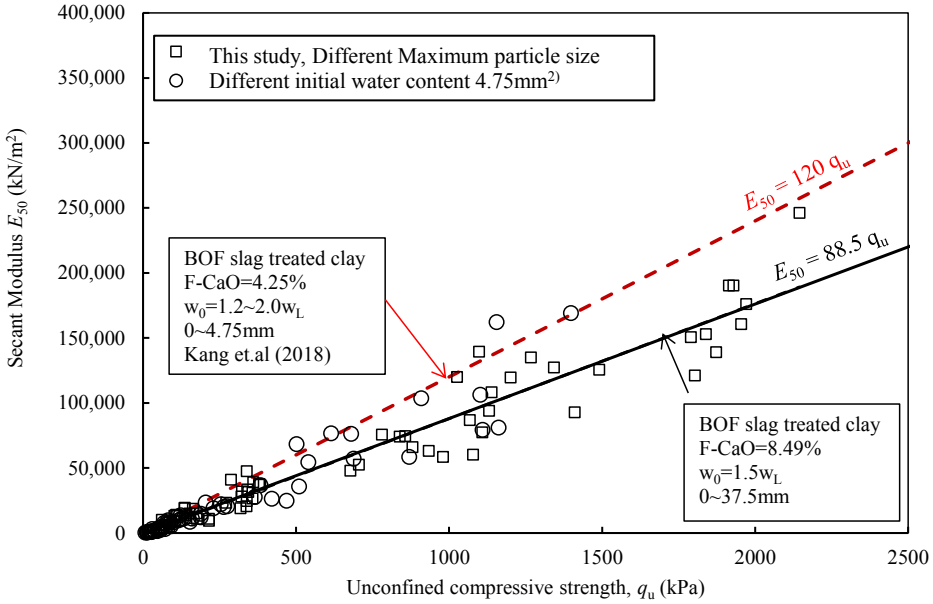

Figure 4- 15 The relationship between compressive strength and the secant modulus of stabilized soils.

maximum grain-sizes. Despite the various range of grain-sizes used in this study, the value of secant modulus can be predicted using a constant value obtained from the relationship between the stress strength of the stabilized soils.

4.3.9 Effect of BOF Slag Grain-size to Strength Mobilization

To compare the difference between this study and the previous study documented in Japan steel-slag manual, the unconfined compressive strength of stabilized soils at 7, 28 and 90 d of curing time as a function of different maximum particle sizes are plotted (Figure 4-16). The previous study also showed a similar effect of the different particle-size to the strength, with a larger maximum particle size of BOF slag. The strength was comparably smaller than the stabilized soils with a smaller particle size. Furthermore, the ratio of strength max grain size 4.75 mm and 20 mm from this study and the previous study is $S_{u(4.75/20)}$ = 1.54 and 1.50, respectively, which indicates that despite the different free lime content, the stabilized soils show a similar strength ratio between the different maximum particle sizes.

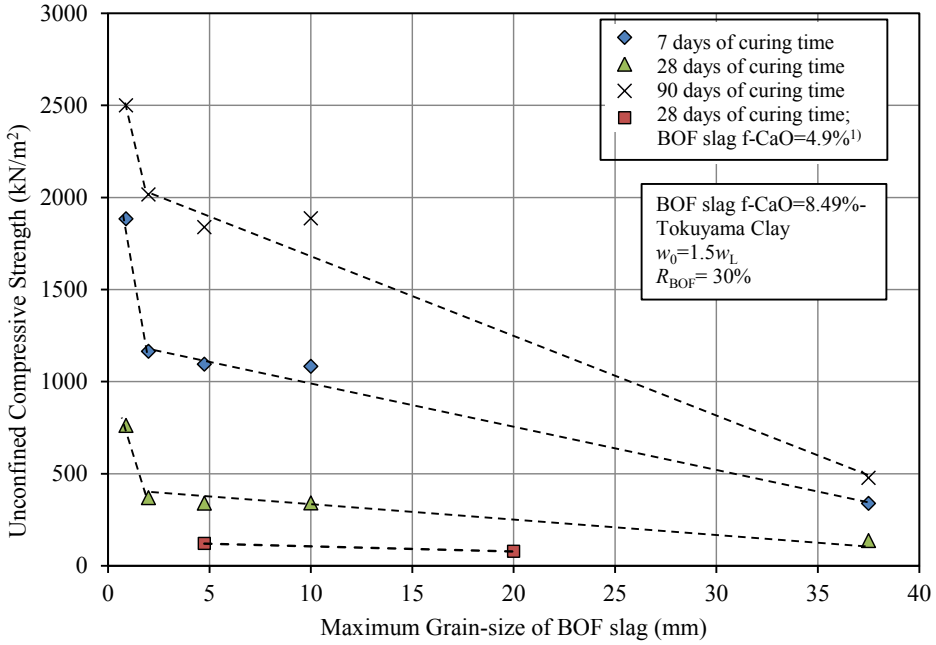

Figure 4- 16 The relationship between the different maximum grain-size of BOF slag and the unconfined compressive strength at 7, 28 and 90 days.

4.3.10 Strength Estimation Equation

Due to the large energy consumption required to grind the BOF slag from the original size to a micro size, a large particle (up to 37.5 mm) is generally adopted in an actual field construction. However, from a practical point of view, the strength measurement of the stabilized soils using the actual grain-size (37.5 mm) in the laboratory is difficult to work with. A large volume of soil and BOF slag are required to prepare the large sample to retain the adequate ratio between the largest particle and the diameter of the sample. Therefore, predicting the actual field strength from a smaller particle size in the laboratory is becoming a common practice.

Although the use of a smaller particle size in the laboratory has been adopted to predict the actual strength in embankment construction, it has been implied that there were substantial differences between actual strength and the laboratory test results (Tanaka et al., 2014; Yuzoh et al., 2012). This was mainly due to the different adopted grain-size distribution in the laboratory and the actual field construction. Consequently, a modification of this method is considered necessary to predict the actual strength.

Figure 4-17 shows the strength of the stabilized soils using various ranges of grain-size (0.85–9.5 mm; 2–9.5 mm; 4.75–9.5 mm and 9.5–37.5 mm) as a function of curing time. With the absence of smaller particles, the strength shows a lower increment than other ranges. The initial strength was produced without a hydration reaction and mostly caused by the lowered initial water content of BOF slag. Strength-test results ranging from 9.5–37.5 mm which lacked a smaller grain size could not exhibit any strength mobilization within the elapsed curing time. From this result, the type of granular BOF slag could be divided into two types: 1) smaller particle sizes (< 9.5 mm) that behaved like cement and 2) larger particle sizes (> 9.5 mm) that behaved with less chemically active material and were similar to aggregate.

According to the results, the rate of addition in Equation 1 was modified to define the mass which is highly active to hydrate, and is described in Equation 7:

$$R_{\text{BOF(hydrate-mass)}} = \frac{M_{\text{BOF(GB)}}}{M_{\text{soil}} + M_{\text{water}} + M_{\text{BOF}}} \times 100 \qquad (\%) \tag{7}$$

where $M_{\text{BOF(GB)}}$ is the mass of chemically-active BOF slag. This value is determined by the boundary of grain-size where the larger size shows no strength gain. The

boundary was taken as 9.5 mm in this study, which may differ from other types of BOF slag.

The contact area between the smaller grain-size of BOF slag and clay particle which produces lime-hydrating minerals is highly related to the surface area of the binder. In a previous study by Zhang and Napier-Munn (1995), the different specific surface area was found to be the reason for the various strength increments of Portland cement at the early and later stages, despite the cement having identical mineral constituents. The measured specific surface area of Portland cement could be accurately determined by their model using particle size distribution.

Equation 8 (Herdan, 1953) was adopted to calculate the specific surface area of granular material with a ball-shape-like assumption:

$$SSA = \frac{6}{\rho}\sum_{i=1}^{n}\left(\frac{w_i}{x_i}\right) \tag{8}$$

and

$$x_i = \left(\frac{\left(x_h^{\,2} + x_j^{\,2}\right)\left(x_h + x_j\right)}{4}\right)^{1/3} \tag{9}$$

where S_s is the surface area (m^2/kg), n is the number of intervals in grain size distribution, w_i is the weight of retained fraction size I, and x_i is the harmonic mean size determined using Equation 9, where x_h and x_j are the upper and lower grain-size interval (mm), respectively, and ρ is the density of the material. The interval of grain-size was divided using the ASTM E11 sieve designation.

The strength development of stabilized soils at a certain curing time can be predicted using the multiplied value of specific surface area with the additional rate of BOF slag. The specific surface SSA of BOF slag, where the grain size is less than 9.5 mm was calculated by Equations (8) and (9). Figure 4-18 shows the relationship between the strength and the total effective specific surface of the BOF slag, SSA^* $R_{\text{BOF(hydrate-mass)}}$. It clarifies that the strength development at later curing time could be well predicted by using the value of $SSA^*R_{\text{BOF(hydrate-mass)}}$ of stabilized soils shown below:

$$q_{u(90d)} = 251.8\left(SSA^* R_{BOF(hydrate-mass)}\right) \tag{10}$$

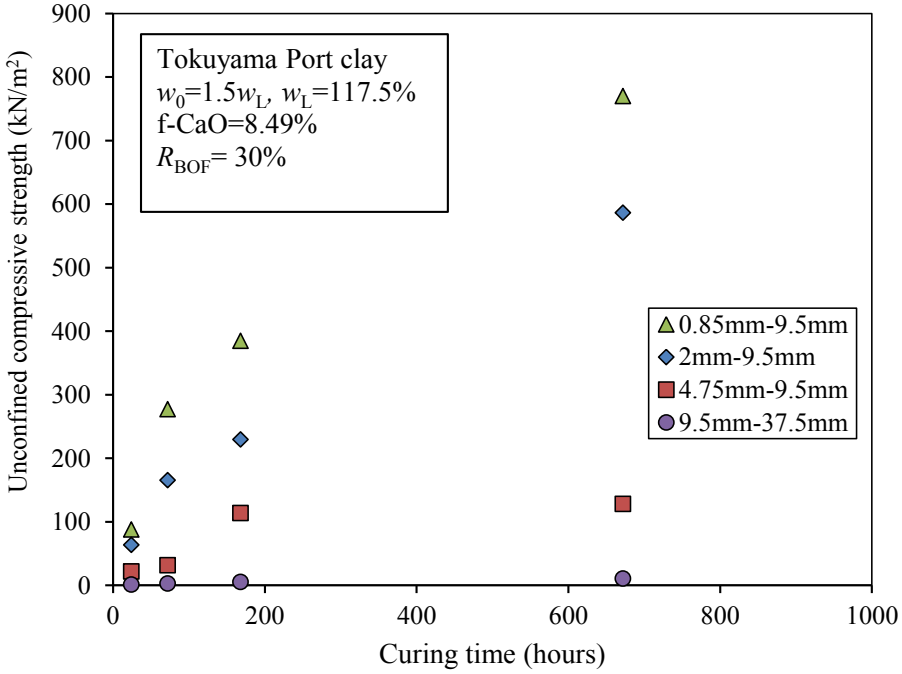

Figure 4- 17 Strength development of the stabilized soils with a lack of fine particle.

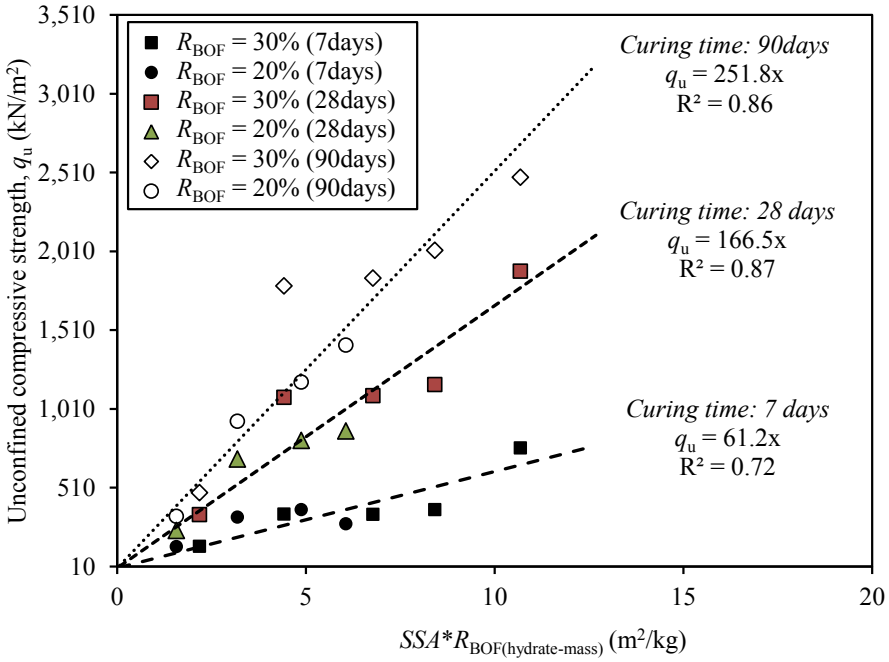

Figure 4- 18 Specific surface area multiplied by the modified rate of addition versus the unconfined compressive strength of stabilized soil using BOF slag.

$$q_{u(28d)} = 166.5\left(SSA * R_{BOF(hydrate-mass)}\right) \quad (11)$$

$$q_{u(7d)} = 61.2\left(SSA * R_{BOF(hydrate-mass)}\right) \quad (12)$$

where $q_{u(d)}$ is an unconfined compressive strength at d curing time of stabilized soils with BOF slag.

Table 4- 6 Calculated *SSA*, *SSA*R*$_{BOF(hydrate-mass)}$ and q_u at 7, 28 and 90 days of curing time.

R_{BOF} (%)	Maximum particle size (mm)	Calculated *SSA* (m^2/kg)	$R_{BOF(hydrate-mass)}$ (%)	$SSA*R_{BOF(hydrate-mass)}$ (m^2/kg)	$q_{u(7\ days)}$ (kN/m^2)	$q_{u(28\ days)}$ (kN/m^2)	$q_{u(90\ days)}$ (kN/m^2)
30	37.5	6.22	40.0	2.50	136.43	338.41	477.46
30	10	8.84	50.0	4.42	341.53	1083.22	1790.00
30	4.75	13.55	50.0	6.77	340.00	1093.70	1838.63
30	2	16.83	50.0	8.42	369.36	1163.70	2015.22
30	0.89	21.37	50.0	10.68	761.57	1884.00	2479.17
20	37.5	6.22	29.0	1.80	136.26	238.00	327.24
20	10	8.84	36.9	3.26	322.71	691.43	930.68
20	4.75	13.55	36.9	5.00	370.55	810.09	1179.13
20	2	16.83	36.9	6.21	279.48	868.79	1414.90

The relationship between the unconfined compressive strength of the stabilized soils and the $SSA*R_{BOF(hydrate-mass)}$ (Table 6 and Figure 4-18) can be used to estimate the strength of the stabilized soils with a varied grain size of the BOF slag. Typically, the maximum grain size of BOF slag in the Japanese construction market is 37.5 mm, and is commonly adopted in many constructions. Using Equations 10, 11 and 12 for various curing times, the strength of BOF slag using the common larger size (37.5 mm) can be predicted using Equation 13 below:

$$q_{u(37.5mm)} = \frac{q_{u(4.75mm)}}{\left(SSA * R_{BOF(hydrate-mass)}\right)_{(4.75mm)}} * \left(SSA * R_{BOF(hydrate-mass)}\right)_{(37.5mm)} \quad (13)$$

where $q_{u(37.5\ mm)}$ is the stress strength of stabilized soils with BOF slag using actual size, and $q_{u(4.75\ mm)}$ is the stress strength of stabilized soils that is obtained in the laboratory using a 4.75 mm grain-size.

4.4 Conclusions

From the data presented in this paper, and considering the limitations of this study, the following conclusions can be drawn:

1. Under similar conditions of initial clay moisture and free lime content, the different grain-size distribution of BOF slag had a significant effect on the strength development of the stabilized marine-dredged clay.
2. At an early stage of curing time, the addition of BOF slag with larger maximum particle sizes produced longer inactive or negligible strength gain. In this study, BOF slag with 37.5 mm of grain size was inactive for up to 10 h, while the smaller maximum grain-size had an average of 5 h of inactivity.
3. The correlation of the secant modulus of BOF slag was between 88.5–120 q_u, where q_u was unconfined compressive strength obtained from the UC test. In this study, the best value to predict the E_{50} was 88.5 q_u. The correlation did not appear to be significantly affected by a different maximum grain-size.
4. Strength estimation equations to predict the stabilized soils using BOF slag were proposed using the specific surface area value obtained from the grain size distribution and the modified BOF rate of addition. It demonstrated good agreement for predicting the actual size used in the field, using a smaller maximum grain-size in the laboratory.
5. Using the proposed Equation 13, the actual strength using a maximum grain-size equal to 37.5 mm can be predicted using the result from the laboratory, with a smaller grain size of 4.75 mm.

4.5 References

Ahmedzade, P., Sengoz, B., 2006. Evaluation of steel slag coarse aggregate in hot mix asphalt concrete. Journal of Hazardous Materials. 165, 300–305.

Arribas, I., Vegas, I., San-Jose, J. T., Manso, J. M., 2014. Durability studies on steelmaking slag concrete. Materials and Design. 63, 168–176.

Asi, I. M., 2007. Evaluating skid resistance of different asphalt concrete mixes. Build. Environ. 42, 325–329.

Belhadj, E., Diliberto, C., Lecomte, A., 2012. Characterization and activation of Basic Oxygen Furnace slag. Cement & Concrete Composites. 34, 34–40.

Coastal Development Institute of Technology (CDIT). 2015. Technical Manual of Dredged soil and Converter slag for Port, Airport, and Coast Facilities. Appendix 2. Influence factor on the strength of dredged soil and converter slag.

Deng, Y. F., Zhang, T. W., Zhao, Y., Liu, Q. W., Wang, Q., 2017. Mechanical behavior and microstructure of steel slag-based composite and its application for soft clay stabilization. European Journal of Environmental and Civil Engineering. 21, 1–16.

The Japan Iron and Steel Federation: Guidebook for Oceanographic Application of Converter Slag. 2008.

Herdan, G. 1953. Small Particle statistics. Elsevier, London. p-413

Horii, K., Tsutsumi, N., Kitano, Y., Kato, T., 2013. Processing and reusing technologies for steelmaking slag. Nippon Steel Technical Report. 104, 123–129.

JHS A 313 1992. Cylinder method for consistency test, Japan Road Association (in Japanese).

JIS A 1216 2008. Method for Unconfined Compression Test of Soils (in Japanese).

Kang, G-O., Tsuchida, T., Athapaththu, A. M. R. G., 2016. Engineering behavior of cement-treated marine dredged clay during early and later stages of curing. Engineering Geology. 209, 163–174.

Kang, G., Tsuchida Takashi, Kim Young-sang, and Baek Won-jin (2017). Influence of Humic Acid on the Strength Behavior of Cement-Treated Clay during Various Curing Stages. J. Mater. Civ. Eng. *29*, 04017057.

Kandhal, P., and Hoffman, G. (1997). Evaluation of Steel Slag Fine Aggregate in Hot-Mix Asphalt Mixtures. Transp. Res. Rec. J. Transp. Res. Board *1583*, 28–36.

Katayama, Y., and Tsuchida, T. (2015). Stability of steel slag mixed with clay slurry of high water content. Journal of Japan Society of Civil Engineers. Vol 31 pages I_1161-I1166. (in Japanese).

Kinoshita, H., Ichii, K., Morikawa, H., Takahashi, H., Shinozaki, H., Takahashi, Y., 2012. Characteristics and assessment of seismic behavior of improved ground by sand compaction pile method using iron and steel slag as base of gravity caisson structure. Japanese Geotechnical Journal. 7 (1), 323–337. (in Japanese).

Kiso, E., Tsujii, M., Ito, K., Nakagawa, M., Gomyo, M., Nagatome, T. 2008. Method of dredged soil improvement by mixing with converter steel-making slag. Kaiyo Kaihatsu Ronbunshu 2008, 24, p 327-332. (In Japanese).

Kitazume, M., Terashi, M., 2013. The deep mixing method. CRC press Taylor & Francis Group, London, UK.

Lee, A. R., 1974. Blastfurnace and steel slag: Production, properties and uses, Edward Arnold, London.

Liu, S., Wang, Z., Li, X., 2014. Long-term properties of concrete containing ground granulated blast furnace slag and steel slag. Magazine of concrete Research. 66 (21), 1095–1103.

Mahieux, P. Y., Aubert, J. E., Escadeillas, G., 2009. Utilization of weathered basic oxygen furnace slag in the production of hydraulic road binders. Construction and Building Materials. 23, 742–747.

Ministry of Transport, The Fifth District Port Construction Bureau, 1999. Pneumatic flow mixing method (in Japanese).

Montgomery, D.G., and Wang, G. (1991). Instant-chilled steel slag aggregate in concrete - strength related properties. Cem. Concr. Res. *21*, 1083–1091.

Motz, H., and Geiseler, J. (2001). Products of steel slags an opportunity to save natural resources. Waste Manag. *21*, 285–293.

Murphy, J.N., Meadowcroft, T.R., and Barr, P.V. (1997). Enhancement of the cementitious properties of steelmaking slag. Can. Metall. Q. *36*, 315–331.

Proctor, D.M., Fehling, K.A., Shay, E.C., Wittenborn, J.L., Green, J.J., Avent, C., Bigham, R.D., Connolly, M., Lee, B., Shepker, T.O., et al. (2000). Physical and Chemical Characteristics of Blast Furnace, Basic Oxygen Furnace, and Electric Arc Furnace Steel Industry Slags. Environ. Sci. Technol. *34*, 1576–1582.

Poh, H. Y., Ghataora, G. S., Chazireh, N., 2006. Soil stabilization using basic oxygen steel slag fines. Journal of Materials in Civil Engineering. 18 (2), 229–240.

Qiang, W., Mengxiao, S., Jun, Y., 2016. Influence of classified steel slag with particle sizes smaller than 20 μm on the properties of cement and concrete. Construction and Building Materials. 123, 601–610.

Rogers, C.D.F., and Roff, T.E.J. (1997). Lime modification of clay soils for construction expediency. Proc. Inst. Civ. Eng. - Geotech. Eng. *125*, 242–249.

Rondi, L., Bregoli, G., Sorlini, S., Cominoli, L., Collivignarelli, C., Plizzari, G., 2016. Concrete with EAF steel slag as aggregate: A comprehensive technical and environmental characterization. Composites Part B. 90, 195–202.

Sato, H., Nishimura, S., Toda K., Sato, S., Arai, Yu. (2016). “Characteristic and Interpretation of Development of Strength and Stiffness for Early-Age Calcia-Stabilized Dredged Soils”. Hokkaido Site Engineering Society, Technical report

No.56, pp 15-20.

Scrivener K. L., 1991. The microstructure of concrete. Materials Science and Concrete (Skalny JP (ed.)). American Ceramic Society, Westerville, OH, USA, 127–161.

Seng, S., Tanaka, H., 2011. Properties of cement-treated soils during initial curing stages. Soils and Foundations. 51 (5), 775–784.

Shen, D. H., Wu, C. M., and Du, J. C., 2009a. Laboratory investigation of basic oxygen furnace slag for substitution of aggregate in porous asphalt mixture. Construction and Building Materials. 23, 453–461.

Shen, W. G., Zhou, M. K., Ma, W., Hu, J. Q., and Cai, Z., 2009b. Investigation on the application of steel slag–fly ash–phosphogypsum solidified material as road base material. Journal of Hazardous Materials. 164 (1), 99–104.

Shi, C. J., and Qian, J. S., 2000. High performance cementing materials from industrial slags–A review. Resources, Conservation Recycling. 29, 195–207.

Shi, C. J., (2004). Steel Slag—Its Production, Processing, Characteristics, and Cementitious Properties. J. Mater. Civ. Eng. *16*, 230–236.

Tanaka, Y., Ko, C., Imamura, T A., Shibuya, T ., Yamagoshi, Y., Yuzoh, A. 2014. Reclamation of the artificial ground made of dredged soil and converter slag. The Japanese geotechnical society, vol 70. No. 2, I_888-I_893 (in Japanese).

Tang, Y. X., Miyazaki, Y., Tsuchida, T., 2001. Practices of reused dredging by cement treatment. Soils and Foundations. 41 (5), 129–143.

Takahashi, H., Morikawa, Y., Shinozaki, H., Kinoshita, H., Maruyama, K., 2011. Ground stability against backfill loading of SCP improved ground using solidified iron–and–steel slag. Japanese Geotechnical Journal. 6 (1), 81–95 (in Japanese).

Technical Manual of Pre-Mix Vessels Method, 2013. Association of Pre-Mix Vessels Method (in Japanese).

Terashi, M. and Katagiri, M., 2005. Key issues in the application of vertical drains to sea reclamation by extremely soft clay slurry, chapter 4 in ground Improvement-Case histories. Elsevier Geo-Engineering Book series, vol. 3 pp 119-143.

The Japan Iron and Steel Federation: Guidebook for Oceanographic Application of Converter Slag. 2008.

Toda, K., Sato, H., Weerakoon, N., Otake, T., Nishimura, S., and Sato, T. (2018). Key Factors Affecting Strength Development of Steel Slag-Dredged Soil Mixtures.

Minerals *8*, 174.

Tsuchida, T., Tang, Y. X., Watabe. Y., 2007. Mechanical properties of lightweight treated soil cured in water pressure. Soils and Foundations. 47 (4), 731–748.

Wachsmuth, F., Geiseler, J., Fix, W., Koch, K., and Schwerdtfeger, K. (1981). Contribution to the Structure of BOF-Slags and its Influence on Their Volume Stability. Can. Metall. Q. *20*, 279–284.

Wang, G., Wang, Y., and Gao, Z. (2010). Use of steel slag as a granular material: volume expansion prediction and usability criteria. J. Hazard. Mater. *184*, 555–560.

Watabe, Y., and Noguchi, T., 2011. Site-investigation and geotechnical design of D-runway construction in Tokyo Haneda Airport. Soils and Foundations. 51 (6), 1003–1018.

Wilkinson, A., Haque, A., Kodikara, J., 2010. Stabilisation of clayey soils with industrial by-products: part A. Ground Improvement. 163 (G13), 149–163.

Worrell, E., Price, L. K., Martin, N., Hendriks, C., Ozawa Meida, L., 2001. Carbon dioxide emissions from the global cement industry. Annual Review of Energy and Environment, 26, 303–329.

Xue, Y., Wu, S., Hou, H., Zha, J., 2006. Experimental investigation of basic oxygen furnace slag used as aggregate in asphalt mixture. Journal of Hazardous Materials. 138 (16), 261–268.

Yuzoh, A., Tanaka, Y., Yamagoshi, Y., Okubo, Y., 2012 Characteristic of the artificial Ground Made of dredged soil and converter slag. The Japanese Geotechnical Society, pp 12-15 (in Japanese).

Yildirim, I.Z., and Prezzi, M. (2011). Chemical, Mineralogical, and Morphological Properties of Steel Slag.

Yildirim Irem Zeynep, and Prezzi Monica (2015). Geotechnical Properties of Fresh and Aged Basic Oxygen Furnace Steel Slag. J. Mater. Civ. Eng. 27, 04015046.

Zhang, Y.M., and Napier-Munn, T.J. (1995). Effects of particle size distribution, surface area and chemical composition on Portland cement strength. Powder Technol. 83, 245–252.

Chapter 5

Expansion Characteristic of Steel Slag Mixed with Dredged Marine Clay

TABLE OF CONTENTS

5.1 Introduction

Countries with large steel manufacturing industries encounter financial and environmental issues regarding the abundant amount of steel slag generated every year (globalslag.com; Geiseler, 1996; Yi et al., 2012). For instance, Japan annually produces over forty million tons of steel slag, and 10%–15% is still sent away to a disposal facility (Horii et al., 2013). The cost-effective utilization of steel slag may not only alleviate the need for disposal facilities but also reduce the use of natural resources. Therefore, a further understanding of the properties of steel slag is required to extensively utilize the large volume of the steel slag.

Steel slag, a by-product of steel manufacturing, has been vastly utilized around the world, especially as an aggregate in the field of road and concrete construction (Arabani and Azarhoosh, 2012; Aziz et al., 2014; Chen et al., 2014; Guo et al., 2019; Montgomery and Wang, 1991; Wang, 2010b; Shen et al., 2009). After a decent treatment, steel slag is able to fulfill the huge demand of aggregate, which is otherwise satisfied using natural resources. Pasetto and Baldo (2010) indicated that steel slag is satisfactory, as an aggregate, in achieving high modulus asphalt even with the use of modified bitumen with a lower polymer concentration. Studies by Montgomery et al. (1991) and Maslehuddin et al. (2003) ascertained that well-aged steel slag can replace natural resources such as limestone as an aggregate in constructions involving concrete, which can preserve the nature. Moreover, Piatak et al. (2015) and Proctor et al. (2000) confirmed that steel slag usage with certain conditions is safe to human life and in compliance with the environmental regulation as a fill.

Even though the environmental reliability of steel slag has been well proven by many researches and field constructions, because of its volume instability, steel slag utilization is relatively lower than the slag from the iron-making process i.e. blast furnace slag. It is widely known that steel slag contains high free lime and free magnesium oxide, which when in contact with water, react and form hydroxides that can cause volume expansion (Shi and Qian, 2000; Motz and Geiseler, 2001). For most applications, such as road pavement constructions, volume instability is a crucial aspect and highly restricted to 0.5% (ASTM D2940). As a result, the utilization of

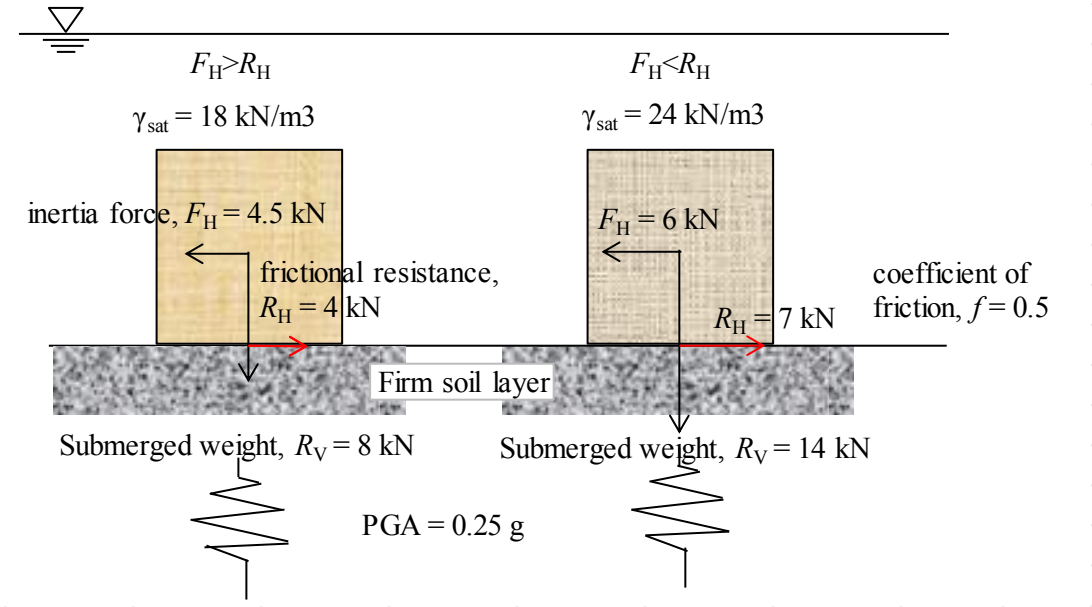

Figure 5- 1 Stability of a submerged geomaterial under an earthquake load.

steel slag consumes a lot of unnecessary energy and time for the treatment and is limited to certain applications that permit a bit of volume instability. Therefore, an alternative treatment with less energy consumption such as steel slag mixed with soft clay is proposed in this paper.

Recent studies (Poh et al., 2006; Yong-Feng et al., 2017; Sato et al., 2016; Kang et al., 2019) have shown that steel slag can improve the strength and durability of soft clays, with or without activators. The strength and workability of soft clay are improved by the drying action of the free lime and low water content of the steel slag. Further stabilization is carried out by the pozzolanic reaction—a reaction between lime, water, and alumina—and silica from the clay that subsequently crystallize to bind the soil skeleton together. Although research on the strength characteristic of the soil treated with steel slag has been distinctively demonstrated over the past decade, little attention has been paid to the expansion behavior of steel slag mixed with soft clay.

The act of adapting steel slag as a heavyweight geomaterial can increase the rate of steel slag utilization; by delicately controlling its volume instability, it can be adapted in offshore embankment constructions. Steel slag is well known to have high specific gravity and bulk density owing to the high content of the ferro mineral; with a

delicate treatment, it can generate a heavyweight geomaterial (Shi, 2004). Figure 5-1 illustrates how the heavyweight material plays an important role in the stabilization of a submerged embankment under an earthquake load. The treated-steel slag with a sufficient unit weight can increase stability in case of an earthquake as compared to a common geomaterial (Tsuchida et al., 2019).

The objectives of this paper are to explain the expansion mechanism of steel slag mixed with dredged soil and to determine the maximum steel slag addition possible such that it remains in compliance with the allowable volume expansion. Chemical properties of both the steel slag and the dredged soil were acquired using X-ray diffraction and X-ray fluorescence test. A series of expansion test on steel slag mixed with various contents of dredged clay was performed and evaluated throughout the curing time. Scanning electron microscopy (SEM) and energy-dispersive spectroscopy (EDS) were performed to describe the microstructure of the expanded material. Our results show that the removal of the fine aggregate in the steel slag is not an effective way to alleviate the volumetric expansion of the steel slag. The soft clay was able to reduce the volume expansion of the steel slag by absorbing the volume expansion and the 60% volumetric addition of steel slag was the maximum addition to achieve the permissible volume expansion with a unit weight of 24.3 kN/m^3.

5.2 Testing Programme

5.2.1 Materials

The soft clay used in this study is the dredged-marine soil of Tokuyama Port, Yamaguchi Prefecture, Japan. The dredged-marine soil of Tokuyama Port is odorless and has a dark-greenish color. It has a liquid limit, a plastic limit, and a plasticity index equal to 119.9%, 45.6%, and 74.3%, respectively. According to the unified soil classification system, the marine-dredged clay is classified as high-plasticity clay. The relative density of the soil is 2.68 g/cm^3.

The steel slag was procured from the JFE steel company in Fukuyama City, Japan. It is a fresh and porous steel slag with a sub-angular shape. It has a maximum diameter of 37.5 mm and a fine-grain content of 10.5%. The original grain size distribution of the steel slag is depicted in Figure 5-2. The average specific gravity of

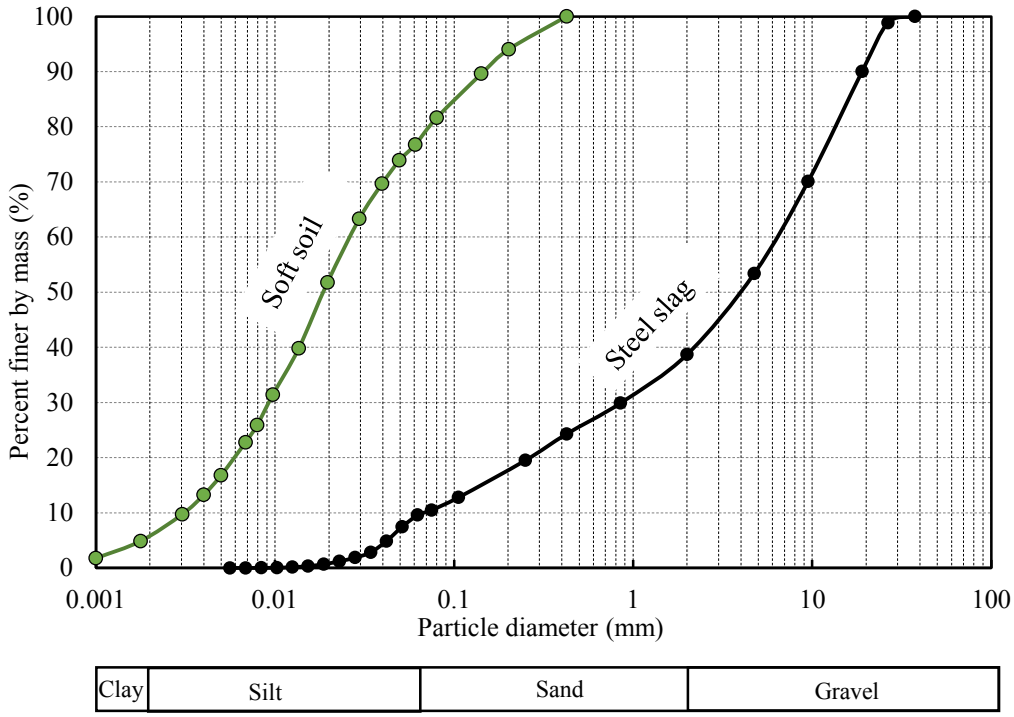

Figure 5- 2 Grain-size distributions of the soft soil and the steel slag.

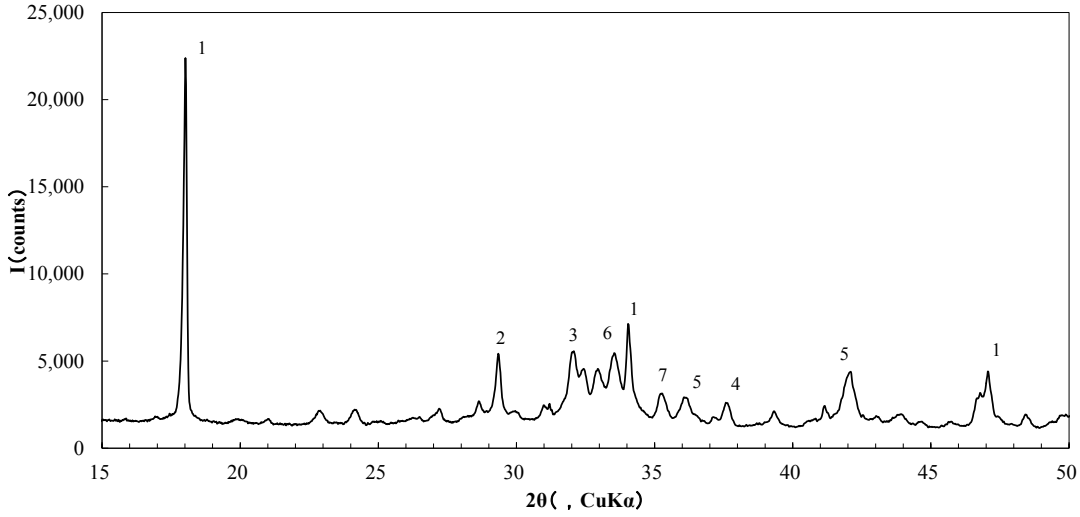

Figure 5- 3 X-Ray diffraction result of the steel slag. [1]portlandite; [2]calcite; [3]larnite; [4]lime; [5]wustite; [6]srebodolskite; [7]magnetite.

the steel slag is 3.15. The free lime content of the steel slag, obtained using an ethylene glycol method, is 8.49%. The surface dry density and the absolute dry density of the steel slag are 3.19 g/cm^3 and 3.08 g/cm^3, respectively.

Table 1 summarizes the basic physical properties of the soft clay and steel slag.

X-ray diffraction and X-ray fluorescence were previously conducted to determine the chemical and mineral composition of steel slag. The mineral

composition of steel slag is summarized in Figure 5-3. The steel slag exhibited minerals such as portlandite ($Ca(OH)_2$), vaterite ($CaCO_3$), wustite (FeO), srebodolskite ($Ca_2Fe_2O_5$), calcite ($CaCO_3$), larnite (Ca2SiO4), lime (CaO), fayalite (Fe2SiO4), and magnetite (FeFe2O4). The crystalline components obtained from the X-ray fluorescence test (Table 2) are mainly 41% CaO, 33% Fe2O3, 14% SiO2, 3% P_2O_5, 3% MnO, 2.6% Al_2O_3, 2.3% MgO, and other minerals such as TiO_2, Cr_2O_3, CuO, ZnO, Se_2O_6, SrO, Y_2O_3, ZrO_2, MoO_3, and BaO.

Table 5- 1 Basic properties of the soft soil and the steel slag.

Property	**Soft soil**
Liquid limit, w_L (%)	119.9
Plastic limit, w_P (%)	45.6
Plastic index, *PI* (%)	74.3
Particle density, *Gs* (g/cm^3)	2.68
Coarse-grained soil (%)	9.98
Fine-grained soil (%)	90.02
Unified soil classification system (USCS)	CH
pH	7.2
Loss of ignition, *LOI* (%)	8.17
Property	**Steel slag**
Initial moisture content, w_0 (%)	8.38
Average specific gravity of the steel slag	3.15
Specific gravity of coarse aggregate <4.75 mm	2.96
Specific gravity of fine aggregate <4.75 mm	3.23
Absolute dry density (g/cm^3)	3.02
Water Absorption rate of coarse aggregate (%)	4.60
Water Absorption rate of fine aggregate (%)	2.49
Largest aggregate size (mm)	<37.5
Coarse-grained size (>75μm) (%)	89.5
Fine-grained size (<75μm) (%)	10.5
Free CaO, (f-CaO) (%)	8.49

Table 5- 2 Chemical Compound of the steel slag (X-Ray Fluorescence)

Chemical compound	Percentage by mass
MgO	2.3
Al_2O_3	2.6
SiO_2	14
P_2O_5	3.0
K_2O	0.15
CaO	41
TiO_2	0.41
Cr_2O_3	0.12
MnO	3.0
Fe_2O_3	33

5.2.2 Mixing Proportions

The experimental mixing proportions, R_{SS}, are 45%, 55%, 60%, 70%, and 100%. The rate of the steel slag addition is determined by using Eq. 1:

$$R_{SS} = \frac{V_{SS}}{V_{soil} + V_{water} + V_{SS}} \times 100 \qquad (\%) \tag{1}$$

where V_{SS} is the solid volume of steel slag, V_{soil} and V_{water} are the volumes of soil and water.

5.2.3 Specimen preparation

Prior to specimen fabrication, the materials were prepared as follows:

- The soft clay was initially filtered by using a 2 mm sieve to remove the coarse particles, shells, and coral reef fractions. Immediately after the sieving, the soft clay was kept in a hermetical box to reduce the loss of moisture.
- Steel slag was air-dried at room temperature, 25±5°C, and 60% relative humidity for 24 h. The moisture content of the steel slag dropped to 3%-5%. Later, the steel slag was sieved to get two types of grain size ranges, 0–19 mm and 9.75–37.5 mm.
- Artificial seawater was prepared by mixing distilled water with salt with 3.5% salinity. The salt water was prepared to represent the actual condition of the sea water on field construction.

To begin the mixing of the steel slag and the soft clay, the moisture content of the soft clay was subsequently brought to 2.0 of the liquid limit of the soft clay by adding the artificial-sea water and mixing it for 2 minutes. Then, the steel slag and the soft clay were uniformly mixed for 5 minutes by using a heavy-duty hand mixer. Soil mixtures were poured into the testing mold and followed by a density measurement.

During specimen preparation, it was observed that the higher the steel slag content is, the harder it is to be mixed. It is obvious as the air-dried steel slag absorbed most of the free water from the soft clay.

5.2.4 Tests Performed

The purpose of this paper is to investigate the expansion behavior of steel slag mixed with soft clay. The maximum steel slag addition at which the expansion ratio produced is still permissible (less than 0.5%) was studied and compared. The ultimate goal was to get a heavyweight geomaterial with a permissible expansion ratio. Therefore, the experimental mixing proportions were varied from low to very high steel slag content along with measuring the unit weight of the mixture.

5.2.4.1 Compaction Test

Before the expansion test was conducted, a compaction test was performed to determine the optimum moisture content and the maximum dry density of the steel slag. The compaction test was applied to generate the expansion specimen of pure steel slag aggregates. Two different energies, the standard (600 kN-m/m^3), and the modified (2700 kN-m/m^3), were applied to the specimen in accordance with ASTM D698 standard test method.

5.2.4.2 Expansion Test

The expansion test was performed in the laboratory and referred to the ASTM D4792 standard test method (Figure 5-4). The test was designated specifically for materials that contained components subject to hydration. The diameter of the testing mold was 15.24 cm, and the initial height of the specimen was 11.643 cm. The specimen was soaked in distilled water, which was carefully maintained at 70 ± 3^{o}C. Both the top and bottom of the specimen were water-permeable. A spacer disk (4.56 kg) was

applied on the top of the specimen as a surcharge load. The volumetric change of the specimen was recorded every 24 h. The expansion test was conducted on three specimens for each mixing proportion.

During the specimen pouring process, it was quite difficult to ascertain a flat and full-contact surface for the spacer disk since the majority of the specimen consisted of large particles. Inevitably, in order to solve the problem, the spacer disk was lifted up and put back multiple times, and light compactions were involved.

In this paper, the expansion test was carried out for a significantly longer time period than those in previous studies (Sorlini et al., 2012; Wang et al., 2010a). The time period ranged from 2 to 6 months for further observing the expansion behavior of the pure steel slag and the steel slag mixed with soft clay.

In an actual construction project, different grain size distributions of the steel slag, followed by different fine grain content will most likely be encountered. Cikmit et al. (2019) reported that the effect of the grain size is significant on the strength development of the steel slag owing to different surface areas for grains of different sizes. The different surface areas are most likely to produce different amounts of hydration products which can lead to a higher expansion ratio. Therefore, to understand the effect of the fine grain content on the expansion ratio of steel slag, the expansion test was carried out on two ranges of grain sizes, 0–19 mm, and 9.5–37.5 mm. The test was terminated after each sample reached its expansion peak and showed no larger than 0.01% of volumetric change in 24 h.

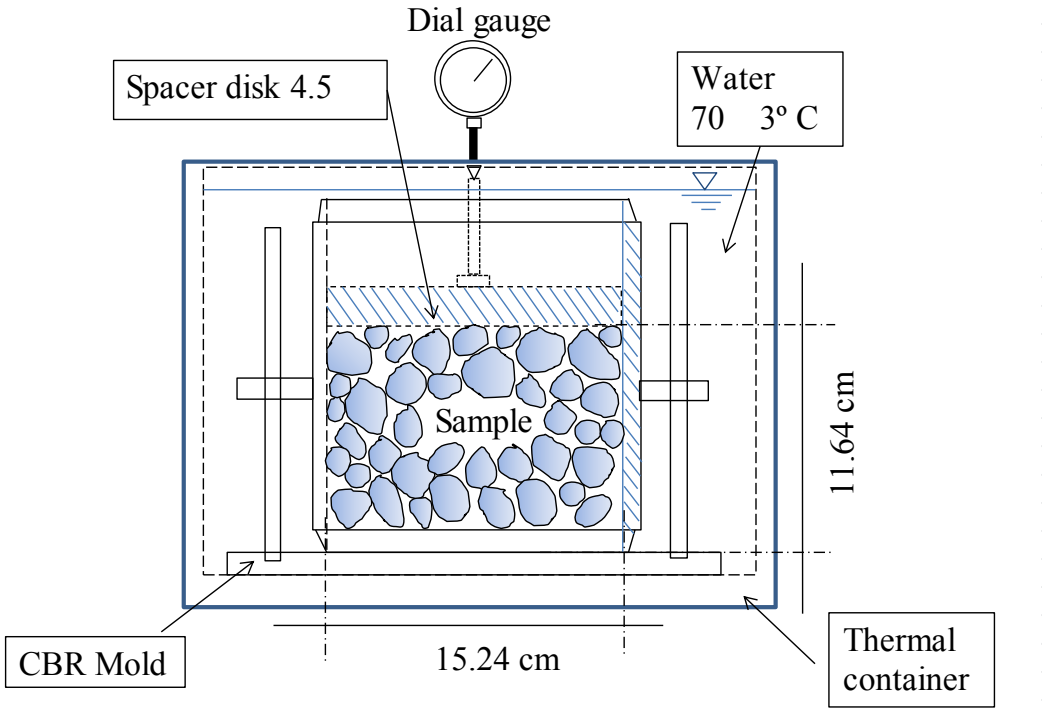

Figure 5- 4 Expansion test apparatus.

5.2.4.3 Strength Test

Unconfined compressive tests following the JGS 0511 standard test method were conducted for the measurement of the strength of the specimens with 45%, 55%, 60%, and 70% rate of steel slag addition at 7 days of curing time. The maximum grain size of the steel slag used was less than 4.75 mm. Three specimens were prepared in molds (ø50 mm x 100 mm) for each curing time. Both ends of the specimen were aligned to get a perfectly flat surface. To avoid the effect of length-to-diameter ratio on the strength of the specimens, the height of the specimens were trimmed such that they had only ± 5 mm inequality. For each test, the loading rate was maintained at one mm/min, and the strain-stress relationship of each specimen was recorded and analyzed.

5.2.4.4 SEM and EDS

SEM analysis and EDS were conducted to investigate the matrix microstructure of the soil mixture after the expansion test. The SEM (JSM-IT300), supplied by JEOL Ltd. was operating at 30 kV and was accompanied by an EDS

analyzer. The EDS was performed using the EDS2000 software. Prior to SEM imaging, a gold coating was applied to the sample surface using JFC-1600 fine coater.

The tests were performed on the pure steel slag with grain sizes between 0–19 mm, and the soil mixtures with 45%, 60%, and 70% steel slag.

5.3 Results and Discussion

5.3.1 Unit Weight of Materials

One of the purposes of this paper is to investigate the feasibility of the soil mixture as a heavyweight geomaterial which can be adapted for multiple purposes in embankment constructions. It needs to point out that the fill using the soil mixture is different from the traditional disposal (directly dumped to disposal facility) as there is an effort to simultaneously recycle dredged soil. Immediately upon the pouring of the soil mixtures, the unit weight of the specimens was measured, and the results are plotted in Figure 5-5. The addition rates of 45%, 55%, 60%, and 70% exhibited an average 22.7, 23.5, 24.3, and 26.1 kN/m^3 of unit weight, respectively.

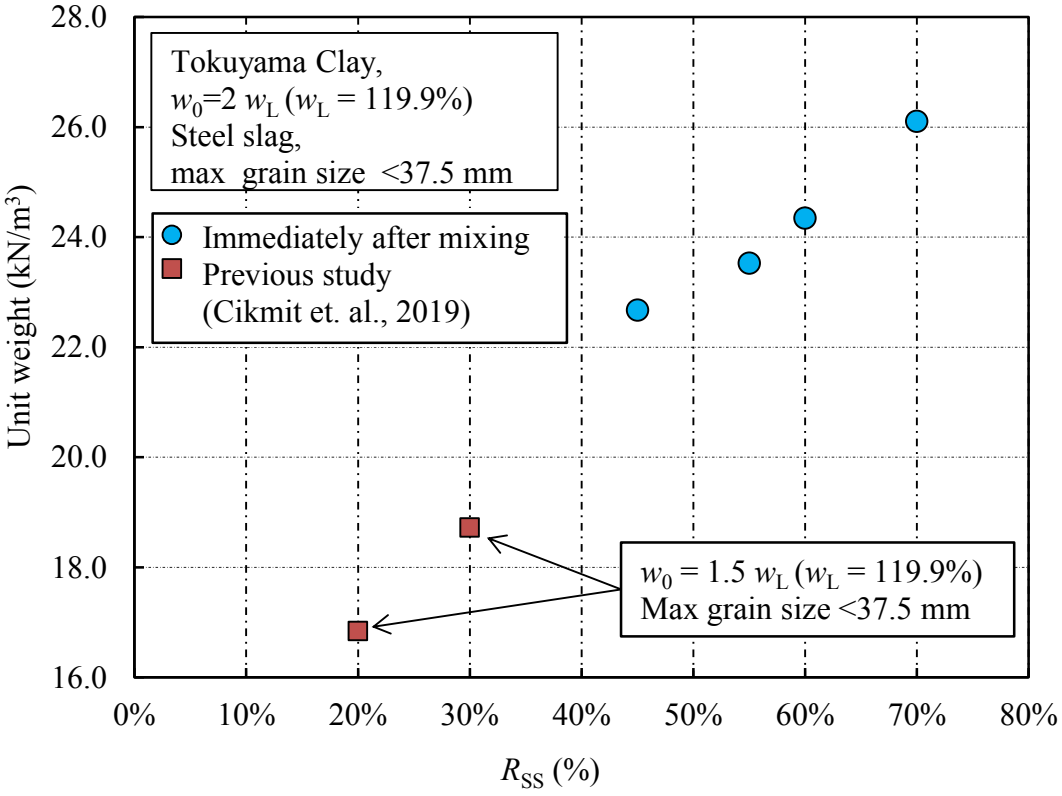

Figure 5- 5 Unit weight of the soil mixtures.

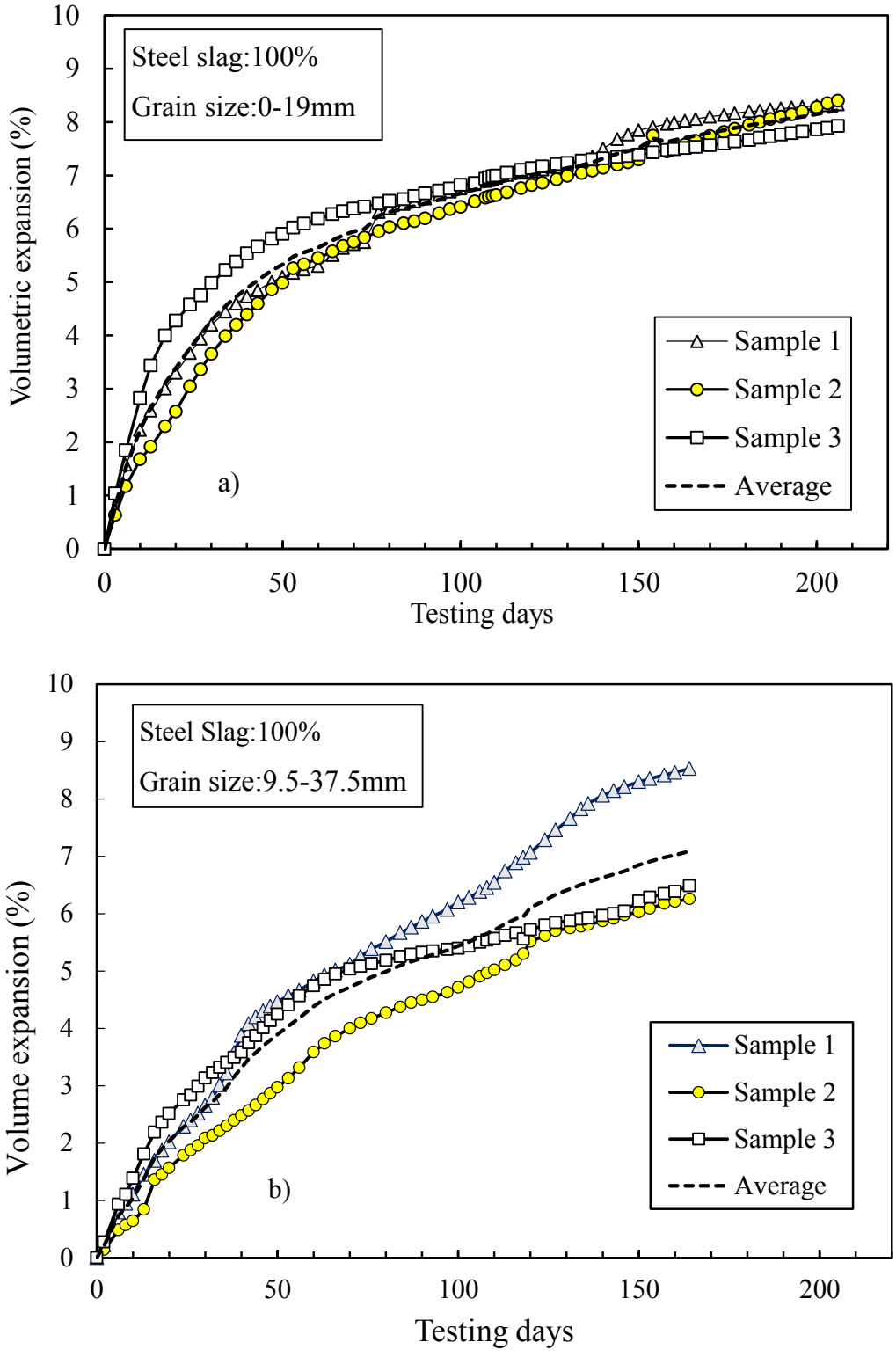

Figure 5- 6 The volume expansion of steel slag as a function of time, a) with fine particle and b) without fine particle.

The Tokuyama soft clay with an initial water content of 1.2–2.0 w_L had ~12.3–13.58 kN/m^3 of unit weight (Kang et al., 2019). Soft clays coming from dredging have a low unit weight depending on the initial moisture and coarse material content (Bartos, 1977). The results show that the addition of steel slag caused a significant increase in the unit weight of the soft clay owing to the fact that the specific gravity of the steel slag was very high, i.e., 3.14.

5.3.2 Effect of fine particles

Prior to the expansion test, the compaction test was conducted on the steel slag to determine the optimum moisture content and the maximum dry unit weight of the steel slag. The optimum moisture content and the maximum dry unit weight of the steel slag were 8.5% and 21.8 kN/m^3 when a standard effort of 600 kN-m/m^3 was applied. A modified effort (2700 kN-m/m^3) increased the dry unit weight to 23.4 kN/m^3 with a 6% optimum moisture content. The steel slag can be categorized as a bulk granular material which contains a void inside its porous structure and has the type of compaction curve that is commonly exhibited by a free draining granular material. Even if it is fully compacted, the material still contains the void, thus, acquiring a larger unit weight that contains an air void close to zero is not reasonable. The results demonstrated a similar range of dry unit weights at the same compaction effort as the study reported by Yildirim and Prezzi (2009), 19.5–21.8 kN/m^3.

Figure 5-6 shows the volume expansion results of the steel slag with different grain sizes as a function of the test period. The results showed that the expansion rate was still significantly increasing after a 7-day test period (minimum test period required in ASTM D 4792). Figure 5-6.a shows the volumetric expansion of the steel slag with fine particles (0–19 mm grain size) at a test period of 206 days. From the results, it can be seen that the increment of volume change can be divided into two phases, highly accelerated and moderate. The highly accelerated phases, 0–40 days, showed a rapid volume change of 5–6%. The next phase, the moderate phase, showed ~3–3.5% of volumetric change in the next 166 days. The average total expansion ratio of the specimen was 8.2 % for a 206-day test period.

The volumetric change of the steel slag without fine particles is shown in Figure 5-6.b. The results show that at 40 days of testing the expansion ratio was 3%–4%, and continued increasing as a linear line of increment to 7% of the average expansion ratio at 164 days.

The expansion of steel slag was mainly caused by two hydrated minerals—hydrated free lime (CaO) and magnesium oxide (MgO). The results showed a consistent ratio of volumetric expansion in time with the previous study performed by Sorlini et al. (2012); the first phase (up to 40 days) exhibited a larger volumetric expansion than the latter phase. The first phase of the expansion was mainly caused by the hydrated free lime, and the latter expansion was caused by the hydrated free lime and magnesium oxide. This is because the hydration process of free lime gets completed relatively faster (weeks) compared to the hydration process of magnesium oxide (years) (Motz and Geiseler, 2001; Juckes, 2003).

A further observation, a comparison between the volumetric expansion of the steel slag with fine particles and the steel slag without fine particles shown in Figure 5-7, was made. It leads to the fact that during the early test period the volume expansion of the steel slag with fine particles was higher than the steel slag without

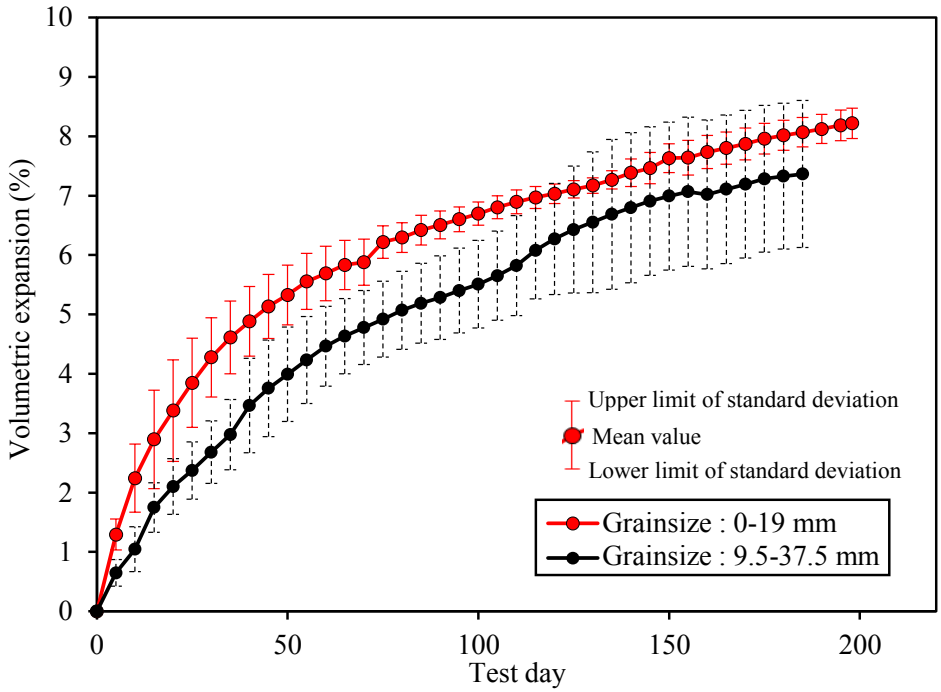

Figure 5- 7 The volumetric change of steel slag at various test days.

fine particles, however, during the final testing days, both had a similar value of volume expansion. The phenomenon can mislead our interpretation on the final volume expansion of steel slag if the judgment in design is taken based only on the early testing period.

It appears that the removal of the fine content in steel slag is not an effective method to reduce the volume expansion for a confined construction purpose. It is extremely probable that the steel slag with fine particles, which had a higher specific surface area, produced a faster hydration process than the steel slag without fine particles (Zhang and Napier-Munn, 1995), thus the volume expansion accelerated in the steel slag with fine particles. However, later, the existence of pores in steel slag body slowly allows the pore water to penetrate the larger aggregate causing hydration and expansion to lead to the same amount of volume change, eventually. Therefore, the amount of free CaO and free MgO most likely controls the final volume expansion, whereas the grain size distribution varies with the increment in volumetric change.

5.3.3 Effect of soft clay mixing

The results of the volumetric expansion, acquired from the three samples of the specimens with 45%, 55%, 60%, and 70% volumetric addition of the steel slag to the soft clay, are shown in Figure 5-8 as a function of time in a semi-logarithmic scale. Each case, with the three samples, showed a marginally-lower standard deviation (less than 0.3) at all the different additions except for when the R_{SS} equaled 70% (0.93). The soil mixture with R_{SS} between 45%–60% exhibited barely 0.02–0.35% of volumetric expansion, whereas the one with 70% addition exhibited 1.37% of volume expansion. The final volumetric expansion of the various steel slag additions is summarized in Table. 3.

It is apparent that the soft clay addition to the steel slag generated lower volumetric expansion values compared to those of the pure steel slag. Each specimen with 45%–60% addition of the steel slag habitually showed a similar behavior of volumetric exchange; starting with an immediate settlement, and after a period of time, expanding. The evidence suggests that the high void ratio of the soft clay provides spaces for the steel slag to expand and causes less change in volume as a whole.

Figure 5-9 shows the volumetric expansion measured at the end of the test as a function of the volumetric steel making slag addition, R_{SS}. It indicates that the volumetric expansion is proportional to the steel slag addition, with a logarithmic increment. The results suggest that the maximum volumetric addition of steel slag is up to 60% to comply with the allowable expansion value. Although one specimen with R_{SS} = 60% showed a value slightly above the allowable expansion ratio (0.67%), as an average, the final volumetric change was only 0.35%.

The results occasionally showed one among three specimens with a relatively higher volumetric expansion than the other two. It most likely occurred because the aggregate coincidentally formed a skeleton (a direct contact between the surfaces of the aggregates) that directly pushed the spacer disk during volume expansion.

Figure 5-10 shows the strength of the specimen obtained by the unconfined compressive test as a function of various R_{SS} values at a curing time of 7 day. The specimen with 45%, 55%, 60%, and 70% R_{SS} exhibited 297.5, 581, 340.7, and 239.02 kN/m^2 unconfined compressive strength, respectively. Strength test data from a previous study (Cikmit et al., 2019) are included for a further comparison; 20% and 30% R_{SS} exhibited 370 and 339 kN/m^2 of unconfined compressive strength, respectively. Tsuchida et al. (2019) reported that the minimum stress strength for a geomaterial to produce a lower earth pressure under an earthquake load was 200 kN/m^2.

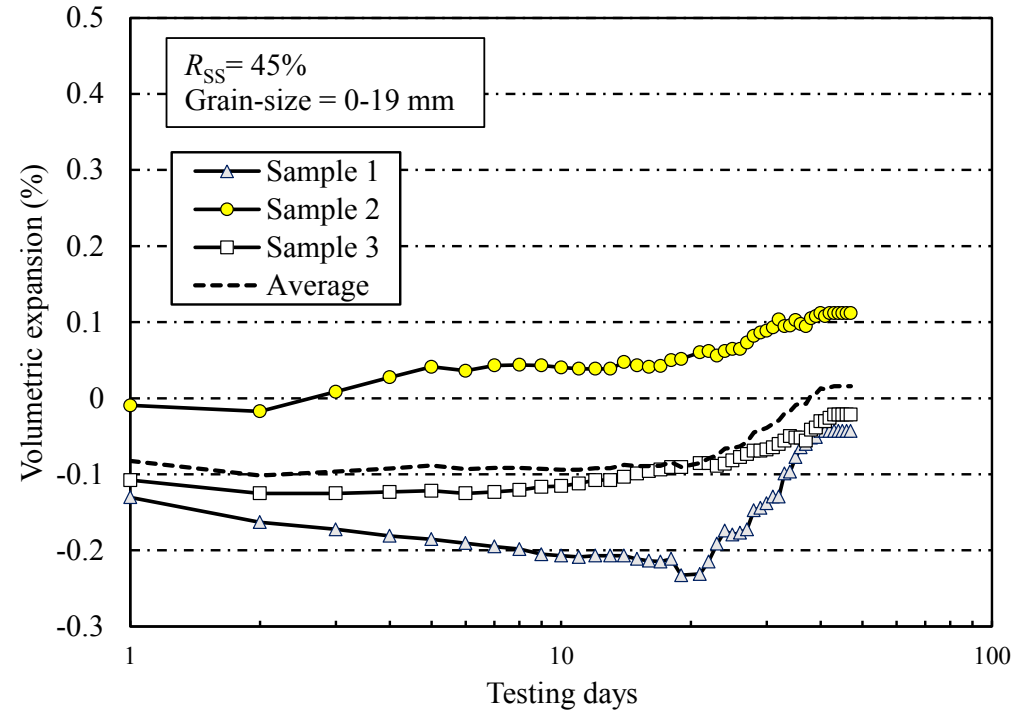

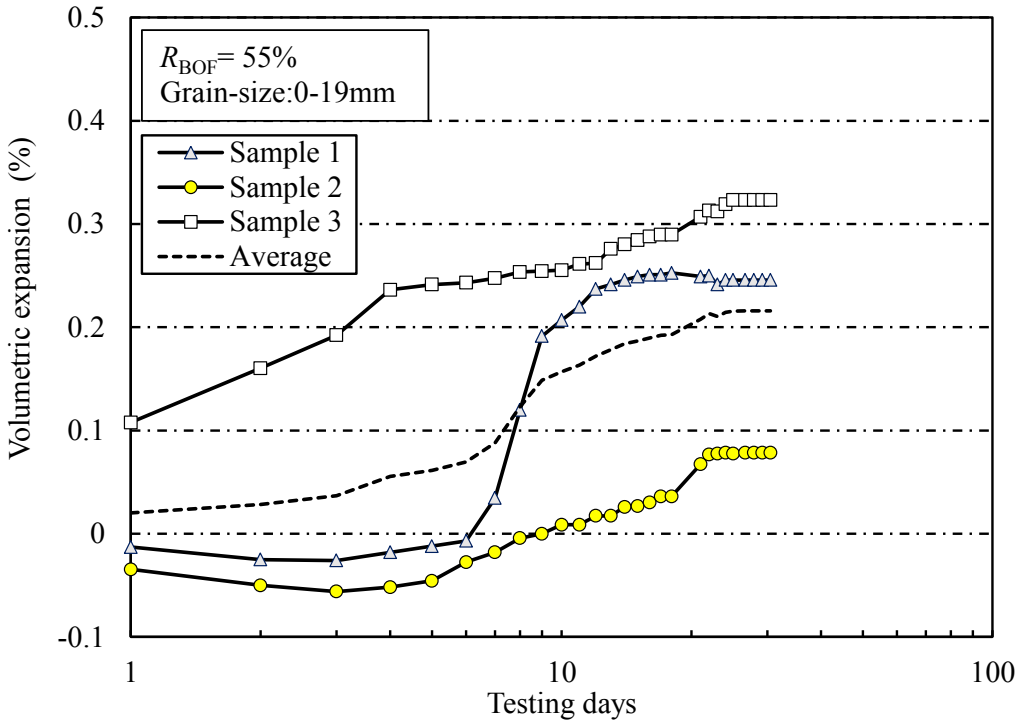

Figure 5- 8.a-b Volumetric expansion of soil mixture (R_{SS} = 45%, 55%, 60% and 70%).

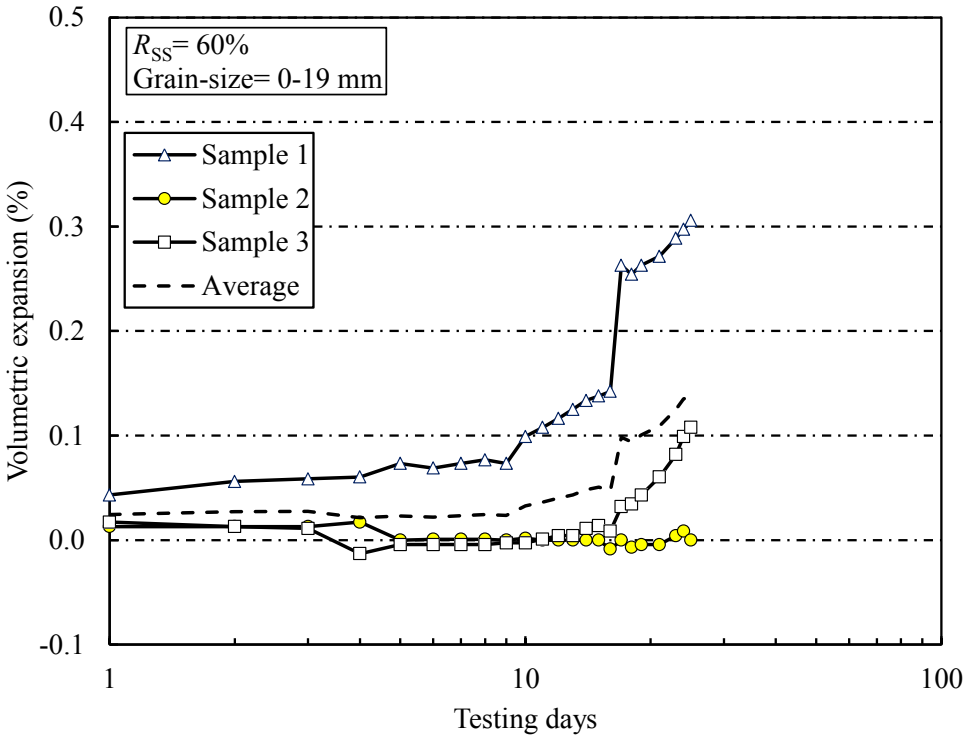

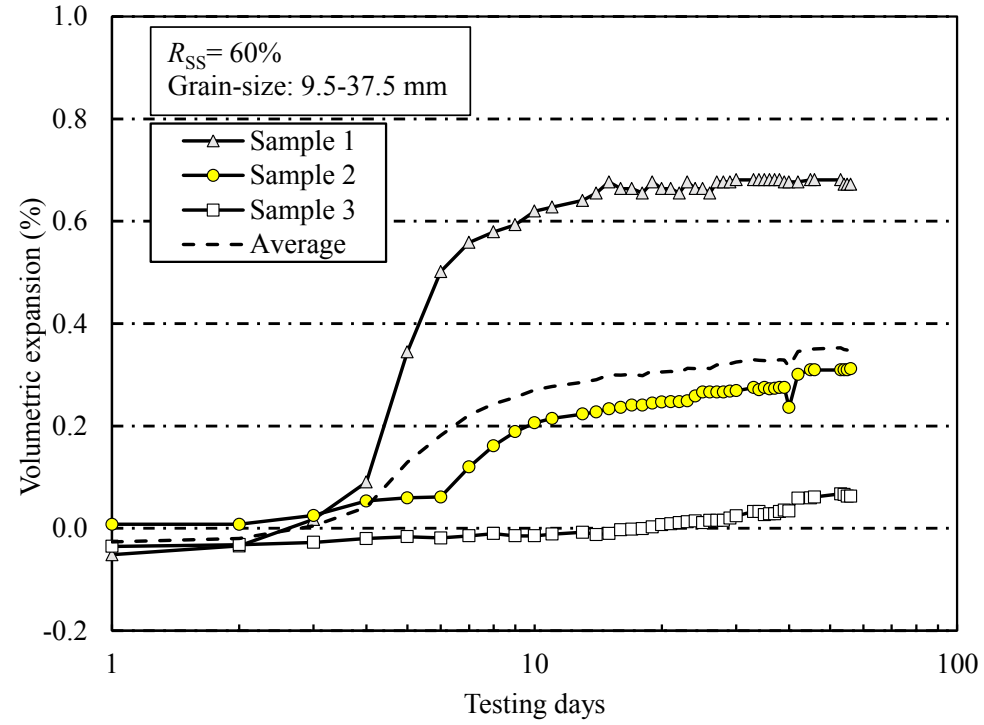

Figure 5-8.c-d Volumetric expansion of soil mixture (R_{SS} = 45%, 55%, 60% and 70%).

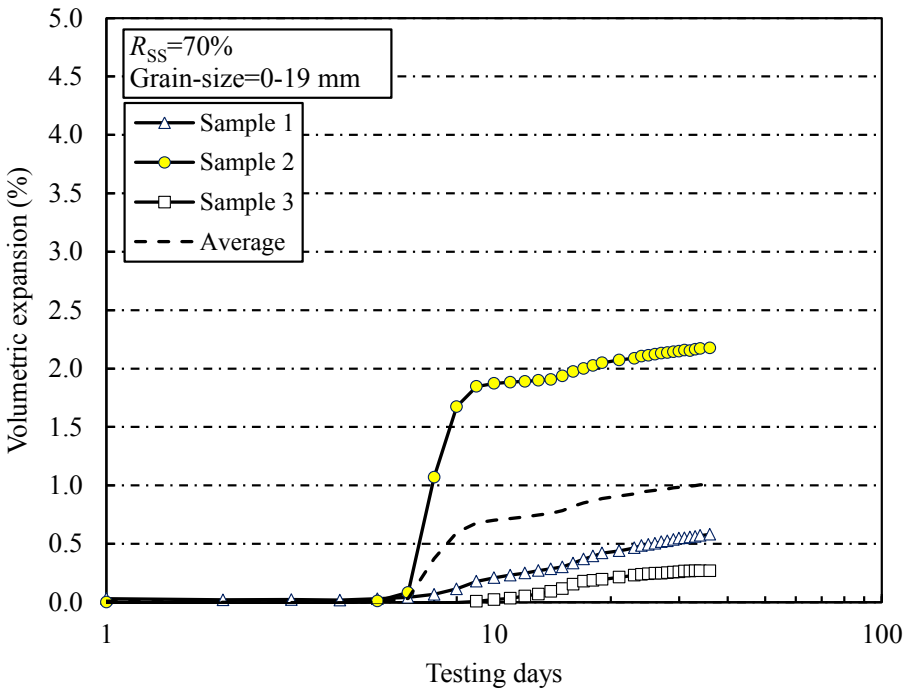

Figure 5-8.e Volumetric expansion of soil mixture (R_{SS} = 45%, 55%, 60% and 70%).

Based on the strength test result, it can be said that although the strength may differ, the specimen exhibited a sufficient strength to be adapted as a submerged geomaterial.

Table 5- 3 Volumetric expansion of various R_{SS}

R_{SS} (%)	Grain-size (mm)	Sample no.	Volumetric expansion, ε_v (%)	Average, $\overline{\varepsilon_v}$ (%)	Test days
45	0-19	1 2 3	-0.04 0.11 -0.02	0.02	47
55	0-19	1 2 3	0.25 0.08 0.32	0.22	52
60	0-19	1 2 3	0.46 0.07 0.19	0.24	72
60	9.5-37.5	1 2 3	0.67 0.31 0.06	0.35	56
70	0-19	1 2 3	0.93 2.35 0.83	1.37	138
100	0-19	1 2 3	8.33 8.40 7.93	8.22	206
100	9.5-37.5	1 2 3	8.53 6.26 6.49	7.09	164

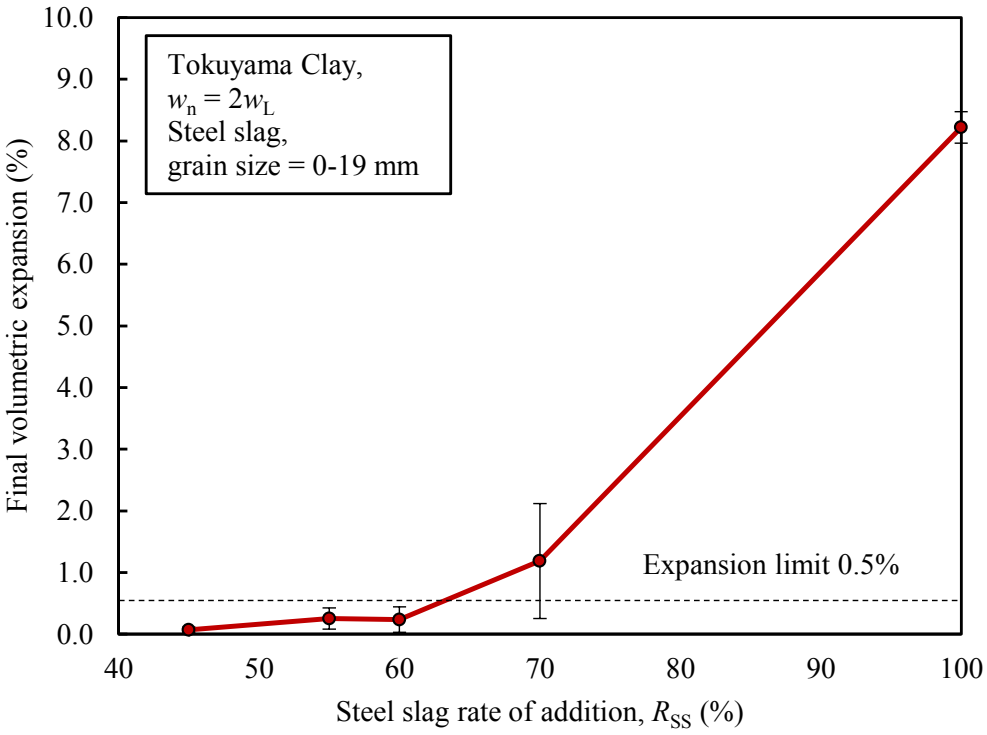

Figure 5- 9 The relationship between the steel slag addition and the final volumetric expansion.

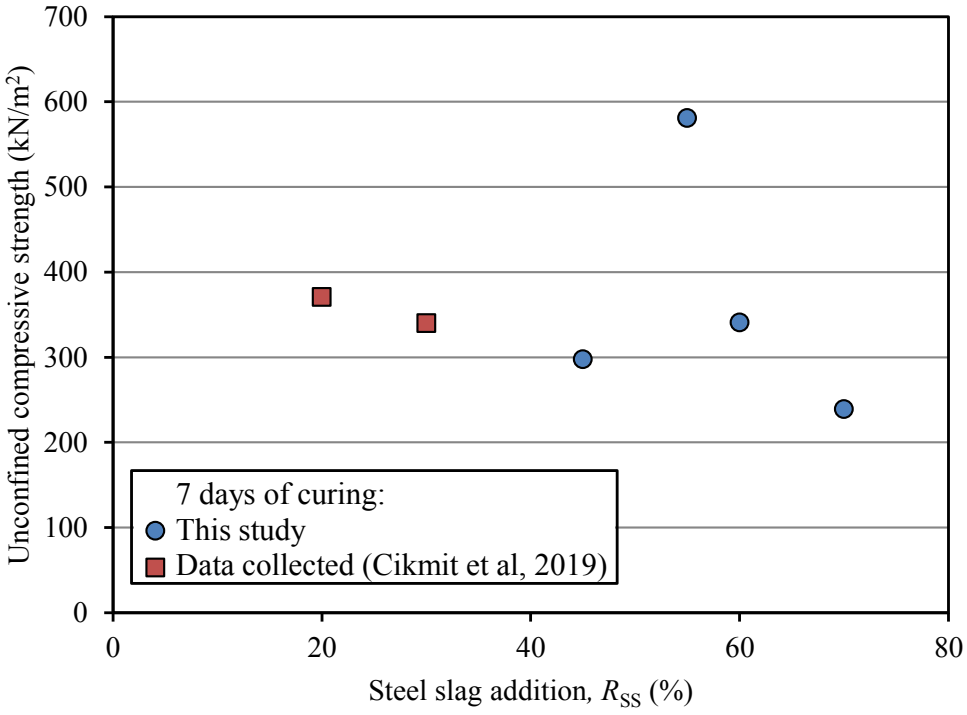

Figure 5- 10 Unconfined compressive strength of soil mixtures with various R_{SS}.

5.3.4 Microstructural observations by SEM and EDS

The representative SEM micrographs of the general structure of steel slag at 200 days after the expansion test are shown in Figures 5-11.a and 5-11.b. It can be seen that there were mainly two types of hydration products produced during the expansion test; a needle-like type, and a fibrous type of hydration structure. The hydration products likely incorporated the C-S-H gel, which interwove with each other.

The EDS data analysis shown in Figure 5-11.c confirmed the existence of the C-S-H gels, which is similar to the results in OPC (Mark and Augustine Osei, 2013). The results exhibited the elements of interest, Ca, Si, and Al. Wang et al. (2010a) reported that the expansion mechanism is mainly caused by the increase in the solid phase of the hydrated limes; lime originally has a specific gravity of 3.34, and when it reacts with water, it produces portlandite ($Ca(OH)_2$) with a specific gravity of 2.23, which results in an increase in volume. Later, the dissolved elements of silica from the steel slag react with the calcium in the portlandite to form the C-S-H phase and produce a close value of specific gravity.

Figures 5-12.a-c show the SEM micrographs of the soil mixtures with R_{SS} values equal to 55%, 60%, and 70%, respectively at a 50-day test period with a 500× magnification. It is clearly seen that there were microcracks in the body of the soil mixtures with 55% and 60% R_{SS}, whereas no crack was found in the soil mixtures with 70% R_{SS}. The microcracks were caused by the shrinkage of the soil mixtures since the soft clay had a large initial void ratio. The results supported the previous claim that the little amount of expansion found in the 55% and 60% was due to the higher void present in the soft clay, which could provide a larger space, as compared to 70%, to absorb the volumetric change of the steel slag.

It is also observed on the SEM micrographs that more hydration products (needle-like type or fibrous type) can be seen in 70% R_{SS} than in 55% and 60% R_{SS}. This is due to the larger free lime (f-CaO) and lime (CaO) content present in 70% R_{SS}.

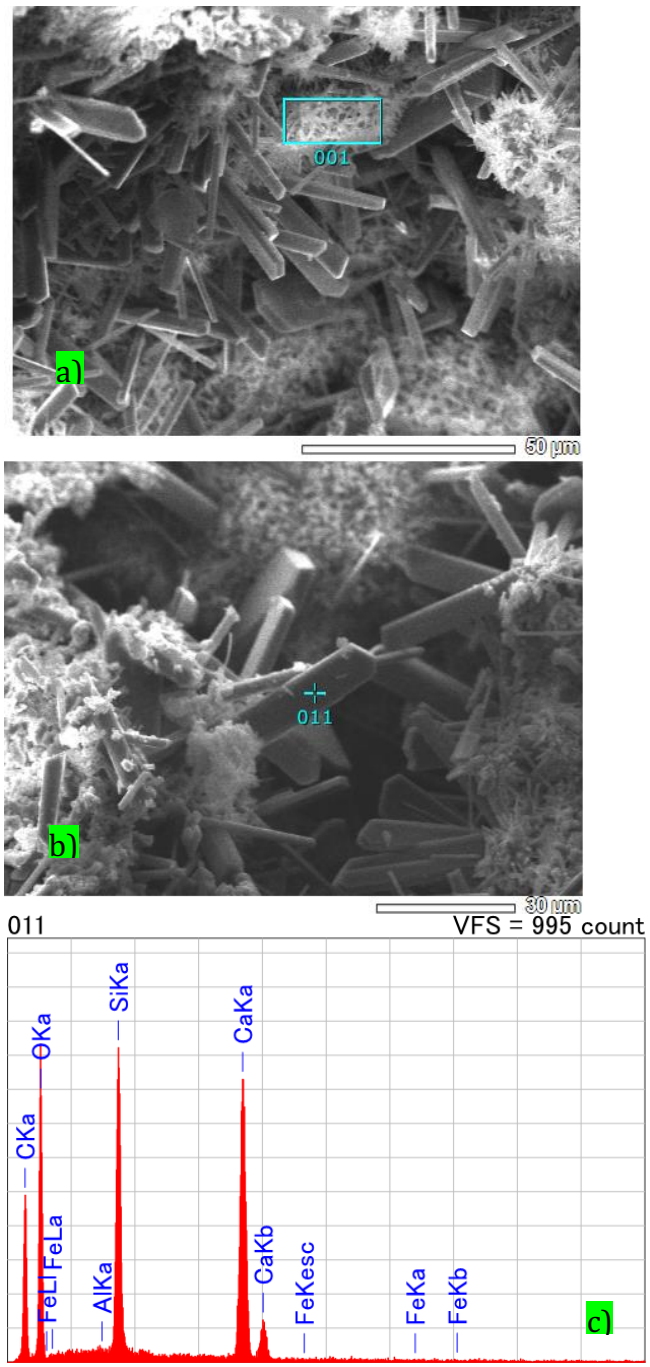

Figure 5- 11 SEM micrographs and an EDS analysis of sample 100% steel slag after expansion test at a 200-day test period (500 magnification).

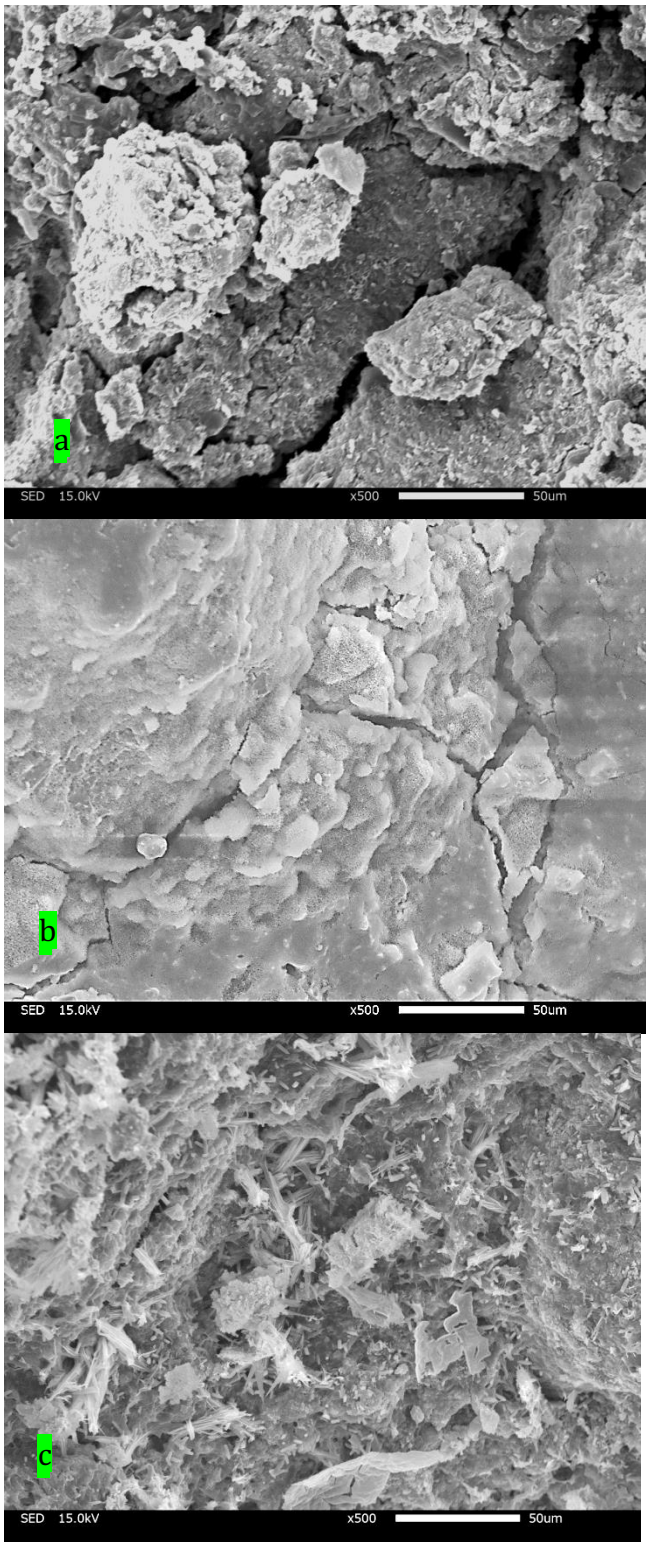

Figure 5- 12 SEM micrographs of the soil mixtures with a steel slag addition, *R*SS, equal to a)55%, b)60%, c) 70%, at a 50-day test period.

5.4 Conclusions

Several expansion tests were performed on different rates of steel slag addition (45%, 55%, 60%, 70%, and 100%) to investigate the volume change of the steel slag-treated soft clay. The maximum rate of steel slag addition to the soft clay that complies with the 0.5% expansion ratio was 60% and it produced 24.3 kN/m^3 of unit weight. It is well ascertained that the addition of soft clay increases the unit weight of the soft clay and reduces the volume expansion of the steel slag. The high void ratio of the soft clay was found to be the likely reason, as it provides more space to absorb the volumetric change. A fewer number of hydration products were observed using a scanning electron microscope in the soil mixtures with an addition of 55%–60% of steel slag as compared to the ones with 70%–100%.

The steel slags with and without fine aggregates were also subjected to the expansion test. The results indicate that the steel slag with fine particles showed a relatively higher value of volume expansion than the steel slag without the fine particles at the early test period (40 days). However, the final volume expansion of steel slag both with and without the fine particles was very similar. It is therefore well ascertained that the removal of the fine aggregate was not an effective way to alleviate the volume expansion.

Our results further explained that the amount of free CaO and free MgO most likely controls the final volume expansion, whereas the grain size distribution varies the increment of the volumetric change.

SEM and EDS analysis results showed more microcracks and less existence of the C-S-H phase for the addition of 45%–60% of steel slag than for 70%–100%, which explains the occurrence of less volumetric expansion.

5.5 References

11th Global Slag conference, Exhibition and Awards 2016. http://www.globalslag.com/conferences/global-slag/review/global-slag-review-2016. Access in 30 March 2019.

Arabani, M., and Azarhoosh, A.R. (2012). The effect of recycled concrete aggregate and steel slag on the dynamic properties of asphalt mixtures. Construction and Building Materials *35*, 1–7.

Aziz, M.M.A., Hainin, M.R., Yaacob, H., Ali, Z., Chang, F.-L., and Adnan, A.M. (2014). Characterisation and utilisation of steel slag for the construction of roads and highways. Materials Research Innovations *18*, S6-255-S6-259.

ASTM D698, Standard Test Methods for Laboratory Compaction Characteristics of Soil Using Standard Effort (12 400 ft-lbf/ft^3 (600 kN-m/m^3)), ASTM International, West Conshohocken, PA, 2012, www.astm.org

ASTM D4792 / D4792M-13(2019), Standard Test Method for Potential Expansion of Aggregates from Hydration Reactions, ASTM International, West Conshohocken, PA, 2019, www.astm.org

ASTM D2940 / D2940M-15, Standard Specification for Graded Aggregate Material For Bases or Subbases for Highways or Airports, ASTM International, West Conshohocken, PA, 2015, www.astm.org

Bartos, M.J. (1977). Classification and Engineering Properties of Dredged Material. (ARMY ENGINEER WATERWAYS EXPERIMENT STATION VICKSBURG MISS).

Chen, Z., Xie, J., Xiao, Y., Chen, J., and Wu, S. (2014). Characteristics of bonding behavior between basic oxygen furnace slag and asphalt binder. Construction and Building Materials *64*, 60–66.

Cikmit, A. A., Tsuchida, T. Kang, G. Hashimoto, R. and Honda, H. (2019). Particle Size Effect of Basic Oxygen Furnace Steel Slag in Stabilization of Dredged Marine Clay. Soils and Foundations. (Accepted).

Geiseler, J. (1996). Use of steelworks slag in Europe. Waste Management *16*, 59–63.

Guo, Y., Xie, J., Zhao, J., and Zuo, K. (2019). Utilization of unprocessed steel slag as fine aggregate in normal- and high-strength concrete. Construction and Building Materials *204*, 41–49.

Horii, K., Kitano, Y., Tsutsumi, N., and Kato, T. (2013). Processing and Reusing Technologies for Steelmaking Slag. 123–129.

Juckes, L.M. (2003). The volume stability of modern steelmaking slags. Mineral Processing and Extractive Metallurgy *112*, 177–197.

Kang, G., Cikmit, A.A., Tsuchida, T., Honda, H., and Kim, Y. (2019). Strength development and microstructural characteristics of soft dredged clay stabilized with basic oxygen furnace steel slag. Construction and Building Materials *203*, 501–513.Maslehuddin, M., Sharif, A.M., Shameem, M., Ibrahim, M., and Barry, M.S. (2003). Comparison of properties of steel slag and crushed limestone aggregate concretes. Construction and Building Materials *17*, 105–112.

Mark, B., and Augustine Osei, F. (2013). Alternative Binders for Increased Sustainable Construction in Ghana—A Guide for Building Professionals. Materials Sciences and Applications *2013*.

Montgomery, D.G., and Wang, G. (1991). Instant-chilled steel slag aggregate in concrete - strength

Motz, H., and Geiseler, J. (2001). Products of steel slags an opportunity to save natural resources. Waste Manag *21*, 285–293.

Pasetto, M., and Baldo, N. (2010). Experimental evaluation of high performance base course and road base asphalt concrete with electric arc furnace steel slags. J. Hazard. Mater. *181*, 938–948.

Piatak, N.M., Parsons, M.B., and Seal II, R.R. (2015). Characteristics and environmental aspects of slag: a review. Applied Geochemistry *57*, 31.

Poh H. Y., Ghataora Gurmel S., and Ghazireh Nizar (2006). Soil Stabilization Using Basic Oxygen Steel Slag Fines. Journal of Materials in Civil Engineering *18*, 229–240.

Proctor, D.M., Fehling, K.A., Shay, E.C., Wittenborn, J.L., Green, J.J., Avent, C., Bigham, R.D., Connolly, M., Lee, B., Shepker, T.O., et al. (2000). Physical and Chemical Characteristics of Blast Furnace, Basic Oxygen Furnace, and Electric Arc Furnace Steel Industry Slags. Environ. Sci. Technol. *34*, 1576–1582.

Sato, H., Nishimura, S., Toda, K., Sato, T., and Arai, Y. (2016). Characteristic and Interpretation of Development of Strength and Stiffness for Early-Age Calcia-

Stabilized Dredged Soils. Hokkaido Site Engineering Society *Techincal report*, 15–20.(In Japanese)

Shen, W., Zhou, M., Ma, W., Hu, J., and Cai, Z. (2009). Investigation on the application of steel slag-fly ash-phosphogypsum solidified material as road base material. J. Hazard. Mater. *164*, 99–104.

Shi, C., and Qian, J. (2000). High performance cementing materials from industrial slags - a review. Resources, Conservation & Recycling *3*, 195–207.

Shi, C. (2004). Steel Slag—Its Production, Processing, Characteristics, and Cementitious Properties. Journal of Materials in Civil Engineering *16*, 230–236.

Sorlini, S., Sanzeni, A., and Rondi, L. (2012). Reuse of steel slag in bituminous paving mixtures. J. Hazard. Mater. *209–210*, 84–91.

Tsuchida, T., Tsurugasaki, K., and Cikmit, A.A. (2019). Study on the Use of Heavy-weight Geo-Material for Design of Quay-wall Structure or Sea-wall. Journal of J.S.C.E Maritim Development Vol.*76 No.1*. (In Japanese).

Wang, G., Wang, Y., and Gao, Z. (2010a). Use of steel slag as a granular material: volume expansion prediction and usability criteria. J. Hazard. Mater. *184*, 555–560.

Wang, G. (2010). Determination of the expansion force of coarse steel slag aggregate. Construction and Building Materials *24*, 1961–1966.

Yi, H., Xu, G., Cheng, H., Wang, J., Wan, Y., and Chen, H. (2012). An Overview of Utilization of Steel Slag. Procedia Environmental Sciences *16*, 791–801.

Yildirim, I., and Prezzi, M. (2009). Use of Steel Slag in Subgrade Applications. JTRP Technical Reports.

Yong-Feng, D., Tong-Wei, Z., Yu, Z., Qian-Wen, L., and Qiong, W. (2017). Mechanical behaviour and microstructure of steel slag-based composite and its application for soft clay stabilisation. European Journal of Environmental and Civil Engineering *0*, 1–16.

Zhang, Y.M., and Napier-Munn, T.J. (1995). Effects of particle size distribution, surface area and chemical composition on Portland cement strength. Powder Technology *83*, 245–252.

Chapter 6

Time-delay effect on the strength development of stabilized soils with BOF slag

TABLE OF CONTENTS

6.1 Introduction

Basic oxygen Furnace slag is a by-product of the conversion of pig iron to steel in a steel manufacturing process (Shi, 2004; Yildirim and Prezzi, 2011). In Japan, for a long time, substantial amounts of BOF slag have simply been dumped to a disposal facility (Horii et al., 2013). The act of landfilling with this by-product could not only be uneconomic but also not environmentally friendly. Therefore, many types of research have been conducted to recycle basic oxygen furnace slag to alleviate the cost and preserve nature.

Most of the research of basic oxygen furnace slag covered chemical, physical, and geometrical properties. There are various applications of basic oxygen furnace slag have been studied, such as aggregates in road construction (Ahmedzade and Sengoz, 2009), aggregate in concrete material (Qasrawi et al., 2009), cementitious material in cement (Shi, 2004), and materials in a fertilizer industry. Also, a geo-material which come from the stabilized soft soil using basic oxygen furnace slag (Cikmit et al., 2017; Kang et al., 2019).

Recent studies (Kang et al., 2019; Poh H. Y. et al., 2006; Sato et al., 2016; Yong-Feng et al., 2017) have shown that steel slag can improve the strength and durability of soft clays, with or without activators. The strength and workability of soft clay are improved by the drying action of the free lime and low water content of the steel slag. The feasibility studies of the stabilized soil with basic oxygen furnace slag in an actual field have been comprehensively performed (Kiso et al., 2008; Tsuchida et al., 2019).

In actual construction, often there is a time gap between the mixing process and the filling construction. It may come from two main factors, whether the distribution time or the waiting time for the material to achieve the minimum strength to be filled in a certain inclination of slope. The time gap might be considered as a disturbance since it will affect the strength development of the stabilized soft soil using basic oxygen furnace slag.

This study aims to comprehensively understand the effect of time gap on the strength development of stabilized soil with various time disturbances, and different additional of basic oxygen furnace slag. From the results, it was found that the

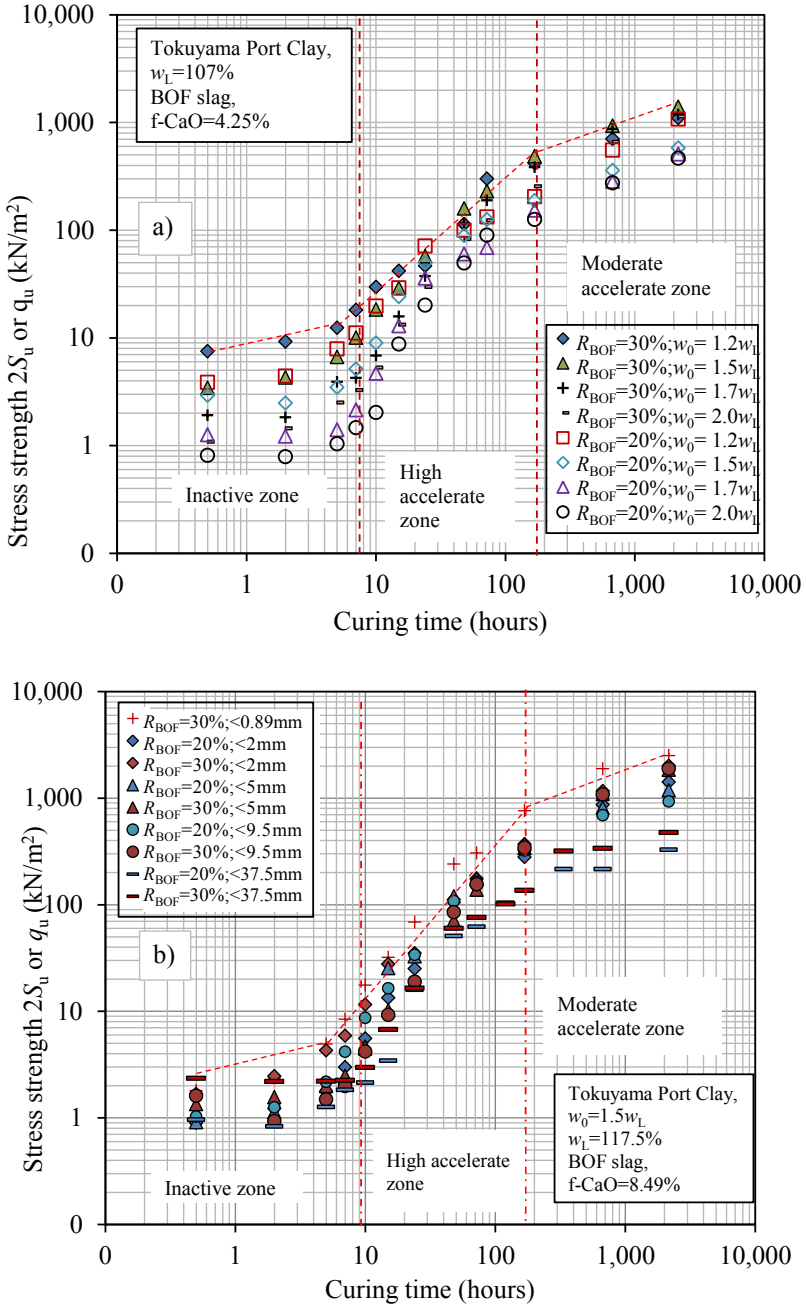

Figure 6- 1 The typical strength development of stabilized soils with steel slag. a) stabilized soils with various initial water and steel slag content (Chapter 1) b) stabilized soils with various steel slag addition and grain-size (Chapter 3).

strength was not affected by the disturbance as long as the time gap still in the dormant period of the strength development of stabilized soil with basic oxygen furnace slag. The strength development of the stabilized soil at 28 and 90 days can be predicted with the strength from 7 and 28 days, respectively.

6.2 The strength development characteristic of SMSS

Previous studies (Sato et al., 2016; Chapter 1; Chapter 2) showed that the strength development of stabilized soils with steel slag is unique compare to the strength development of stabilized soil with Portland cement. Figures 6-1 shows the time-strength characteristic of stabilized soils with steel slag. The strength development of stabilized soils with steel slag can generally be divided into three zone; inactive zone, high accelerate zone, and moderate accelerate zone.

On one hand, in an actual construction, the stabilized soils with steel slag is cured for several hours or days to gain a minimum strength which is crucial to construct the fill with a stiff slope (vertical to horizontal 1:2 or 1:3) (Tanaka et al., 2014; Yamagoshi et al., 2014). On the other hand, the duration of delay time from mixing to the filling construction can give a significant effect to the strength development of stabilized soils with steel slag. Therefore, the optimum time (between mixing and fill construction) to fill the stabilized soils is necessarily considered in this study.

6.3 Methodology

The definition of disturbance in this study is the time delay from the mixing process to the pouring process into molds. The time delay portrays the interval time between the mixture process in batching plan and the fill process in an actual construction. The delay could simply be caused by the distribution or most of the time to achieve minimum strength for keeping minimum turbidity of the ocean during the fill construction (reference).

In order to cemprehend the delayed-cast disturbance effect to the strength development of stabilized soil with steel slag, a series of strength test was performed in laboratory; using a laboratory vane shear (LVS) test and an unconfined compressive (UC) test. The disturbance was varied from 2, 5, 7 hours and 1, 2 and 3 days.

6.3.1 Materials

The soft clay used in this study is the dredged-marine soil of Tokuyama Port, Yamaguchi Prefecture, Japan. The dredged-marine soil of Tokuyama Port is odorless and has a dark-greenish color. It has a liquid limit, a plastic limit, and a plasticity index equal to 119.9%, 45.6%, and 74.3%, respectively. According to the unified soil classification system, the marine-dredged clay is classified as high-plasticity clay. The relative density of the soil is 2.68 g/cm^3. Table 1 summarizes the basic physical properties of the soft clay.

The steel slag was supplied by JFE steel company in Fukuyama City, Japan. It is a fresh steel slag with a sub-angular shape. It originally has a maximum diameter of 37.5 mm and a fine-grain content of 10.5%. The original grain size distribution of the BOF slag is depicted in Figure 6-2. The average specific gravity of the steel slag is 3.15. The free lime content of the steel slag, obtained using an ethylene glycol method, is 8.49%. The surface dry density and the absolute dry density of the steel slag are 3.19 g/cm^3 and 3.08 g/cm^3, respectively. Table 2 summarizes the basic physical properties of the steel slag.

Figure 6-2 shows the grain-size distribution of the soft soil and the BOF slag.

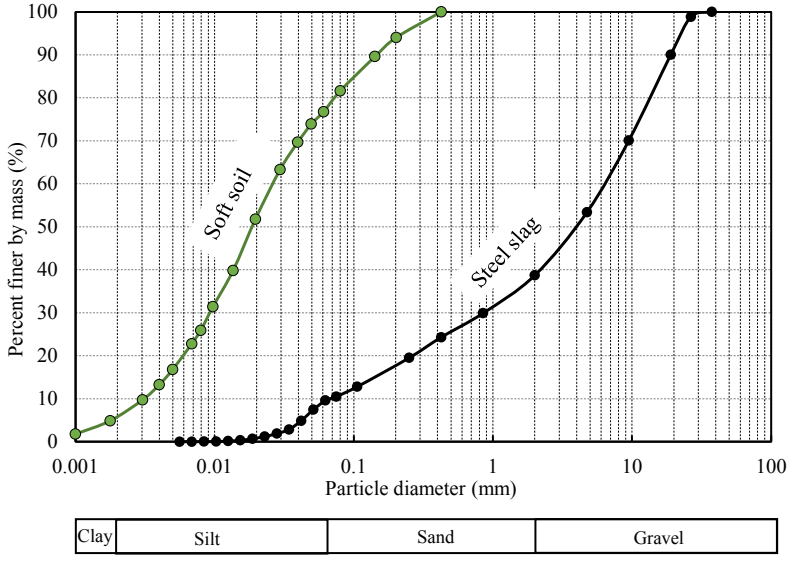

Figure 6- 2 Grain-size distribution of the soft soil and steel slag.

From X-ray diffraction, the result showed that the steel slag exhibited minerals such as portlandite ($Ca(OH)_2$), vaterite ($CaCO_3$), wustite (FeO), srebrodolskite ($Ca_2Fe_2O_5$), calcite ($CaCO_3$), larnite (Ca2SiO4), lime (CaO), fayalite (Fe2SiO4), and magnetite (FeFe2O4). The crystalline components obtained from the X-ray fluorescence test are mainly CaO, Fe_2O_3, SiO_2, P_2O_5, MnO, Al_2O_3, MgO.

Table 6- 1 Properties of the soft clay.

Property	Soft clay
Liquid limit, w_L (%)	119.9
Plastic limit, w_P (%)	45.6
Plastic index, PI (%)	74.3
Specific gravity, Gs (g/cm^3)	2.68
Coarse-grained Soil (%)	9.98
Fine-grained soil (%)	90.02
Unified soil classification system (USCS)	CH
pH	7.2
Ignition loss, LOI (%)	8.17
Salinity (%)	3.48

Table 6- 2 Engineering properties of the BOF slag.

Property	BOF slag
Specific gravity, Gs (gr/cm^3)	3.15
Absolute dry density (gr/cm^3)	3.02
Water absorption rate (%)	4.6
Maximum particle size (mm)	37.5
Coarse-grained Soil (%)	89.5
Fine-grained Soil (%)	10.5
Free CaO, f-CaO (%)	8.49

6.3.2 Mixing Proportions

The mixing proportion of the specimens is shown in Table 3. The steel slag additions ranged from 20%-30%, and curing time varied from 0.5 hours to 90 days. The

experimental mixing proportions were similarly determined as in the previous study (Cikmit et al., 2018) using Equation 1.

$$R_{BOF} = \frac{V_{\text{BOF}}}{V_{\text{soil}} + V_{\text{water}} + V_{\text{BOF}}} \times 100 \qquad (\%) \tag{1}$$

where V_{SS} is the solid volume of steel slag, V_{soil} and V_{water} are the volumes of soil and water.

Table 6- 3 Mixing proportion and curing time of BOF slag treated clay

Clay initial water content (%)	BOF slag R_{BOF} (%)	Time Disturbance	Curing Time
178.5% (1.5w_{L})	20, 30	2, 5, 7 hours 1, 2, 3 days	0.5, 2, 3, 5, 7, 10, 15 (hours) 1, 2, 3, 7, 28, 90 (days)

6.3.3 Specimen preparation

Prior to specimen fabrication, the materials were prepared as follows:

- The soft clay was initially filtered by using a 2 mm sieve to remove the coarse particles, shells, and coral reef fractions. Immediately after the sieving, the soft clay was kept in a hermetical box to reduce the loss of moisture.
- Steel slag was air-dried at room temperature, 25±5$^{\text{o}}$C, and 60% relative humidity for 24 hours. The moisture content of the steel slag dropped to 3%-5%. Later, the steel slag was sieved to get grain size distribution 0-4.75 mm.
- Artificial seawater was prepared by mixing distilled water with salt with 3.5% salinity. The salt water was prepared to represent the actual condition of the sea water on field construction.

To begin the mixing of the steel slag and the soft clay, the moisture content of the soft clay was subsequently brought to 2.0 of the liquid limit of the soft clay by adding the artificial-sea water and mixing it for 2 minutes. Then, the steel slag and the soft clay were uniformly mixed for 5 minutes by using a heavy-duty hand mixer.

The disturbance was applied to the sample by delaying the time of pouring of the sample to the mold from the mixing process. Soil mixture was poured into the testing mold after 0.2, 5, 7 hours, 1, 2, and 3 days after mixing. For instance, 1 day disturbance means that there was 24 hours' time interval from mixing to the pouring process. The curing time started from 0.5 hours after the mixing process.

6.3.4 Tests Performed

Strength development of stabilized dredged clay with steel slag at various disturbances and curing time contents were measured using two types of strength test. An LVS test in was adopted using (Japan Geotechnical Standard) JGS 1441-2012 to measure the low strength of samples. Samples were tested at 6 degrees/minutes of rotation speed. A rectangular vane with height to diameter ratio (H/D=1) is used, height and diameter of the blade were 20mm. Series LVS test was conducted on the specimen at 0.5h to 15h curing time which was predicted to have low strength. Tests were taken 40-60 degrees of rotation (peak of measured torque).

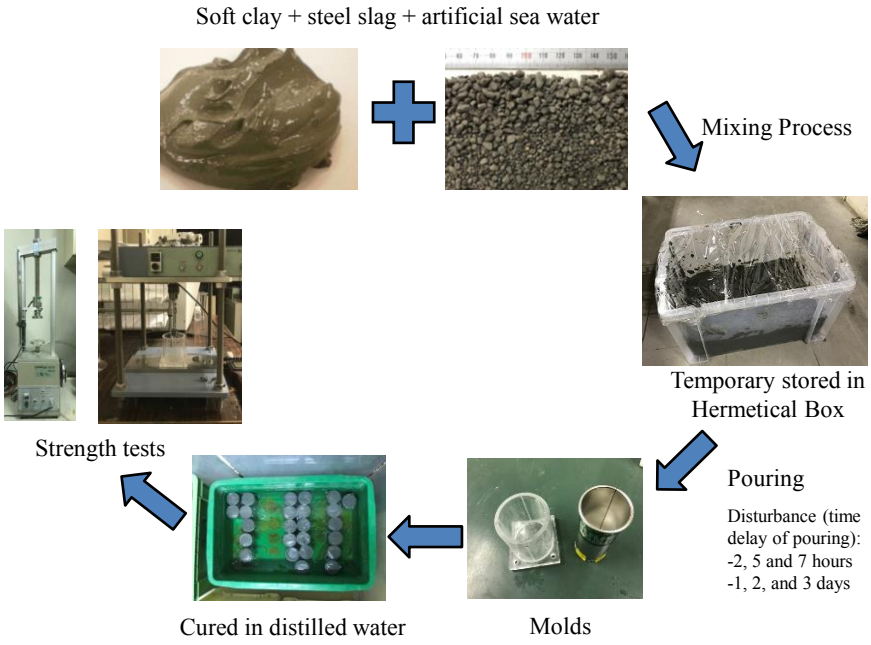

Figure 6- 3 Flow of sample preparation

The UC test (JGS 0511-2014), a prevalent testing to determine the strength of soil in Japan, was used to measure the strength of the specimen at 1-90 days of curing. Sample surfaces were aligned using a spatula before conducting the test. In this study, 1% per minute strain rate was accounted to perform the UC test. Both stress and strain were recorded and plotted and analyzed to obtain the secant modulus.

6.4 Test Result and Discussion

6.4.1 Stress-Strain

Figure 6-4 and 6-5 show the stress-strain curves of the specimens of 20% and 30% R_{BOF} after 3 days disturbance at 3, 7, 28 and 90 days after mixing. The specimens at 3 and 7 days after mixing exhibited stress-strain curves similar to soft soil. At 28 and 90 days after mixing, the stress-strain of the specimens developed to one that similar to stiff clay behavior. The results show that even though the disturbance affected the strength development of the stabilized soil, the stabilized soil has the ability to self-recover and develop the strength after period of time.

Fig. 6-6 shows stress-strain curves of the specimens of R_{BOF} 30% after 2 hours and 3 days disturbance at 28 and 90 days after mixing. The specimens after 2 hours and 3 days disturbance failed at 1.2% and 1.45% strain, respectively.

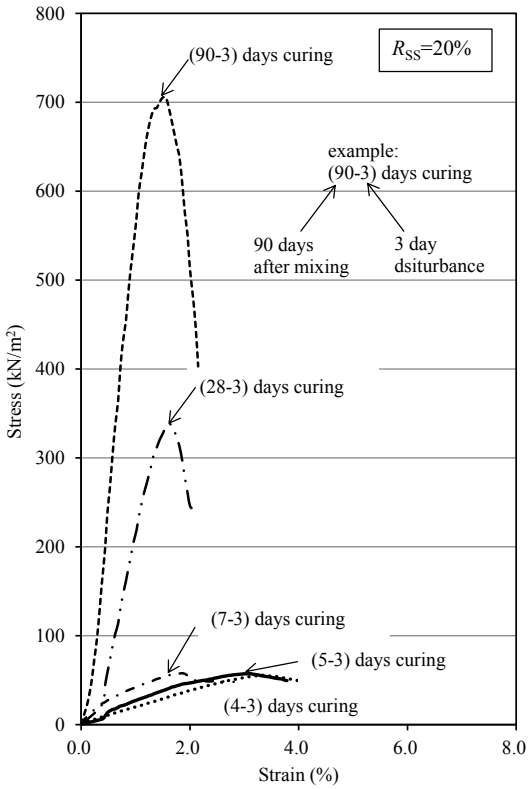

Figure 6- 4 Stress-strain curves of the specimen of R_{BOF} 20% after 3 days disturbance.

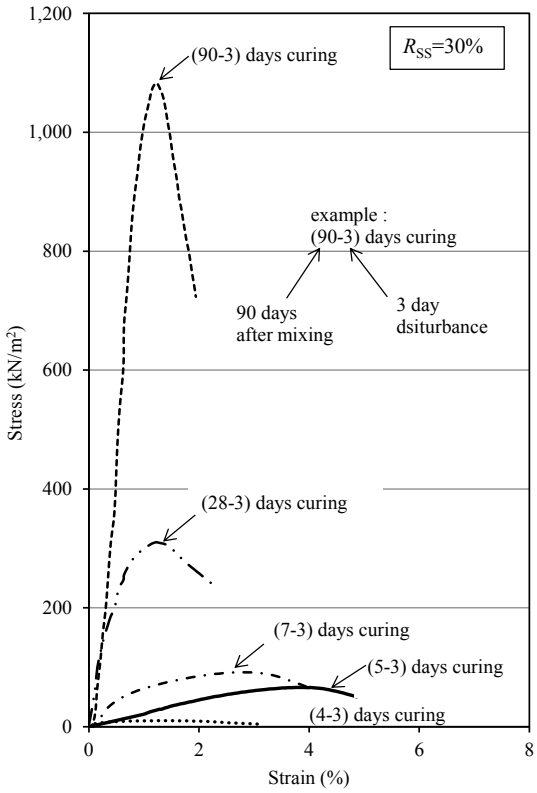

Figure 6- 5 Stress-strain curves of the specimen of R_{BOF} 30% after 3 days disturbance.

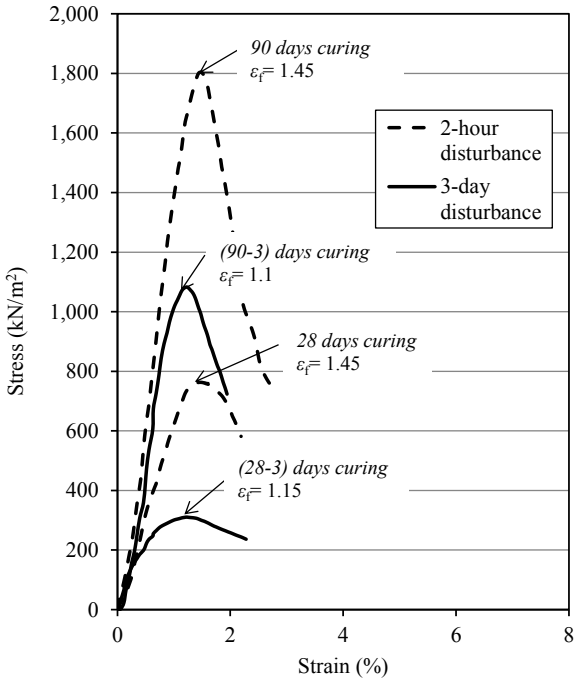

Figure 6- 6 Stress-strain curve of soil mixture at 90 days curing time after 2-hour disturbance and 3 day-disturbance.

6.4.2 Time-strength mobilization.

Figs. 6-7 and 6-8 show the strength mobilization of specimen of R_{BOF} 20% and 30% after 2, 5, 7 hours, 1, 2, and 3 days disturbance at various curing time. Fig. 6-7 shows that at the early curing time, the disturbance of 2, 5, 7 hours, 1, 2 and 3 days caused the specimen to exhibit lower stress strength than that without the disturbance. However, after 7 days, the specimens with 2, 5, and 7 hours disturbance surpassed the strength of the specimen without disturbance. The rest of specimens with 1, 2, and 3 days disturbance were able to develop with a strength ratio of 0.7, 0.5 and 0.52 to that without disturbance, respectively.

The specimens of 2, 5, and 7 hours disturbance were most likely had less moisture content than the specimen without disturbance since the hydration reaction had partially started. Thus, the specimen had less void and denser in unit weight which cause its higher in strength than the specimen without disturbance.

Fig. 6-8 shows the strength of the specimen of 2, 5 and 7 hours disturbance were less affected by the disturbance. At the early curing time, all the samples had lower strength than the specimen without disturbance. Later, after 28 days, the specimen of 2, 5, and 7 hours of disturbance achieved similar strength as what the

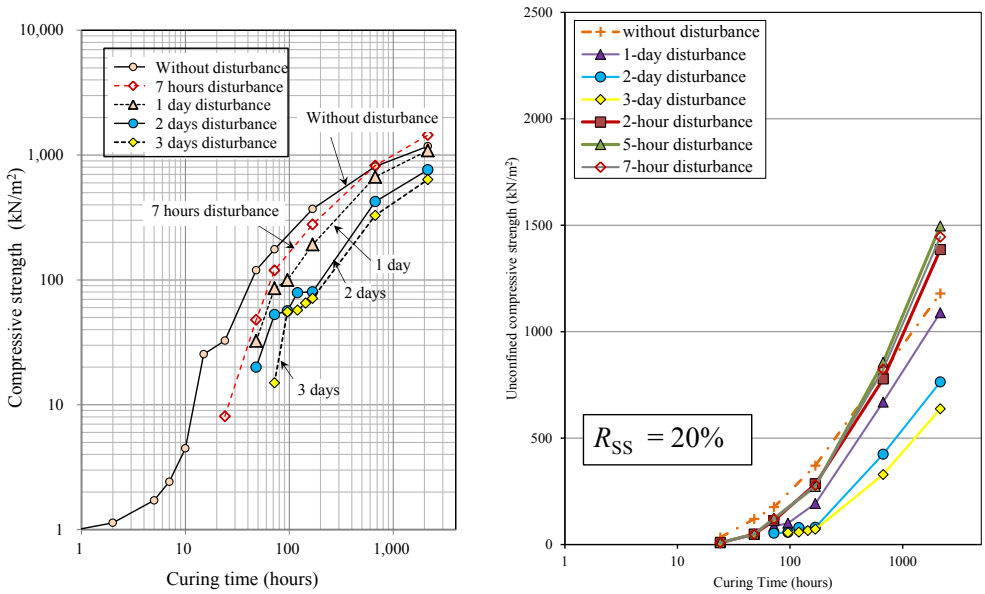

Figure 6-7 Strength development of soil mixture R_{BOF} = 20% with various disturbances.

specimen without strength exhibited. The specimens of 1, 2, and 3 days disturbance exhibited strength ratio of 0.92, 0.64, and 0.54, respectively.

From the results, it can be ascertained that up to its dormant period (10 hours), the strength of the stabilized soils at later curing time was close or higher than the specimen without disturbance.

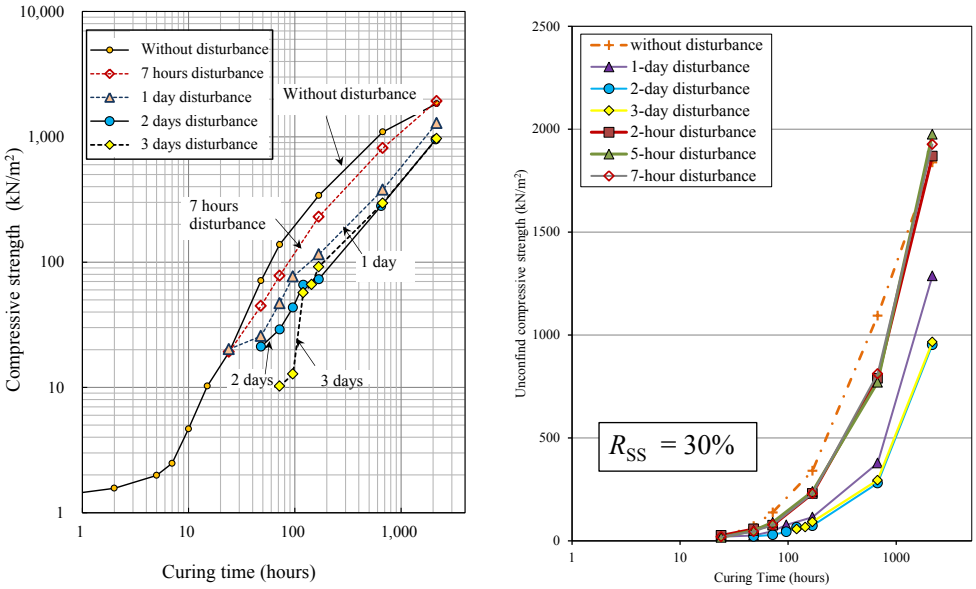

Figure 6-8 Strength development of soil mixture R_{BOF} = 30% with various disturbances.

Figure 6-9 and 6-10 show the strength ratio of the specimen with various disturbances at 7, 28 and 90 days after mixing. Fig. 6-9 shows the strength ratio of the specimen at 7 and 28 days after mixing. It is clearly seen that even though the data consist of various R_{BOF} values and different time-disturbances, the strength ratio can be referred by a single with a high coefficient determination, 0.94. From the results, we can predict the specimen strength from the results no matter the disturbance is with the equation as follow:

$$q_{u(28d)} = 2.6.q_{u(7d)} + 128 \quad (4)$$

where $q_{u(7d)}$ is the unconfined compressive strength of specimen at 7 days curing, and $q_{u(28d)}$ is the unconfined compressive strength at 28 days.

Fig. 6-10 shows a series of the strength ratio of the stabilized soils at 28 days and 90 days after mixing. The results show that the strength ratio of 28 to 90 days

($q_{u(90d)}$ / $q_{u(28d)}$) can be categorized based on the amount of its addition. The specimens of 30% R_{BOF} and 20% R_{BOF} can be represented by equation as follows:

$$q_{u(90d)} = 2.1q_{u(28d)} + 300 \quad \text{for } R_{BOF} = 20\% \qquad (3)$$

$$q_{u(90d)} = 1.75.q_{u(28d)} \quad \text{for } R_{BOF} = 30\% \qquad (4)$$

where $q_{u(90d)}$ is the unconfined compressive strength at 90 days.

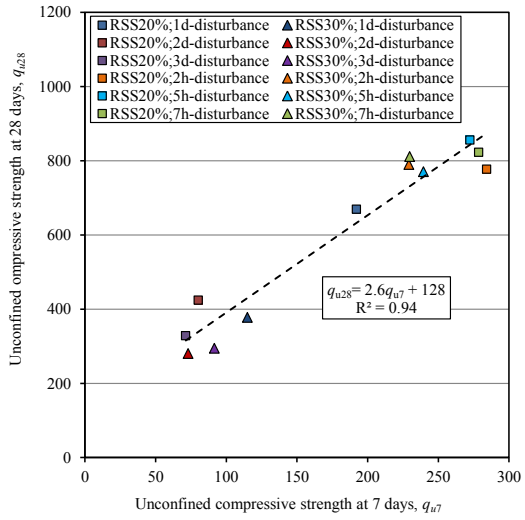

Figure 6-9 Strength ratio between strength at 7 days and 28 days after mixing.

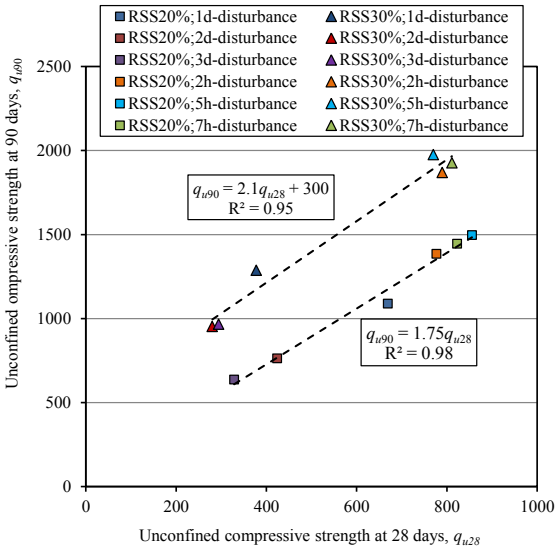

Figure 6-10 Strength ratio between strength at 28 days and 90 days.

6.5 Conclusions

From the data results obtained from the experiments in this study, conclusions are taken:

1. The disturbance significantly affected the strength development of the stabilized soil. However, the stabilized soil has the ability to self-recover and develop the strength after period of time.
2. Up to its dormant period (10 hours), the strength of the stabilized soils at later curing time (after 28 days) is close or higher than the specimen without disturbance.
3. For 30% R_{BOF}, the strength of the specimens with 2, 5, and 7 hours disturbance were fully recovered after 7 days close to the specimen without disturbance. The specimens with 1, 2, and 3 days disturbance were able to develop with a strength ratio of 0.7, 0.5 and 0.52 to that without disturbance, respectively.
4. For 20% R_{BOF}, after 28 days, the specimen of 2, 5, and 7 hours of disturbance achieved similar strength as what the specimen without strength exhibited. The specimens of 1, 2, and 3 days disturbance exhibited strength ratio of 0.92, 0.64, and 0.54, respectively.
5. Although the data consist of various R_{BOF} values and different time-disturbances, the strength ratio between 7 days and 28 days after mixing can be referred by a single with a high coefficient determination, 0.94.

The strength development can be predicted using strength Equation 4, 5 and 6.

6.6 References

Ahmedzade, P., and Sengoz, B. (2009). Evaluation of steel slag coarse aggregate in hot mix asphalt concrete. J. Hazard. Mater. *165*, 300–305.

Horii, K., Kitano, Y., Tsutsumi, N., and Kato, T. (2013). Processing and Reusing Technologies for Steelmaking Slag. 123–129.

Kiso, E., Tsujii, M., Ito, K., Nakagawa, M., Gomyo, M., Nagatome, T. 2008. Method of dredged soil improvement by mixing with converter steel-making slag. Kaiyo Kaihatsu Ronbunshu 2008, 24, p 327-332. (In Japanese).

Kang, G., Cikmit, A.A., Tsuchida, T., Honda, H., and Kim, Y. (2019). Strength development and microstructural characteristics of soft dredged clay stabilized

with basic oxygen furnace steel slag. Construction and Building Materials *203*, 501–513.

Poh H. Y., Ghataora Gurmel S., and Ghazireh Nizar (2006). Soil Stabilization Using Basic Oxygen Steel Slag Fines. Journal of Materials in Civil Engineering *18*, 229–240.

Qasrawi, H., Shalabi, F., and Asi, I. (2009). Use of low CaO unprocessed steel slag in concrete as fine aggregate. Construction and Building Materials *23*, 1118–1125.

Sato, H., Nishimura, S., Toda, K., Sato, T., and Arai, Y. (2016). Characteristic and Interpretation of Development of Strength and Stiffness for Early-Age Calcia-Stabilized Dredged Soils. Hokaido Site Engineering Society *Techincal report*, 15–20.

Shi, C. (2004). Steel Slag—Its Production, Processing, Characteristics, and Cementitious Properties. Journal of Materials in Civil Engineering *16*, 230–236.

Tanaka, Y., Ko, C., Imamura, T., Shibuya, T., Yamagoshi, Y., Akashi, Y., Kitano, Y., and Kanno, H. (2014). Reclamation of the artificial ground made of dredged soil and converter slag. Japanese Society of Civil Engineering B3 70, I_888-I_893.

Tsuchida, T., Tsurugasaki, K., and Cikmit, A.A. (2019). Study on the Use of Heavy-weight Geo-Material for Design of Quay-wall Structure or Sea-wall. Journal of J.S.C.E Maritim Development *76*.

Yildirim, I.Z., and Prezzi, M. (2011). Chemical, Mineralogical, and Morphological Properties of Steel Slag.

Yamagoshi, Y., Akashi, Y., Kanno, H., Nobuhiro, T., and Tanaka, Y. (2014). Reclamation by CaO improved soil. Nippon Steel and Sumitomo Metal Technical Bulletin *399*, 65–72.

Yong-Feng, D., Tong-Wei, Z., Yu, Z., Qian-Wen, L., and Qiong, W. (2017). Mechanical behaviour and microstructure of steel slag-based composite and its application for soft clay stabilisation. European Journal of Environmental and Civil Engineering *0*, 1–16.

Chapter 7

Summary

TABLE OF CONTENTS

7.1 Conclusion

From the experimental and discussions presented above, the main conclusions of the thesis can be summarized as follows:

7.1.1 Strength Development and Microstructural Characteristics of Soft Dredged Clay with Basic Oxygen Furnace Steel Slag

In **Chapter 3**, an attempt to further understand the strength development of the stabilized dredged marine soils with basic oxygen furnace (BOF) slag was performed. The main conclusions are as follows:

1. The strength development of stabilized dredged marine clay can be divided into three stages: a dormant/inactive period, active/high accelerated period, and moderate accelerated period.
2. 3. For the inactive zone, the equation for estimating the strength was proposed according to the volumetric solid content, initial water content, and strength increment rate. The strength in the active and moderate zones could be estimated based on the equation consisting of the normalized specific volume (v'/v_{LL}) and strength increment rates for each of the active and moderate zones.
3. The rate of strength increment of the stabilized soil changed according to the active and moderate zones. Moreover, the value and range of the strength increment rate varied with the type of binder, BOF, and cement. For the active zone, the increment rate of the BOF strength increased significantly with an increase in the BOF mass due to the hydration reaction. The rate of strength increment in the moderate zones differed with the change in the BOF slag content. Based on this result, the effect of the pozzolanic reaction in increasing the strength at the long-term curing time can be changed with the R_{BOF} content.
4. The reticulation structures of the amorphous C-S-H gel and platy AFm phases on all samples were observed with rod-like intergrowths. The degree of cementitious compounds became more evident with an increase in the R_{BOF} content and curing time. The C-S-H gel and ettringite with large openings, and the voids among the cementitious compounds of the BOF-treated clay, differed compared to cement-treated clay.

7.1.2 Particle Size Effect of Basic Oxygen Furnace Steel Slag in Stabilization of Dredged Marine Clay

The experimental work in **Chapter 4** was executed to comprehend the effect of different grain size distributions (GSD) of BOF slag in the stabilization of dredged marine clay. Mainly conclusions and finding are as follows:

6. Under similar conditions of initial clay moisture and free lime content, the different grain-size distribution of BOF slag had a significant effect on the strength development of the stabilized marine-dredged clay. The larger the max GSD, the lower final strength are observed within the stabilized marine clay with BOF slag.
7. At an early stage of curing time, the addition of BOF slag with larger maximum particle sizes produced longer inactive or negligible strength gain. In this study, BOF slag with 37.5 mm of grain size was inactive for up to 10 h, while the smaller maximum grain-size had an average of 5 h of inactivity.
8. The correlation of the secant modulus of BOF slag was between 88.5–120 q_u, where q_u was unconfined compressive strength obtained from the UC test. In this study, the best value to predict the E_{50} was 88.5 q_u. The correlation did not appear to be significantly affected by a different maximum grain-size.
9. Strength estimation equations to predict the stabilized soils using BOF slag were proposed using the specific surface area value obtained from the grain size distribution and the modified BOF rate of addition. It demonstrated good agreement for predicting the actual size used in the field, using a smaller maximum grain-size in the laboratory.
10. Using the proposed Equation 13, the actual strength using a maximum grain-size equal to 37.5 mm can be predicted using the result from the laboratory, with a smaller grain size of 4.75 mm.

7.1.3 Expansion Characteristic of Steel Mixed with Dredged Marine Clay

A comprehensive study on the behavior of soil mixture consisted of dredged marine clay and BOF slag was performed in **Chapter 5**. The following are the conclusions:

1. The maximum rate of steel slag addition to the soft clay that complies with the 0.5% expansion ratio was 60% and it produced 24.3 kN/m^3 of unit weight. It is well ascertained that the addition of soft clay increases the unit weight of the soft clay and reduces the volume expansion of the steel slag. The high void ratio of

the soft clay was found to be the likely reason, as it provides more space to absorb the volumetric change. A fewer number of hydration products were observed using a scanning electron microscope in the soil mixtures with an addition of 55%–60% of steel slag as compared to the ones with 70%–100%.

2. The steel slags with and without fine aggregates were also subjected to the expansion test. The results indicate that the steel slag with fine particles showed a relatively higher value of volume expansion than the steel slag without the fine particles at the early test period (40 days). However, the final volume expansion of steel slag both with and without the fine particles was very similar. It is therefore well ascertained that the removal of the fine aggregate was not an effective way to alleviate the volume expansion.
3. Our results further explained that the amount of free CaO and free MgO most likely controls the final volume expansion, whereas the grain size distribution varies the increment of the volumetric change.
4. SEM and EDS analysis results showed more microcracks and less existence of the C-S-H phase for the addition of 45%–60% of steel slag than for 70%–100%, which explains the occurrence of less volumetric expansion.

7.1.4 Time-delay effect to the strength development of stabilized soils with BOF slag

The study on **Chapter 6** was carried out to understand the effect of time delay between mixing and pouring/casting on the strength development of the stabilized marine clay with BOF slag. The conclusions are as follow:

1. The disturbance significantly affected the strength development of the stabilized soil. However, the stabilized soil has the ability to self-recover and develop the strength after period of time.
2. Up to its dormant period (10 hours), the strength of the stabilized soils at later curing time (after 28 days) is close or higher than the specimen without disturbance.
3. For 30% R_{BOF}, the strength of the specimens with 2, 5, and 7 hours disturbance were fully recovered after 7 days close to the specimen without disturbance. The specimens with 1, 2, and 3 days disturbance were able to develop with a strength ratio of 0.7, 0.5 and 0.52 to that without disturbance, respectively.

4. For 20% R_{BOF}, after 28 days, the specimen of 2, 5, and 7 hours of disturbance achieved similar strength as what the specimen without strength exhibited. The specimens of 1, 2, and 3 days disturbance exhibited strength ratio of 0.92, 0.64, and 0.54, respectively.

7.2 Recommendation for future work

Based on the studies presented in this dissertation, I would like to draw recommendations for future work. I encountered limitations that can be overcome in the next study. The recommendations are as follows:

1. This study was conducted as a fundamental study to understand the engineering properties of SMSS. It is essential to have a comprehensive understanding before one could use it widely as geomaterial. Therefore, more studies on field construction shall be conducted in the next study. More different types of soils and different types of BOF slag should be further studied and compare with the current result. It is then, the variability can be investigated and overcome.
2. The strength observed in **Chapter 4**, the strength of different GSD might still be affected by the smaller particle attached on the surface of the bigger particle. The complication was due to the method used to sieve the different grain size distributions. The mechanical sieve can be replaced with other methods, or assist with an additional step such was, brush or water jetting.
3. The further study shall be carried on the effect of MgO on the expansion behavior of stabilized soils with BOF slag. **In Chapter 5**, the study mostly covered the expansion part caused by free lime; it is assumed that the MgO is also contributing to the expansion, however, the portion of MgO in the expansion is still unknown. Therefore, a further study on how to measure the expansion of MgO is essential.
4. The disturbance in **Chapter 6** is only limited to time delay, the time delay between the mixing process and pouring or casting process. Often other disturbances can exist, such as drilling, or earthquake. Other experiments to accurately represent the disturbance can be proposed in the next study.
4. As it had been described in **Chapter 6**, the stabilized marine clay with BOF slag has a self-recovery feature. It is necessary to know whether the self-recover feature still exists at later curing, say 1 year, 2 years or 5 years. The experiment model can

be approached with accelerated curing process; high temperature, vapor, etc. (Ramachandran et al., 1964)

7.3 References

Ahmedzade, P., and Sengoz, B. (2009). Evaluation of steel slag coarse aggregate in hot mix asphalt concrete. J. Hazard. Mater. *165*, 300–305.

Horii, K., Kitano, Y., Tsutsumi, N., and Kato, T. (2013). Processing and Reusing Technologies for Steelmaking Slag. 123–129.

Kiso, E., Tsujii, M., Ito, K., Nakagawa, M., Gomyo, M., Nagatome, T. 2008. Method of dredged soil improvement by mixing with converter steel-making slag. Kaiyo Kaihatsu Ronbunshu 2008, 24, p 327-332. (In Japanese).

Kang, G., Cikmit, A.A., Tsuchida, T., Honda, H., and Kim, Y. (2019). Strength development and microstructural characteristics of soft dredged clay stabilized with basic oxygen furnace steel slag. Construction and Building Materials *203*, 501–513.

Poh H. Y., Ghataora Gurmel S., and Ghazireh Nizar (2006). Soil Stabilization Using Basic Oxygen Steel Slag Fines. Journal of Materials in Civil Engineering *18*, 229–240.

Qasrawi, H., Shalabi, F., and Asi, I. (2009). Use of low CaO unprocessed steel slag in concrete as fine aggregate. Construction and Building Materials *23*, 1118–1125.

Ramachandran, V.S., Sereda, P.J., and Feldman, R.F. (1964). Mechanism of Hydration of Calcium Oxide. Nature *201*, 288.

Sato, H., Nishimura, S., Toda, K., Sato, T., and Arai, Y. (2016). Characteristic and Interpretation of Development of Strength and Stiffness for Early-Age Calcia-Stabilized Dredged Soils. Hokaido Site Engineering Society *Techincal report*, 15–20.

Shi, C. (2004). Steel Slag—Its Production, Processing, Characteristics, and Cementitious Properties. Journal of Materials in Civil Engineering *16*, 230–236.

Tanaka, Y., Ko, C., Imamura, T., Shibuya, T., Yamagoshi, Y., Akashi, Y., Kitano, Y., and Kanno, H. (2014). Reclamation of the artificial ground made of dredged soil and converter slag. Japanese Society of Civil Engineering B3 70, I_888-I_893.

Tsuchida, T., Tsurugasaki, K., and Cikmit, A.A. (2019). Study on the Use of Heavy-weight Geo-Material for Design of Quay-wall Structure or Sea-wall. Journal of J.S.C.E Maritim Development *76*.

Yildirim, I.Z., and Prezzi, M. (2011). Chemical, Mineralogical, and Morphological Properties of Steel Slag.

Yamagoshi, Y., Akashi, Y., Kanno, H., Nobuhiro, T., and Tanaka, Y. (2014). Reclamation by CaO improved soil. Nippon Steel and Sumitomo Metal Technical Bulletin *399*, 65–72.

Yong-Feng, D., Tong-Wei, Z., Yu, Z., Qian-Wen, L., and Qiong, W. (2017). Mechanical behaviour and microstructure of steel slag-based composite and its application for soft clay stabilisation. European Journal of Environmental and Civil Engineering *0*, 1–16.